REGULATORY DOCKET FILE COPY

INDIANA & MICHIGAN POWER COMPANY
P. O. BOX 18
BOWLING GREEN STATION
NEW YORK, N. Y. 10004

October 24, 1978
AEP:NRC:00085

Donald C. Cook Nuclear Plant Unit 1
Docket No. 50-315
License DPR No. 58

Mr. Harold R. Denton, Director
Office of Nuclear Reactor Regulation
Nuclear Regulatory Commission
Washington, D.C. 20555

Dear Mr. Denton:

In fulfillment of the statement made in my letter to Mr. Edson G. Case dated May 12, 1978 please find attached to this letter two (2) copies of the Startup Test Report for Cycle 3 of Unit No. 1 of the Donald C. Cook Nuclear Plant, dated October 10, 1978.

Under separate cover we are mailing you twenty-five (25) additional copies of the subject report for distribution to your staff. Additional copies are being sent to Mr. J. G. Keppler, Regional Director Office of Inspection and Enforcement, Region III, to Mr. W. G. McDonald, Director Office of Management and Program Analysis, and to Ms. M. M. Mlynczak, Project Manager for the Donald C. Cook Nuclear Plant, Units No. 1 and 2.

Very truly yours,

John Tillinghast
Vice President

JT:em

Sworn and subscribed to before me this 24th day of October, 1978 in New York County, New York

Gregory M. Gurican
Notary Public

GREGORY M. GURICAN
Notary Public, State of New York
No. 01-4643431
Qualified in New York County
Commission Expires March 30, 1979

cc: (attached)

7811030103

A027
S
1/25
REPRO
LTR'S

cc: John G. Davis, Acting Director, I.E. (2)
W. G. McDonald, Director, M.P.A. (2)
M. M. Mlynczak (2)
G. Charnoff (1)
R. C. Callen (1)
R. J. Vollen (1)
P. W. Steketee (1)
R. Walsh (1)
R. W. Jurgensen w/att
D. V. Shaller -Bridgman (60)

A017

REGULATORY INFORMATION DISTRIBUTION SYSTEM

DOCKET NBR: 50-315 COOK 1 DOC DATE: 781114

RECIPIENT: DENTON, H.R. ACCESSION NBR: 7811210260

ORIGINATOR: TILLINGHAST, J. COPIES RECEIVED:

COMPANY: IN & MI PWR LTR 1 ENCL 40

SUBJECT: SIZE: 2+98

Forwards rept "Reactor Containment Bldg Integrated Leak Rate Test" for subj facil conducted 780527-29..

(see report)

DISTRIBUTION CODE: A017

DISTRIBUTION TITLE: NOTARIZED ✓

CONTAINMENT LEAK RATE TESTING-APPENDIX J.

NAME	ENCL?	FOR ACTION
BR CHIEF	W/7 ENCL	ORB#1 BC
REG FILE	W/ENCL	
NRC PDR	W/ENCL	
I & E	W/2 ENCL	
OELD	W/ENCL	
HANAUER	W/ENCL	
CONTAINMENT SYSTEMS	W/ENCL	
AD FOR SYS & PROJ	W/ENCL	
ENGINEERING BR	W/ENCL	
REACTOR SAFETY BR	W/ENCL	
PLANT SYSTEMS BR	W/ENCL	
EEB	W/ENCL	
M FAIRTILE	W/ENCL	
EFFLUENT TREAT SYS	W/ENCL	
LPDR	W/ENCL	
TERA	W/ENCL	
NSIC	W/ENCL	
ACRS	W/16 ENCL	

TOTAL NUMBER OF COPIES REQUIRED:

LTR 40

ENCL 40

NOV 29 1978

NOTES: I & E 3 CYS ALL MATL

GD

DONALD C. COOK
NUCLEAR PLANT

UNIT 1

CYCLE III

INDIANA & MICHIGAN
POWER COMPANY

STARTUP
TEST REPORT

AMERICAN ELECTRIC
AEP
POWER SYSTEM

Docket # 50-315
Control # 7811030103
Date 10/24/78 of Document
REGULATORY DOCKET FILE

TABLE OF CONTENTS

SECTION	TITLE	PAGE NUMBER
1.0	INTRODUCTION	1-1
2.0	SUMMARY	2-1
3.0	CORE LOADING	3-1
4.0	INSPECTION OF IRRADIATED FUEL ASSEM.	4-1
5.0	INITIAL CRITICALITY	5-1
6.0	LOW POWER PHYSICS TESTING	6-1
7.0	POWER ASCENSION TESTING	7-1
7.1	PLANT CHEMISTRY HISTORY DURING POWER ASCENSION	7.1-1
7.2	PLANT RADIATION SURVEYS	7.2-1
7.3	LOOSE PARTS MONITORING SYSTEM	7.3-1
7.4	POWER RANGE NOISE MEASUREMENTS	7.4-1
7.5	POWER ASCENSION TESTS	7.5-1
8.0	CORE POWER DISTRIBUTION MEASUREMENTS	8-1
APPENDIX A	FUEL EXAMINATION CORE 2	A-1
APPENDIX B	SUMMARY OF EXXON FUEL EXAMINATION	B-1

SECTION 1.0

INTRODUCTION

The Donald C. Cook Nuclear Plant consists of two 1100 MWe pressurized water reactors. The Nuclear Steam Supply Systems for both units are Westinghouse supplied with a General Electric Turbine-Generator on Unit 1 and a Brown Boveri Turbine-Generator on Unit 2.

The attached report summarizes the results of the Unit 1 - Cycle III Start-Up and Power Ascension Testing.

At 1500 hours on April 6, 1978, the generator was manually tripped from the Unit 1 Control Room to complete a Unit 1 Cycle I testing requirement. This manual actuation resulted in a turbine and reactor trip through normal logic circuitry actuation, which marked the commencement of the Unit 1 Refueling Outage. Following the outage, initial criticality of Unit 1 - Cycle III was obtained at 1349 hours on June 18, 1978. The turbine was rolled at 1610 hours on June 24, 1978 with the generator paralleled to the system at 1746 hours.

SECTION 2.0

SUMMARY

Unit 1, Cycle II was completed on April 6, 1978. Fuel shuffling for Cycle III began on April 26, 1978 and was completed on May 2, 1978. A total of 64 new fuel assemblies were placed in the core, and the Cycle II burnable poison rods were removed. During the fuel shuffle, delays were encountered as a result of the following equipment problems: abnormal fuel transfer system operation due to a clogged air motor exhaust filter; manipulator crane limit switch malfunctions, upender microswitch malfunction and a source range detector failure.

A thorough inspection of irradiated fuel assemblies was conducted during the fuel shuffle. A binocular inspection of all irradiated fuel assemblies found five assemblies with apparent rod bow, three assemblies with scraped grid straps, and one assembly with a variation in crud discoloration. An independent fuel vendor conducted a TV inspection of eight irradiated assemblies which found some minor rod bowing and corrosion sites, but no significant defects or structural damage. Exxon Nuclear Corporation made measurements of the fuel rod spacing on two fuel assemblies and length measurements for one of the two assemblies. No significant abnormalities were observed.

Cycle III core cirticality was achieved on June 18, 1978 at 1349 hours with an all rods out boron concentration of 1297 ppm (design prediction was 1333 ppm). The range selected for zero power testing was 10^{-7} to 10^{-8} amps on the reactivity computer.

Low power physics testing began at 1830 hours on June 18, 1978, and was completed at 1130 hours on June 23, 1978. Parameters measured included; critical boron endpoints, rod worths, minimum shutdown margin verification and boron worth. Also several flux maps were taken at low power levels with various control rod bank configurations. New power distribution mapping equipment made it possible to obtain more accurate data in less time with the lower power level required for measurements. The all rods out moderator temperature coefficient was positive (+2.45 pcm/^{o}F). With the Doppler coefficient of -1.66 pcm/^{o}F, the isothermal temperature coefficient was measured at +0.79 pcm/^{o}F. The total worth of the control rod banks (CBA, B, C and D) was measured at 3.60%, compared to the design value of 3.58%.

The positive moderator temperature coefficient determined during low power physics testing required early cycle operation with a boron concentration below 1180 ppm, or criticality with control bank C below 150 to 170 steps to insure a negative moderator temperature coefficient as required by the Technical Specifications.

Power operation with Control Bank C above 150 steps was necessary to insure no violation of $F_{\Delta H}$ power peaking factors. The Unit was operated with control bank C withdrawn 150 to 170 steps until sufficient Xenon was built into the core to resume normal operations.

Plant chemistry measurements have shown that the Iodine-131 activity in the reactor coolant for Cycle III is less than one-tenth of the activity at a comparable time during Cycle II. Also the Iodine 131/133 ratio is about one-quarter as high in Cycle III as in Cycle II. Both of these parameters indicate better clad integrity for the Cycle III core fuel. No primary to secondary leakage has been detected.

During plant start-up a mixed bed demineralizer was inadvertently put into service with high reactor coolant ammonia concentrations. The demineralizer resin was exhausted and released chlorides. The reactor coolant chlorides reached about 1 ppm (specification calls for 0.15 ppm max.). Reactor coolant drainage to 1/2 loop and refill reduced the chloride concentration to less than 0.05 ppm in about 1 day.

Plant radiation surveys during start-up have shown no significant changes in the gamma radiation levels throughout the plant.

Spectral traces were taken from the loose parts monitoring system on June 19, 1978 at zero reactor power, and on July 18, 1978 at 99% reactor power. No significant increases in the system vibrations are present in Cycle III compared with those present before refueling.

Power range noise measurements were obtained on July 19, 1978 at 98% of full reactor power. Comparison with earlier measurements shows that the power noise present at a frequency of 6.8 cps continues to increase. This frequency corresponds to the natural frequency of the core barrel. The baseline measurements made in April, 1975 indicated a core barrel motion of about 20 mils (peak-to-peak). Three measurements made since the baseline measurements indicate the magnitude has increased to about 39 mils with an increase of about 6 mils/year.

Power coefficient measurements were performed at 50, 70 and 90% of rated thermal power. The power coefficient was determined from data measured using the boron substitution technique, and from data obtained by combining Doppler and moderator temp. coefficient measurements. All measured data met the review criteria. Moderator coefficient measurements showed values consistently more positive than design values. The measured data averaged 5 pcm/^{o}F above design data.

An incore-excore calibration was performed with data measured at a power level of 50%. Five full core power maps were taken. The first map was at 0544 hours on June 27, 1978 and the last map was at 0847 hours on June 28, 1978. Additional core power distribution measurements were obtained at various power levels in the power ascension testing program. All measurements were within Technical Specification limits and the measured horizontal power distribution agreed well with design values. Although the power level was initially limited to 97% because of the APDMS, subsequent burnup has allowed the unit to operate at 100%.

SECTION 3.0

CORE LOADING

PURPOSE

The purpose of this section is to briefly describe the fuel shuffle, the reactivity monitoring performed during the shuffle and the problems encountered which caused delays in the shuffle.

SUMMARY OF RESULTS

The fuel shuffle commenced on April 26, 1978 and was completed on May 2, 1978. A total of 64 new fuel assemblies were placed in the core while 64 old assemblies and the Cycle II burnable poison rods were removed. Inverse Count Rate Ratios (ICRR) were obtained as the assemblies were withdrawn from or inserted into the core. Verification that the fuel assemblies were in their proper core locations after the shuffle was completed, on May 2, 1978, was made by using a video tape camera. There were several equipment malfunctions which caused delays in the fuel shuffle.

DISCUSSION OF TEST

The fuel shuffle began on April 26, 1978 at 0920 hours and consisted of 193 major steps and many more sub-steps. The procedure was completed on May 2, 1978 at 1052 hours. Initial and final core locations, for fuel assemblies and inserts, are shown in Figures 3-1 and 3-2, respectively.

Source range channels N31 and N32 were used to monitor reactivity changes during core alterations. Base counts were taken prior to the start of the procedure. ICRR's were obtained as each assembly was either removed from or inserted into the core. Figures 3-3 and 3-4 show the ICRR versus the number of assemblies positioned in final locations for N31 and N32, respectively. None of the plots indicated any unusual changes in reactivity during the fuel shuffle.

Several equipment malfunctions caused delays in the fuel shuffle. Typical of the problems encountered were:

1. Fuel transfer system was jerky and stopped several times due to a clogged exhaust filter on the air motor.

2. The brake on the manipulator crane would not release for normal travel in the north direction due to a bad limit switch.

3. After removal of an assembly from the upender, the upender would not go down because of a bad microswitch.

4. A source range detector failed.

5. The manipulator crane hoist control ran only in fast speed because of a bad switch.

After the fuel shuffle was complete, a television camera was lowered into the vessel and the proper locations and orientation of all fuel assemblies was verified.

Figure 3-1 Cook Unit I Cycle II Fuel Loading Pattern

NSD

FP-AEP-R2

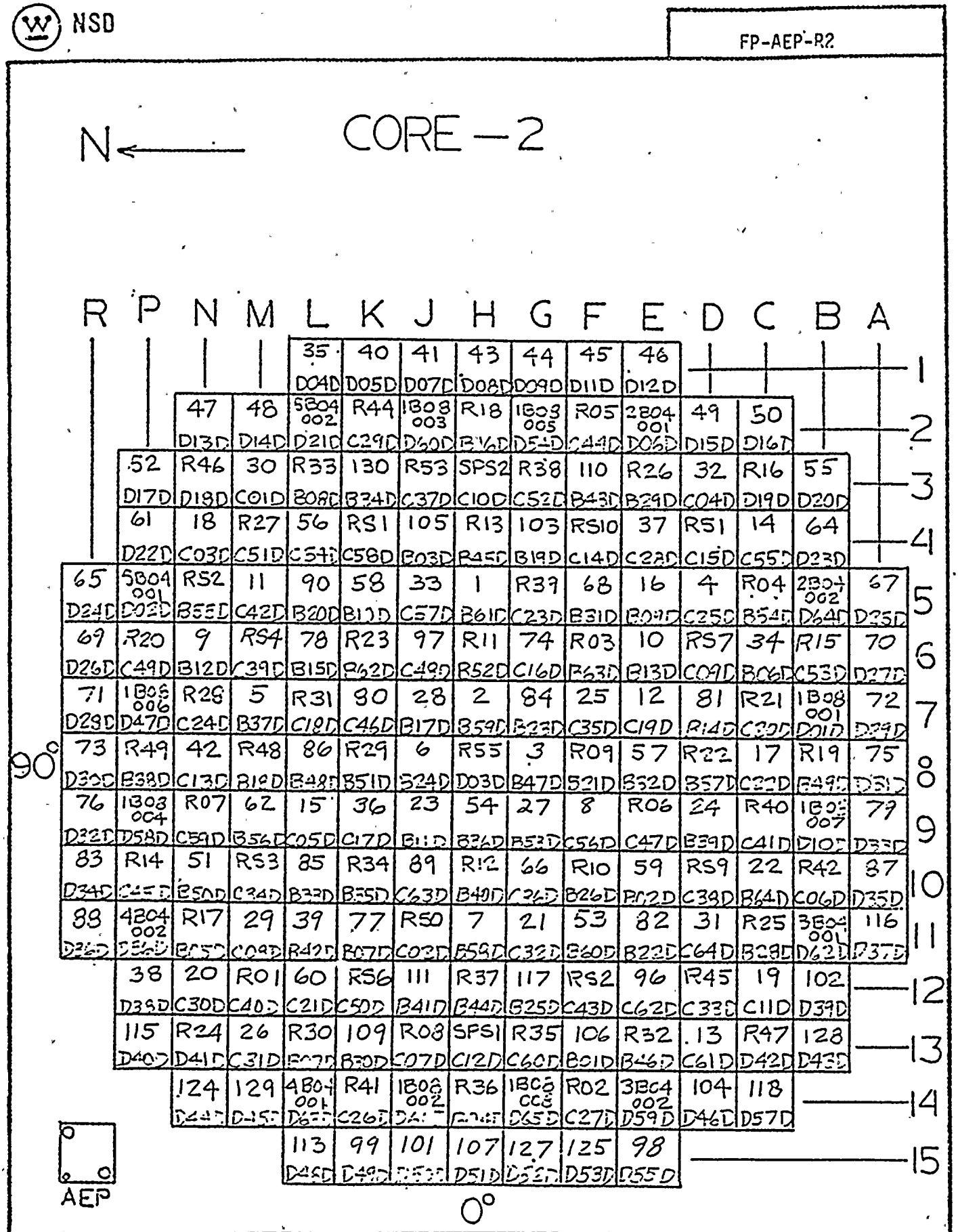

EFFECTIVE DATE	MAR 31 1978	PAGE	245	REVISED DATE	

WESTINGHOUSE FORM 55348

Figure 3-2 Cook Unit I Cycle III Fuel Loading Pattern

NSD

FP-AEP-R2

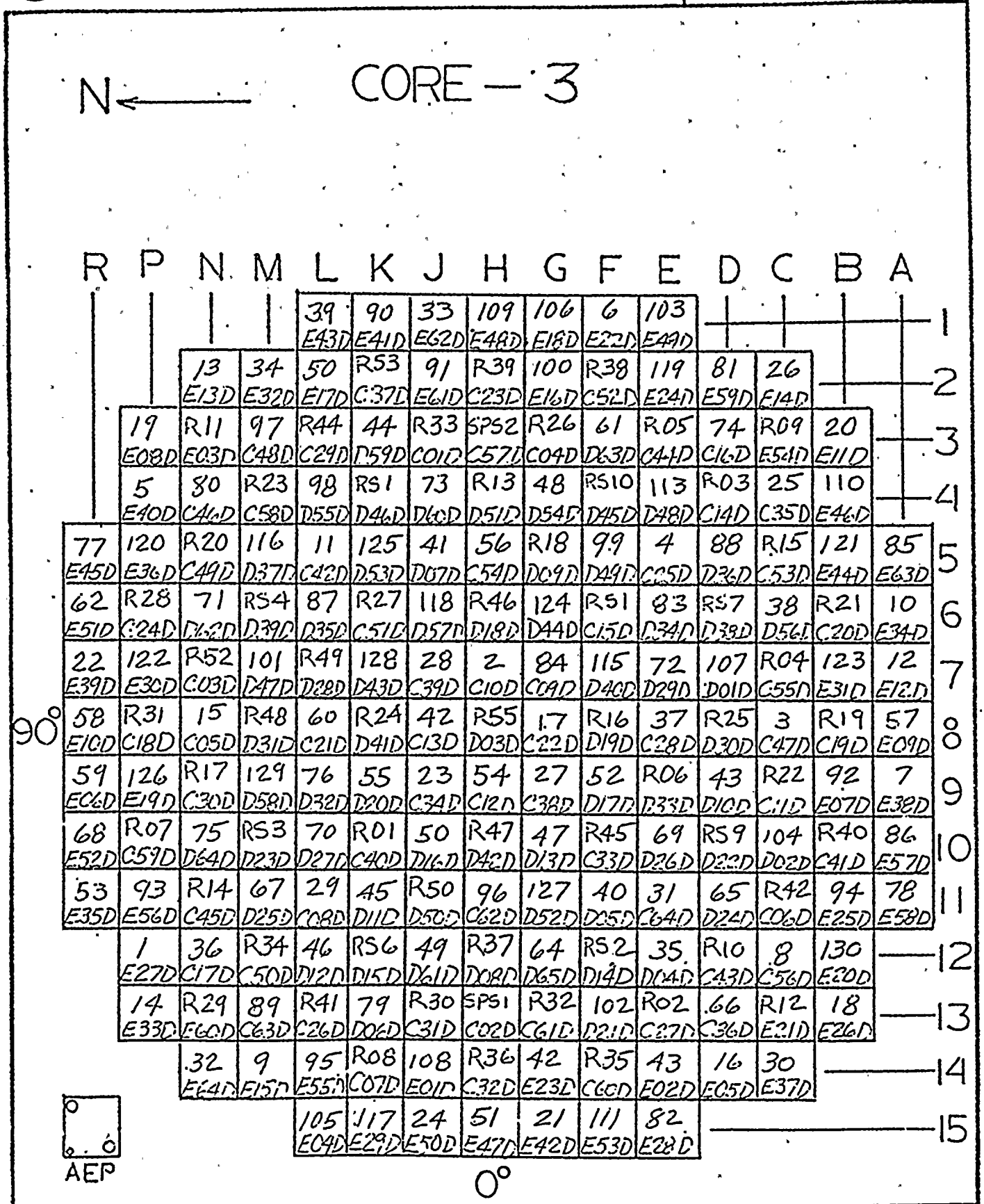

EFFECTIVE DATE MAR 31 1978	PAGE 311	REVISED DATE	

WESTINGHOUSE FORM 55348

Figure 3-3 ICRR vs. Procedure Step - N31

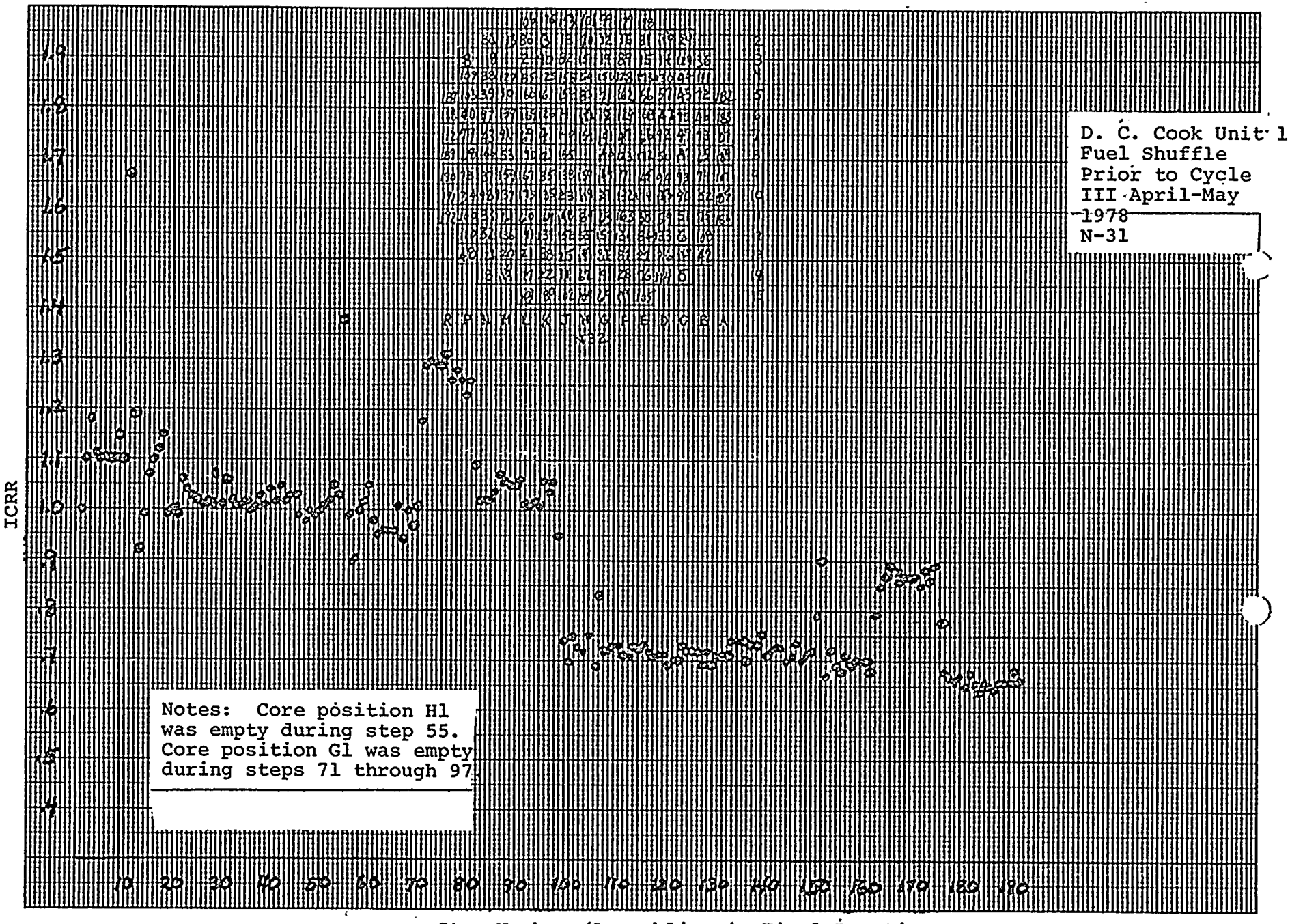

SECTION 4.0

INSPECTION OF IRRADIATED FUEL ASSEMBLIES

PURPOSE

The purpose of this inspection was to determine if any structural damage occurred to any irradiated fuel assemblies during Cycle II operation or subsequent handling during the fuel shuffle for Cycle III.

SUMMARY OF RESULTS

The irradiated fuel inspection commenced on April 26, 1978 and continued until the fuel shuffle was completed on May 2, 1978. During the fuel shuffle, 193 irradiated fuel assemblies were inspected with binoculars, including 64 fuel assemblies that were removed from the core (Region B), and 129 fuel assemblies which were rearranged within the core (Regions C and D). Eight assemblies were inspected by television camera. One fuel assembly was measured for rod-to-rod spacing and assembly length.

The results of the binocular inspection indicates 5 assemblies had apparent rod bow, 3 assemblies were scraped on the grid straps, and one assembly had a variation in the crud discoloration. These disparaties were not deemed significant enough to warrant more in depth inspection.

The television and measurement inspections did not reveal any structural damage or other significant abnormalities.

DISCUSSION OF TEST

During the fuel shuffle, two inspectors were stationed at the refueling cavity and one at the spent fuel pit using binoculars to inspect the irradiated fuel assemblies. The inspectors tried to check all four sides of each assembly, but where this wasn't possible, as many sides as manageable were inspected. No gross structural damage was seen on any of the assemblies. A list of minor discrepancies is given in Table 4-2.

Eight other irradiated assemblies underwent a TV inspection by an independent fuel vendor. The original sample of five assemblies was chosen because those assemblies were among the highest burnup fuel assemblies in their respective regions or because they exhibited minor discrepancies the previous cycle. Table 4-1 shows the fuel assemblies inspected, their burnup in MWD/MTU, and the region average burnup in MWD/MTU. No structural damage was found during the TV inspection, however, local crud

Figure 3-4 ICRR vs. Procedure Step - N32

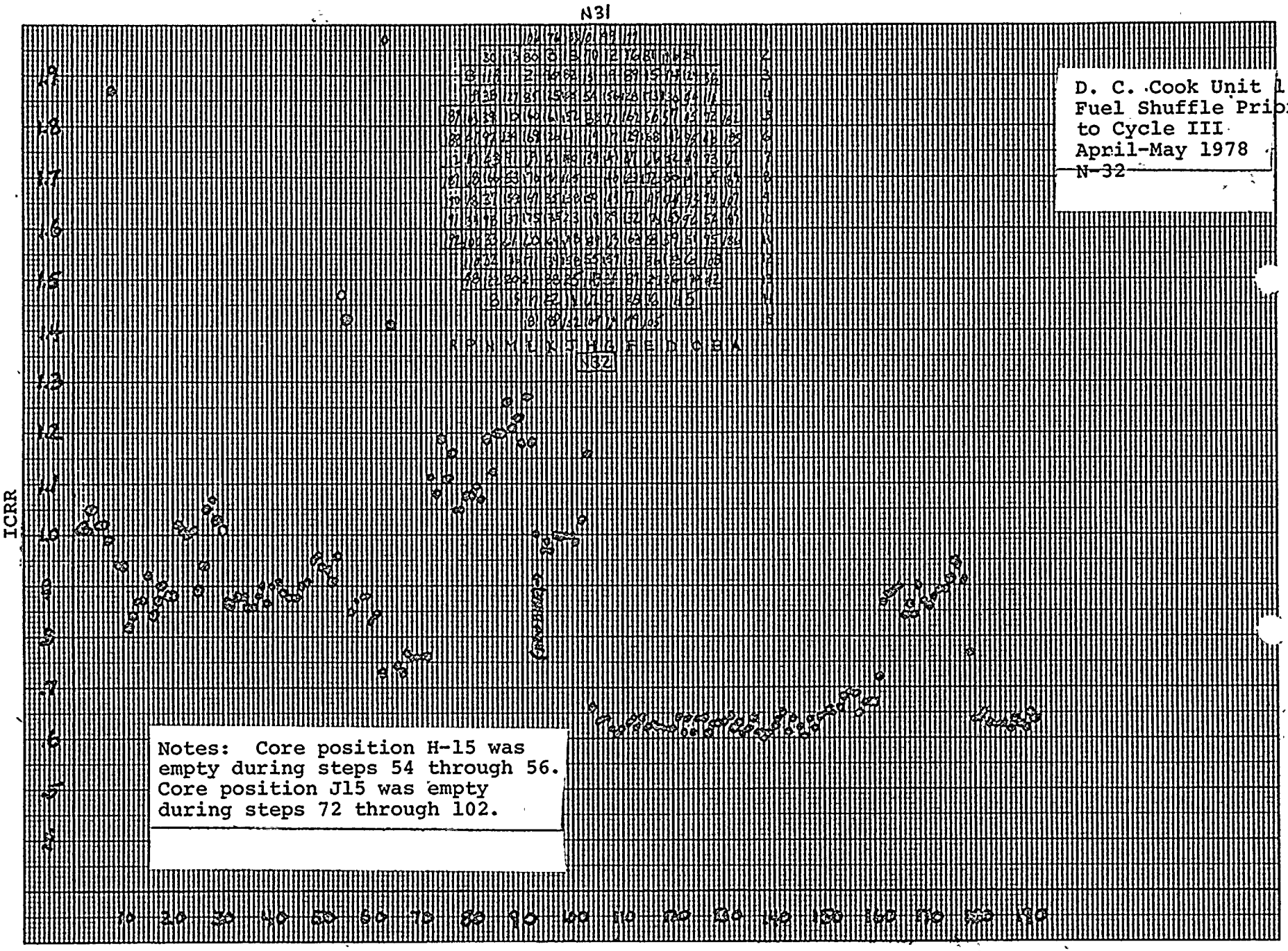

deposits known as "snails" were found on Region B & C fuel assemblies. In order to obtain additional data on this phenomenon, two additional Region B assemblies were inspected. Snails are oval shaped, darker crud deposits usually associated with a scratch on the fuel rod which occurred during insertion into the grid assembly. Although the frequency of the "snails" is high, there is no apparent adverse effect on fuel rod performance. This conclusion was confirmed by Westinghouse review of the data.

One additional Region D assembly was inspected because time was available.

One other fuel assembly was inspected by Exxon Nuclear Corporation for rod-to-rod spacing, and fuel assembly length. The results of this series of measurements did not reveal any serious problems with rod bow (gap closure) or fuel rod growth.

Appendix A contains the Babcock and Wilcox report discussing the detailed TV inspection of the fuel assemblies listed in Table 4-1. Appendix B contains a letter from Exxon Nuclear Corporation summarizing their preliminary results.

Table 4-1

Fuel Assemblies Inspected By Television Camera

Fuel Assembly Serial Number	Fuel Assembly Burnup MWD/MTU	Region Average Burnup MWD/MTU
B26	29,260	
*B57	29,930	29,050
B63	28,970	
*C11	29,410	
*C42	27,890	25,170
*D58	13,560	
D60	13,190	10,620
*D61	13,430	

*Original Sample

Table 4-2

Fuel Assemblies With Discrepancies[1] Seen By Binocular Inspection

	Fuel Assembly	Burnup MWD/MTU
Rod Bow	B11	29,230
	B15	28,490
	C13	25,050
	C21	27,940
Scrape Marks	D11	10,160
	D35	10,190
	D39	10,880
Crud Discoloration	D32	10,800

[1] These discrepancies were not severe enough to warrant more in depth inspection.

SECTION 5.0

INITIAL CRITICALITY

PURPOSE

The purpose of this test was to achieve criticality, establish the neutron flux level limits for zero power physics testing, determine the all rods out critical boron concentration, verify the proper operation of the reactivity computer, and verify the proper amount of overlap between the source and intermediate range detectors.

SUMMARY OF RESULTS

Criticality was achieved at 1349 hours on June 18, 1978 with an all rods out boron concentration of 1297 ppm. The flux level range for zero power testing was set at 1×10^{-8} amps to 10×10^{-8} amps. The reactivity computer was checked by using the built in exponential test and by reactor transients. A maximum average error of 0.92% was found using the exponential test method. During the increase of flux level, more than the required one decade of overlap was observed between source and intermediate range detectors.

DISCUSSION OF TEST

Prior to the withdrawal of the part length bank and shutdown banks, subcritical noise data was taken (Table 5.1) to help determine the proper flux level for zero power physics testing. The reactivity computer was checked and found to have a large noise signal which was eliminated by placing a 20μfd capacitor across the input. The ρ-computer was then checked using the exponential test. The results are given in Table 5.2

The part length rods were withdrawn at 0129 hours on June 18, 1978. RPI primary and secondary voltages were checked to verify their positions. The shutdown banks were then pulled and source range base counts were taken in preparation for pulling out the control banks.

The control banks were then withdrawn in the overlap mode until CBD reached 198 steps. N31 and N32 counts were taken at 50 step intervals and ICRR vs. control bank position data was plotted (Figure 5-1).

Dilution to critical started at 0540 hours on June 18, 1978 at a rate of 70 gpm. Every 20 minutes, N31 and N32 data was taken and plots of ICRR vs. Boron Concentration, ICRR vs. Time, and ICRR vs. Primary Water Integrator readings were made (Figure 5-2 through 5-4). When the ICRR reached 0.05, dilution was stopped and the RCS was allowed to mix. At 1349 hours on June 18, 1978, the reactor was declared critical.

The flux level was then raised to 5×10^4 cps to verify the proper overlap between the source and intermediate range detectors. More than the required one decade overlap was found.

While raising the flux level to check overlap, it was noticed that the ρ-computer responded sluggishly and had a large noise signal. The original 20μFd capacitor was replaced with a 35μFd capacitor which was placed across the input from N44 and the ρ-computer started responding normally, with a small noise signal.

The flux level was then raised to determine the start of nuclear heating. Three tries showed nuclear heat to begin at 1×10^{-6} amps. The range for the flux level for zero power physics testing was chosen as 1×10^{-8} amps to 10×10^{-8} amps. This range was below the nuclear heating level, but not quite above a level where background was ∿ 1%. All measurements except boron end points and ρ-computer checks were then made in the upper half of the range to minimize the background effects.

The reactivity computer was checked using reactor transients for different periods (Table 5.2). The average error (-0.05%) and each individual period error was well within the allowable ± 4% error.

The all rods out boron concentration was calculated using the reactivity measured from three consecutive rod movements. The rods were withdrawn from their original just critical position to full out and then inserted back to their original position. By knowing the just critical boron concentration, the reactivity change due to rod motion, and the design boron worth, the all rods out boron concentration was determined to be 1297 ppm. The design value for the boron concentration was 1333 ppm ± 75 ppm.

TABLE 5-1

Determination of the Flux Range for Zero Power Physics

Noise Level

Flux Level (N-44)	ΔFlux Level (Noise)	% Noise $\frac{\Delta \phi}{\phi} \times 100$
9×10^{-10} amps	0.03×10^{-10} amps	0.33%
9×10^{-9} amps	0.025×10^{-9} amps	0.28%
5.8×10^{-8} amps	0.01×10^{-8} amps	0.17%
9×10^{-7} amps	0.005×10^{-7} amps	0.06%

Subcritical Signal 7×10^{-10} amps $\frac{7 \times 10^{-10} \text{ amps}}{1 \times 10^{-8} \text{ amps}} = 7 \times 10^{-2}$

Nuclear Heating

Test Number	Flux Level for Heat	Average Flux Level
1	1×10^{-6} amps	
2	1×10^{-6} amps	1×10^{-6} amps
3	1×10^{-6} amps	

Flux range for zero power physics testing 1×10^{-8} amps to 10×10^{-8} amps.

TABLE 5-2

Reactivity Computer Check

6-18-78 Exponential Test

ρ calculated (pcm)	ρ indicated (pcm)	Error (%)	Average Error (%)	Standard Deviation
55.81	56.26	0.80		
92.67	93.20	0.57	0.92	0.44
31.59	31.83	0.75		
16.89	17.16	1.57		

6-18-78 Reactor Transient Test

ρ calculated (pcm)	ρ indicated (pcm)	Error (%)	Average Error (%)	Standard Deviation
62.96	63.5	0.85		
-40.65	-39.7	-2.39 [1]	-0.05	1.63
43.46	43.5	0.09		
19.75	20.0	1.25		

[1] The increase in error magnitude was due to not waiting long enough for period to stabilize.

FIG. 5-1 ICRR vs. Control Bank Position Initial Criticality Unit 1, Cycle II

June 1978

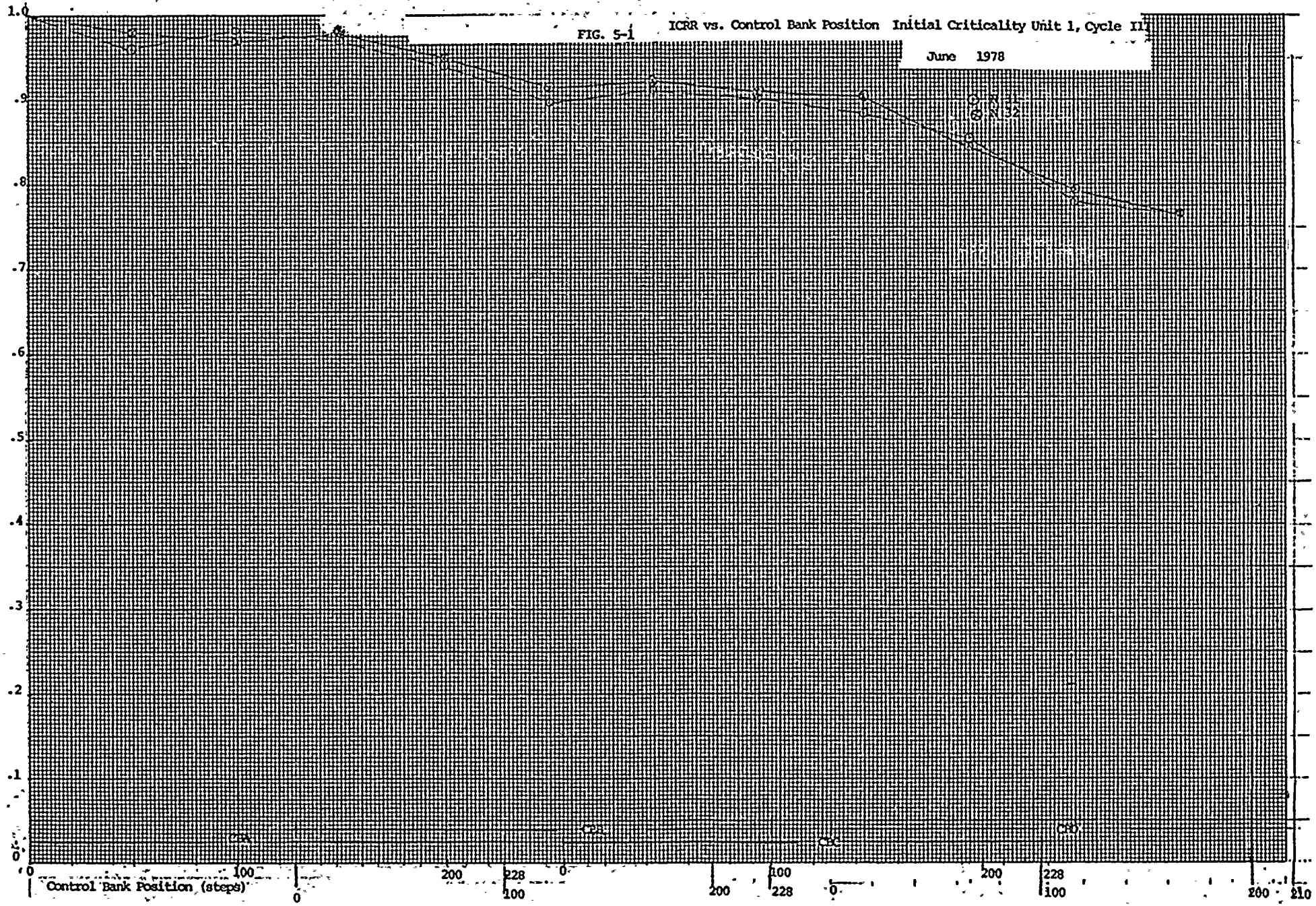

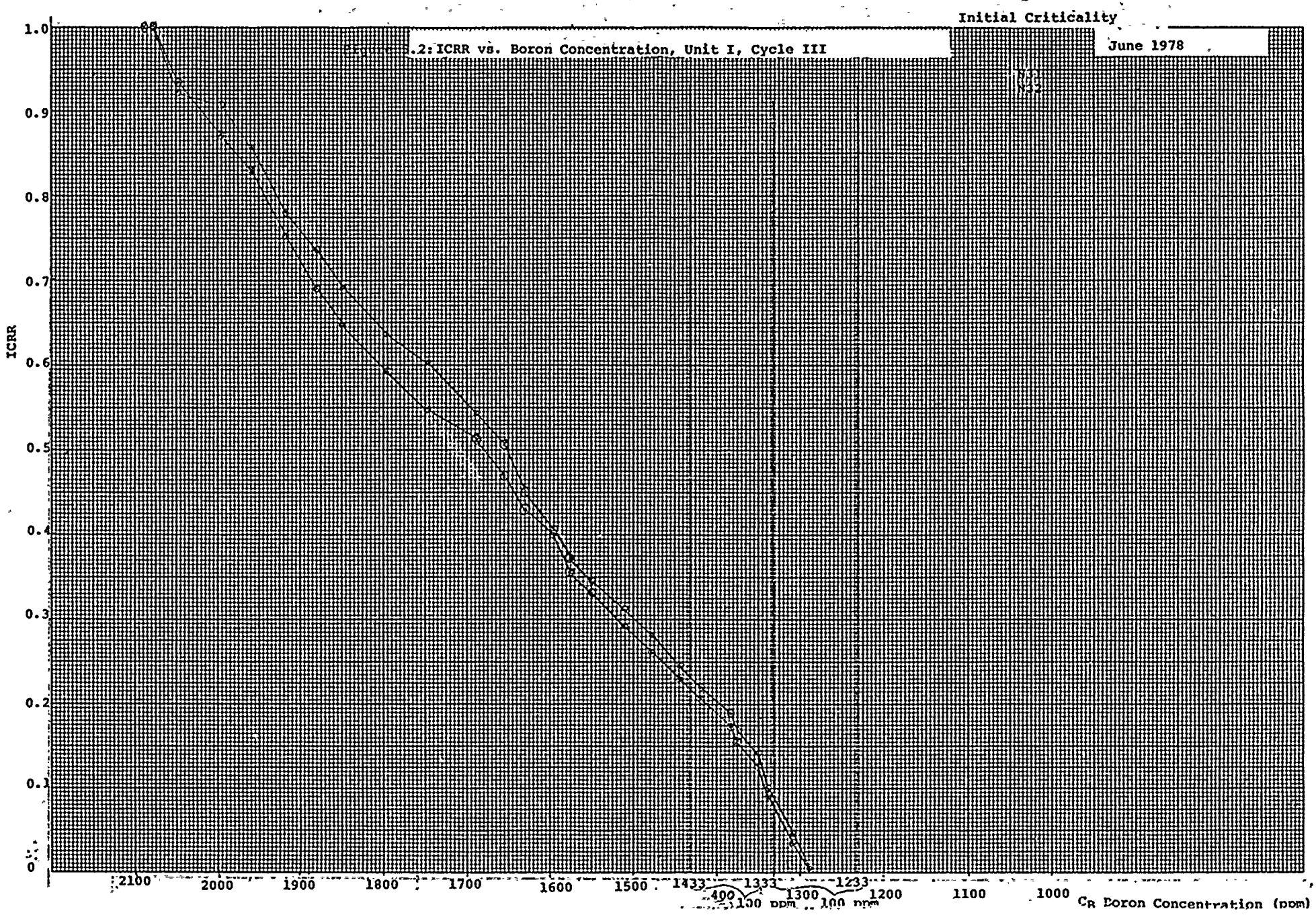
Initial Criticality
June 1978
.2: ICRR vs. Boron Concentration, Unit I, Cycle III
ICRR
1.0
0.9
0.8
0.7
0.6
0.5
0.4
0.3
0.2
0.1
0
2100
2000
1900
1800
1700
1600
1500
1433
1333
1233
1300
1200
1100
1000
400
100 ppm
100 ppm
C_B Boron Concentration (ppm)

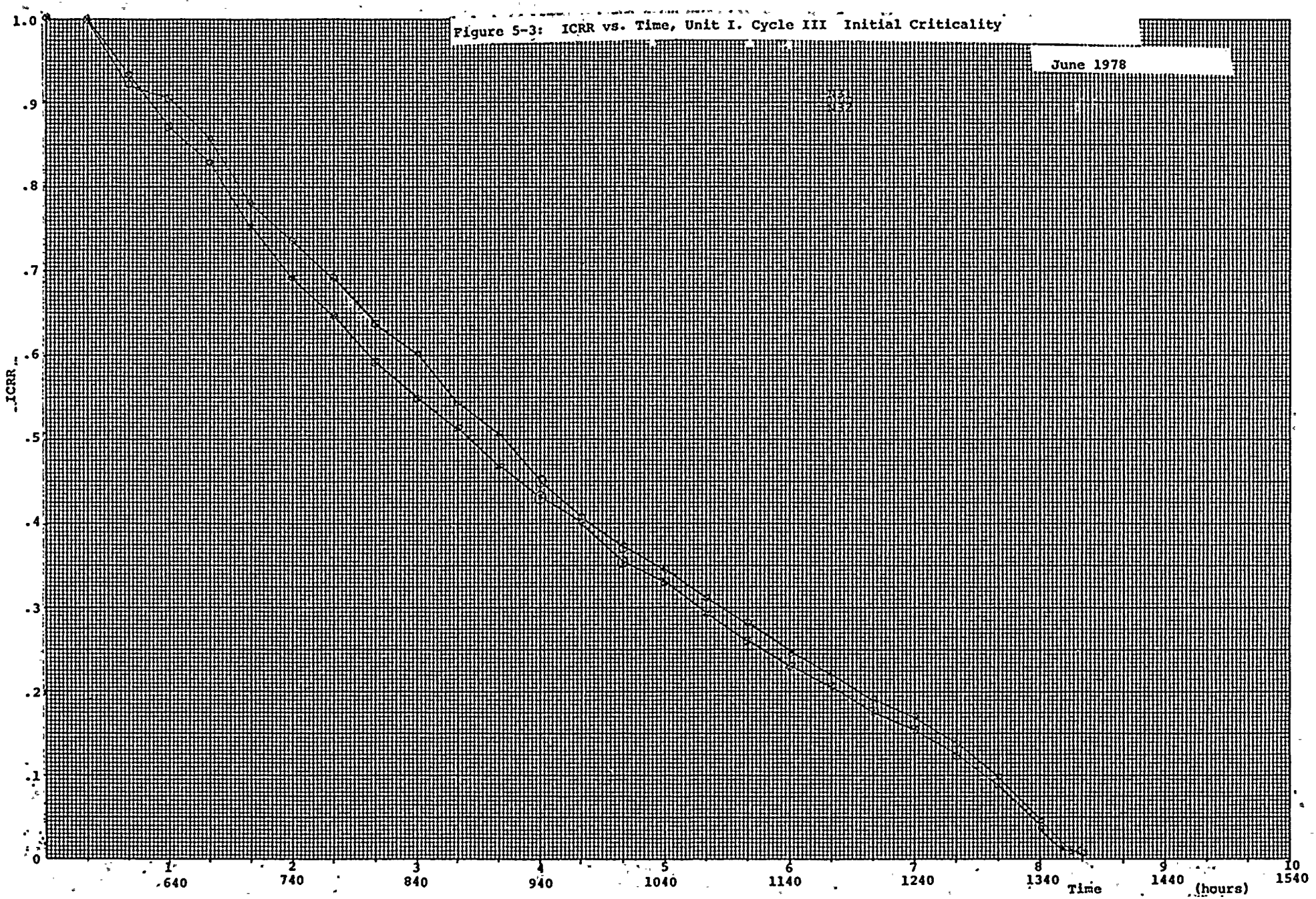
Figure 5-3: ICRR vs. Time, Unit I. Cycle III Initial Criticality
June 1978
731
732
ICRR
1.0
.9
.8
.7
.6
.5
.4
.3
.2
.1
0
1
640
2
740
3
840
4
940
5
1040
6
1140
7
1240
8
1340
9
1440
10
1540
Time
(hours)

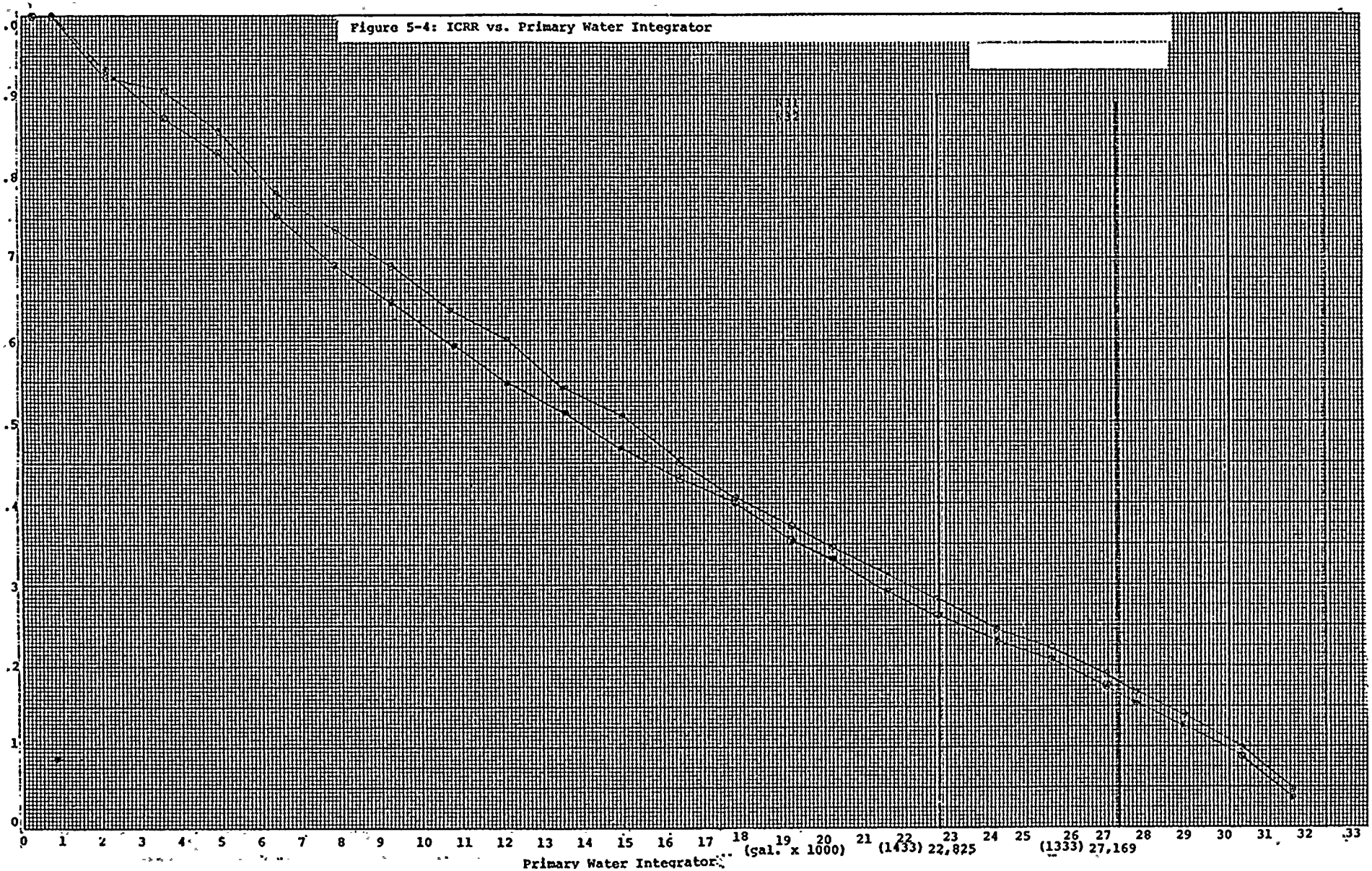
Figure 5-4: ICRR vs. Primary Water Integrator
.0
.9
.8
7
6
.5
.4
3
.2
1
0
0 1 2 3 4 5 6 7 8 9 10 11 12 13 14 15 16 17 18 19 20 21 22 23 24 25 26 27 28 29 30 31 32 33
(gal. x 1000)
(1433) 22,825
(1333) 27,169
Primary Water Integrator

SECTION 6.0

LOW POWER PHYSICS TESTING

PURPOSE

The purpose of the Low Power Physics Testing program was to obtain the following reactor physics characteristics in order to verify design predictions and to demonstrate compliance with the appropriate Technical Specifications:

1. Isothermal temperature coefficients at various boron concentrations and control rod configurations.
2. Boron end points at various rod configurations.
3. Rod worths for the control banks.
4. Power distributions through incore flux maps at various rod configurations.
5. Boron worth during movement of control rod banks.
6. Verify shutdown margin.

SUMMARY OF RESULTS

Low power physics testing began at approximately 1830 hours on June 18, 1978 and was completed on June 23, 1978 at 1130 hours. Two days were lost during the test to repair a problem in the feedwater system. A summary of the results for each parameter measured is displayed in the following tables:

Parameter	Table
Isothermal Temperature Coefficient	6-1
Boron Endpoint	6-2
Rod Worths	6-3
Boron Worths	6-4
Power Distribution	6-5

Table 6-1 Isothermal Temperature Coefficient

Rod Configuration	Bank Position	C_B(ppm)	Heatup(pcm/°F)	Cooldown(pcm/°F)	Average(pcm/°F)	Design(pcm/°F)
ARO	CBD @ 218	1289	+ 0.136	+ 1.667	0.789	- 2.75±3
ARO	CBD @ 214.5	1289	+ 0.727	+ 0.840		
ARO	CBD @ 210	1297	+ 0.784	+ 0.783		
ARO	CBD @ 210	1297	+ 0.547	+ 0.824		
CBD_{in}	CBC @ 214.5	1221	- 0.841	+ 0.900	- 0.311	- 5.22±3
CBD_{in}	CBC @ 216	1211	- 1.000	- 0.302		
CBD_{in} & CBC_{in}	CBB @ 228	1116	- 3.48	- 2.93	-3.325	- 7.7±3
CBD_{in} & CBC_{in}	CBB @ 199	1118	- 4.17	- 2.72		

Table 6-2

Boron Endpoint Data[1]

Rod Configuration	C_B (ppm)[2] Individual	C_B (ppm)[2] Average	C_B (ppm) Design	ΔC_B (ppm) Design-Measured
ARO	1294 1300	1297	1333±30	36
CBD_{in}	1224.3 1211.3	1217.8	1244±30	26.2
CBD & CBC_{in}	1118.8 1114.3	1116.6	1139±30	22.4
CBD,CBC,CBB_{in}	1062.4	1062.4	1067±30	4.6
All control banks in	975.3	975.3	960±30	-15.3

[1]The boron endpoint is the just critical boron concentration for the particular rod configuration.

[2]Corrected to the no xenon condition

Table 6-3

Rod Worth Data

Bank	Measured Integral Worth (pcm)	Design Worth (pcm)	% Error[1]
Control D	845	853 ± 85	+ 0.9
Control C	1074	996 ± 100	- 7.3[2]
Control B	656	695 ± 70	+ 5.9
Control A	1025	1035 ± 104	+ 1.0
Total Control Banks	3600	3579 ± 358	- 0.6
Control Banks in Overlap	3528	3600 ± 144[3]	+ 2.1

[1] % Error = $\frac{\text{Design - Measured}}{\text{Measured}} \times 100$

[2] The higher measured worth of CBC is due to heavy shadowing of detector N-44 (input to reactivity computer) by CBC.

[3] Sum of measured individual worths ± 4%.

Table 6-4

Boron Worth Data[1]

Bank	Measured Worth(pcm/ppm)	Design Worth(pcm/ppm)	% Error[2]
CBD	- 10.7	- 9.6	- 10.3
CBC	- 10.6	- 9.5	- 10.4
CBB	- 12.1	- 9.7	- 19.8
CBA	- 11.8	- 9.7	- 17.8
Least Squares Fit (slope)	- 11.2	- 9.7	- 13.4

[1]The differential boron worth was obtained by dividing the bank worth by the change in boron concentration over the bank movement.

[2]$\% \text{ Error} = \frac{\text{Design} - \text{Measured}}{\text{Measured}} \times 100$

Table 6-5 Power Distribution During Zero Power Testing

Rod Configuration	Map Number	Power (%)	F^m_{xy}	F^c_{xy}	$F^m_{\Delta H}$	$F^c_{\Delta H}$	F^m_Q	F^c_Q
ARO	103-01	0.26	1.6261	1.577 $\pm$ 0.07	1.4870	1.432 $\pm$ 0.07	2.4010	2.258 $\pm$ .11
CBD in	103-02	0.25	1.8125	1.874 $\pm$ 0.09	1.7009	1.672 $\pm$ 0.08	2.8967	2.757 $\pm$ .14
CBD & CBC in	103-03	2.86	1.9732	2.061 $\pm$ 0.10	1.8484	1.773 $\pm$ 0.09	3.1786	2.936 $\pm$ .15
CBC @ 147	103-04	3.60	1.9972	2.0397*	1.7521	1.8011*	2.5910	3.9000*

F^m - denotes penalized measured value

F^c - denotes value calculated by fuel vendor, with penalties

* - calculated technical specification limit

DISCUSSION OF TEST

6.1 Isothermal Temperature Coefficient Measurement

Isothermal temperature coefficient measurements were performed at various rod configurations and boron concentrations during low power physics testing. A summary of this data is given in Table 6-1.

The measurement was done by monitoring core reactivity while changing Tave between 542°F and 547°F. The temperature change was accomplished by controlling the amount of steam to the condenser through the steam dump valves. The temperature and reactivity changes were plotted on an X-Y plotter. The isothermal temperature coefficient is determined by calculating the slope of the plot. A typical plot is shown in Figure 6.1-1.

As a result of this testing, it was determined that the all rods out (ARO) moderator temperature coefficient was positive. With control bank D at ∿216 steps, the isothermal temperature coefficient was determined to be + 0.789 pcm/°F. The Doppler contribution is -1.66 pcm/°F, giving an ARO moderator coefficient at BOL of + 2.45 pcm/°F. In order to insure a negative moderator temperature coefficient during normal operations, the boron concentration had to be reduced from the ARO boron endpoint.

The most conservative way to accomplish this end is to correct the design HZP, ARO moderator coefficient as a function of boron concentration. The design values for this function were supplied by the fuel vendor. The design function was normalized to the measured ARO value. The resulting boron concentration for a zero moderator coefficient was 1118 ppm.

This is a very low value for the boron concentration and would have required both control banks D and C near full insertion. Operating in this configuration would have violated insertion limits. Furthermore, examination of the power distribution maps, discussed in Section 6.4, indicated that control bank C should be about 150 to 170 steps to insure no violation of $F_{\Delta H}$ on entry into Mode 1.

Therefore, it was necessary to take into account the decrease in moderator coefficient brought about by rod insertion. This effect is the result of increased neutron leakage. When this was done, it was determined that a boron concentration of 1180 ppm would produce a rod configuration that would not violate $F_{\Delta H}$ or moderator coefficient restrictions. The unit was operated in this configuration until sufficient Xenon was built into the core to resume normal operations.

Figure 6.1-1 Typical Isothermal Temp. Coefficient Plot

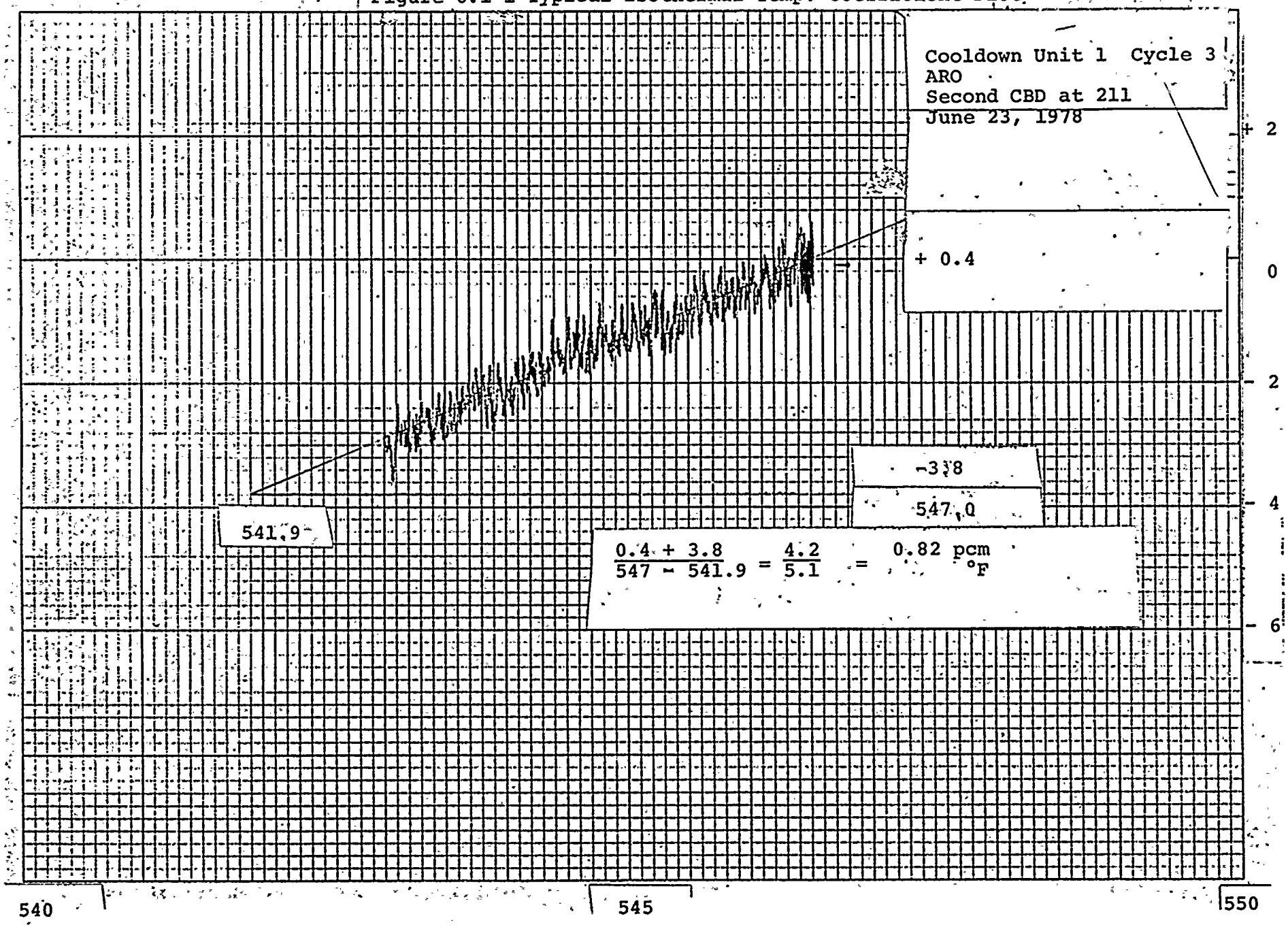

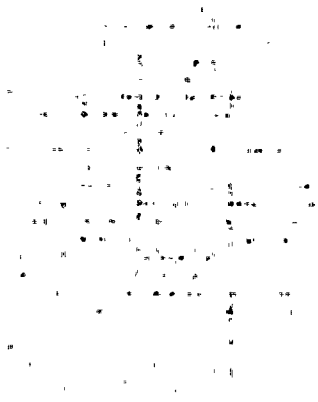

6.2 Boron Endpoints and Boron Worths

During rod movements for measurement of rod worth and differential boron worth, the dilution was stopped when the rods were near the bottom to obtain boron endpoint data. The rod configuration and boron concentration are summarized in Table 6-2.

After dilution was stopped, reactor coolant system (RCS) was allowed to mix until boron samples of the RCS and pressurizer showed their boron concentrations to be within 20 ppm of each other. The control rods were then moved to the position indicated in Table 6-2 and the resulting reactivity insertion was measured using the reactivity computer. This measurement was repeated several times. The design boron worth was used to adjust the measured boron concentration for the change in reactivity due to the rod movement to obtain the boron endpoint. Table 6-2 shows both individual measurements and their average values.

The results of the boron endpoint and rod worth measurements are used in Figure 6.2-1 to obtain a differential boron worth. The slope of the line is equal to the differential boron worth (slope= -11.2 pcm/ppm). The results of a least square fit to both the design and measured values in Figure 6.2-1 showed that the measured differential boron worth is 13.4% larger than the design value.

The differential boron worth for each control rod bank was calculated by dividing the worth of the control bank by the change in boron concentration for that control bank movement. The results for the individual control rod banks are shown in Table 6-4.

Figure 6.2-2 shows the differential boron worth vs boron concentration. The values for the differential boron worth have been scaled up to account for the difference between the measured and the design differential boron worth.

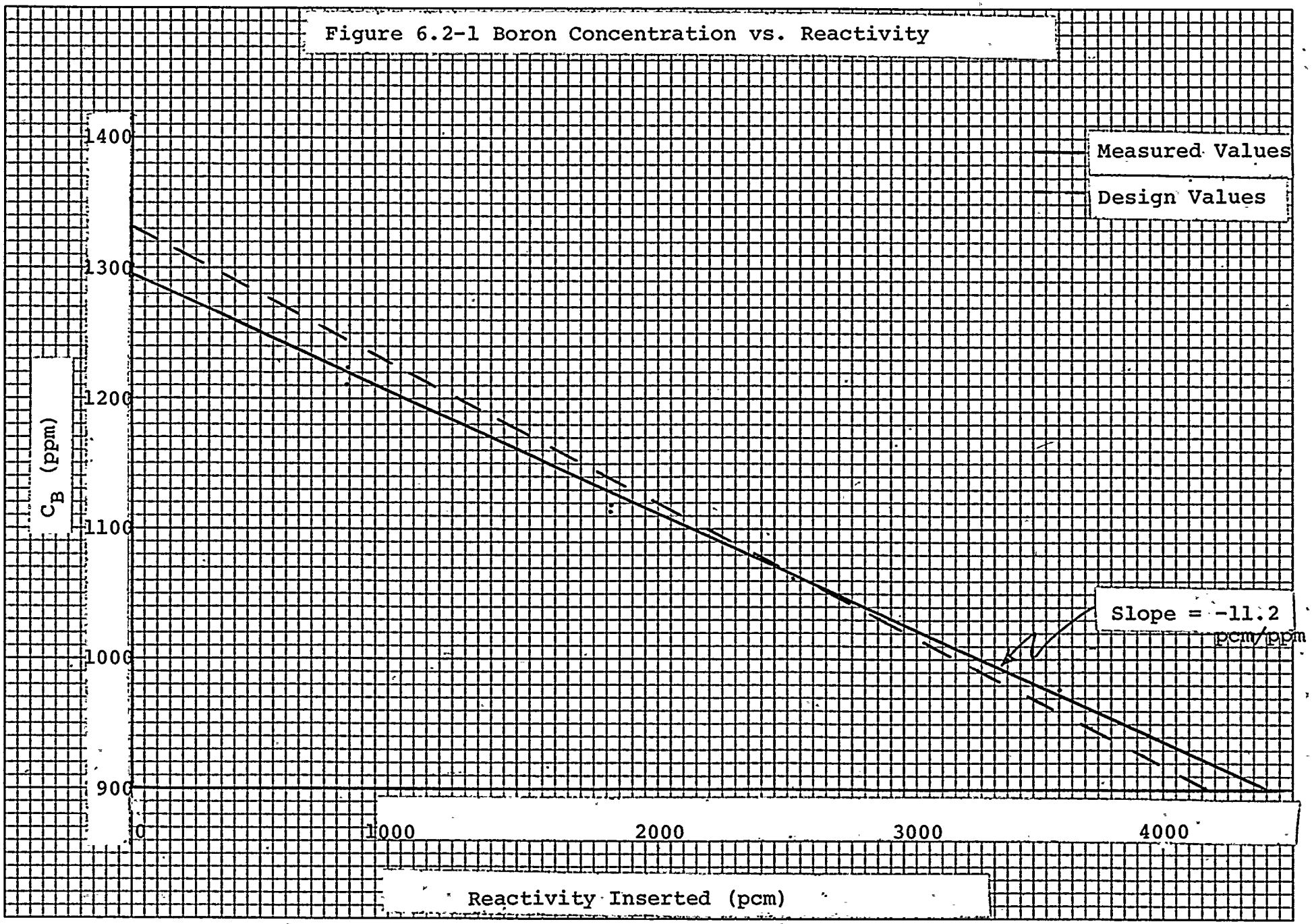
Figure 6.2-1 Boron Concentration vs. Reactivity
Measured Values
Design Values
Slope = -11.2 pcm/ppm
C_B (ppm)
1400
1300
1200
1100
1000
900
0
1000
2000
3000
4000
Reactivity Inserted (pcm)

Figure 6.2-2 Differential Born Worth vs. Boron Concentration

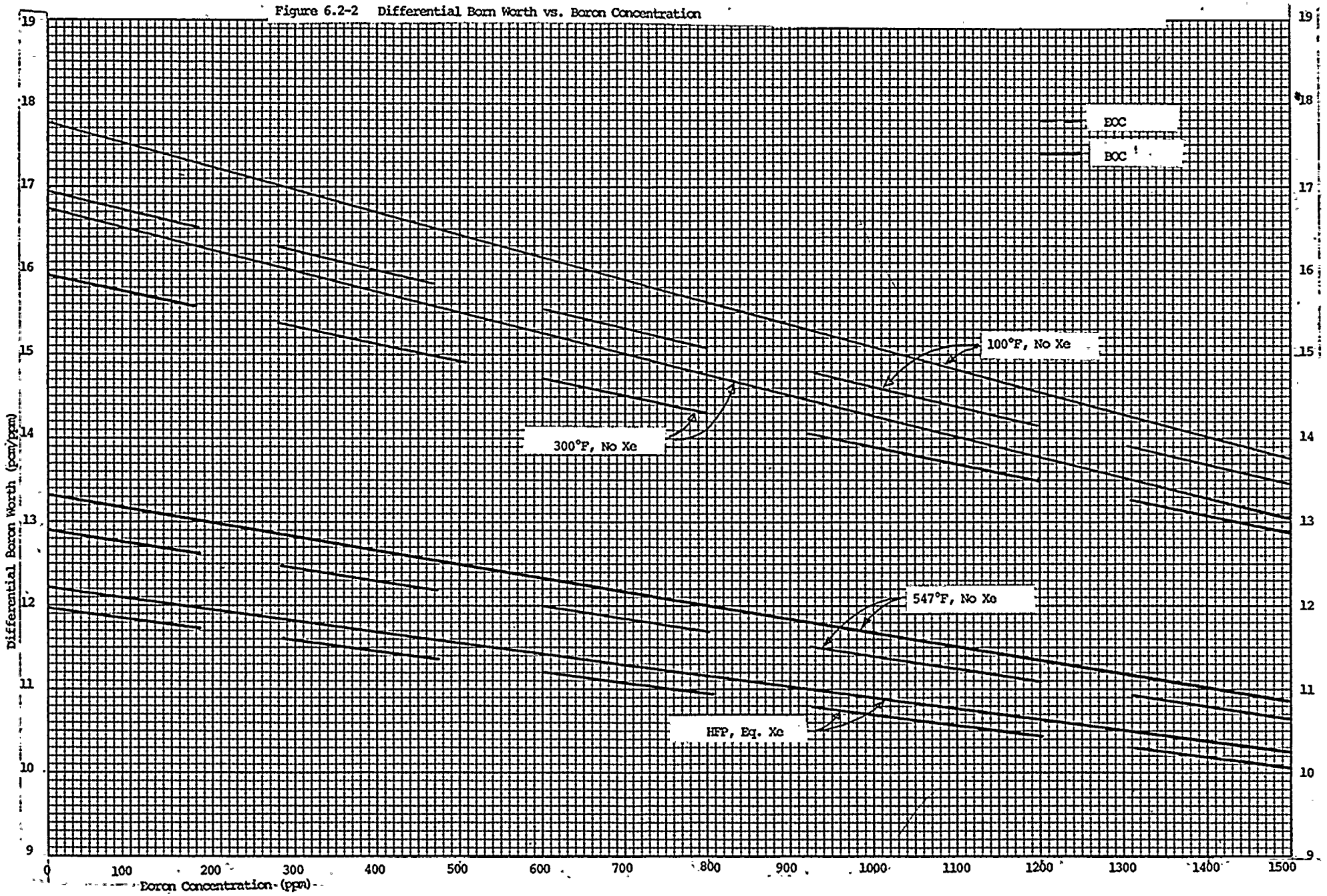

47 0782

6.3 Rod Worths

Rod worths were measured for each individual control rod bank, starting with control bank D. The worths were determined by diluting at a constant rate of about 500 pcm per hour and stepping the rod bank in to compensate for the change in reactivity. The change in reactivity was measured on the reactivity computer. A typical rod worth trace is shown in Figure 6.3-6.

After control banks D and C were measured, there was a unit trip caused by a turbine trip while warming the steam lines. Problems with a feed pump delayed a return to criticality. The feed pump was repaired in two days, the reactor was brought critical, and the rod worth tests continued.

Control banks B & A were then measured by the dilution method. It was not necessary to measure any shutdown banks because each bank agreed within $\pm$ 15% of design worth and the total control bank worth agreed within $\pm$ 10% of design prediction. Figures 6.3-1 to 6.3-4 show the integral and differential rod worth for each control rod bank.

All four control banks were then measured in the overlap mode. This was accomplished by borating at a constant rate (about -500 pcm/hr.) and stepping the control banks out to compensate for the changing reactivity. The worth of the control banks in the overlap mode differed by only 2% from the sum of the individual bank measurements. Integral and differential rod worth graphs for control banks in overlap are shown in Figure 6.3-5. A summary of all rod worth data is given in Table 6-3.

The reactivity computer was checked prior to rod worth measurements, after the reactor trip, and after the rod worth measurements. Each individual period error and average error was within the acceptance limit of $\pm$ 4%. A summary of the reactivity computer checks is given in Table 6.3-1.

Figure 6.3-1

D. C. Cook Unit I, Cycle III HZP, BOC 3

Integral & Differential Worth of CBA

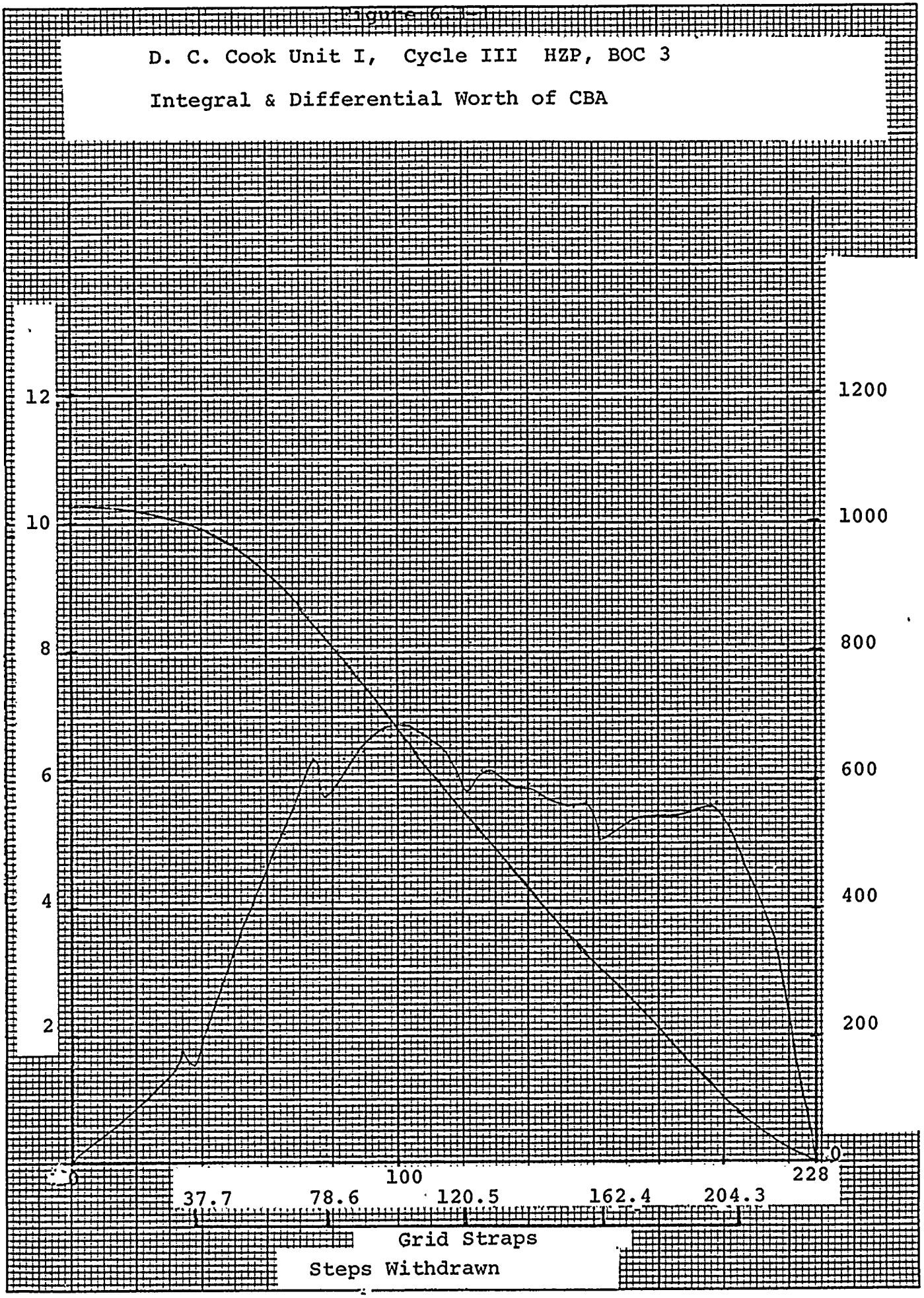

Figure 6.3-2
D. C. Cook Unit 1, Cycle III, HZP, BOC 3
Integral & Differential Worth of CBB

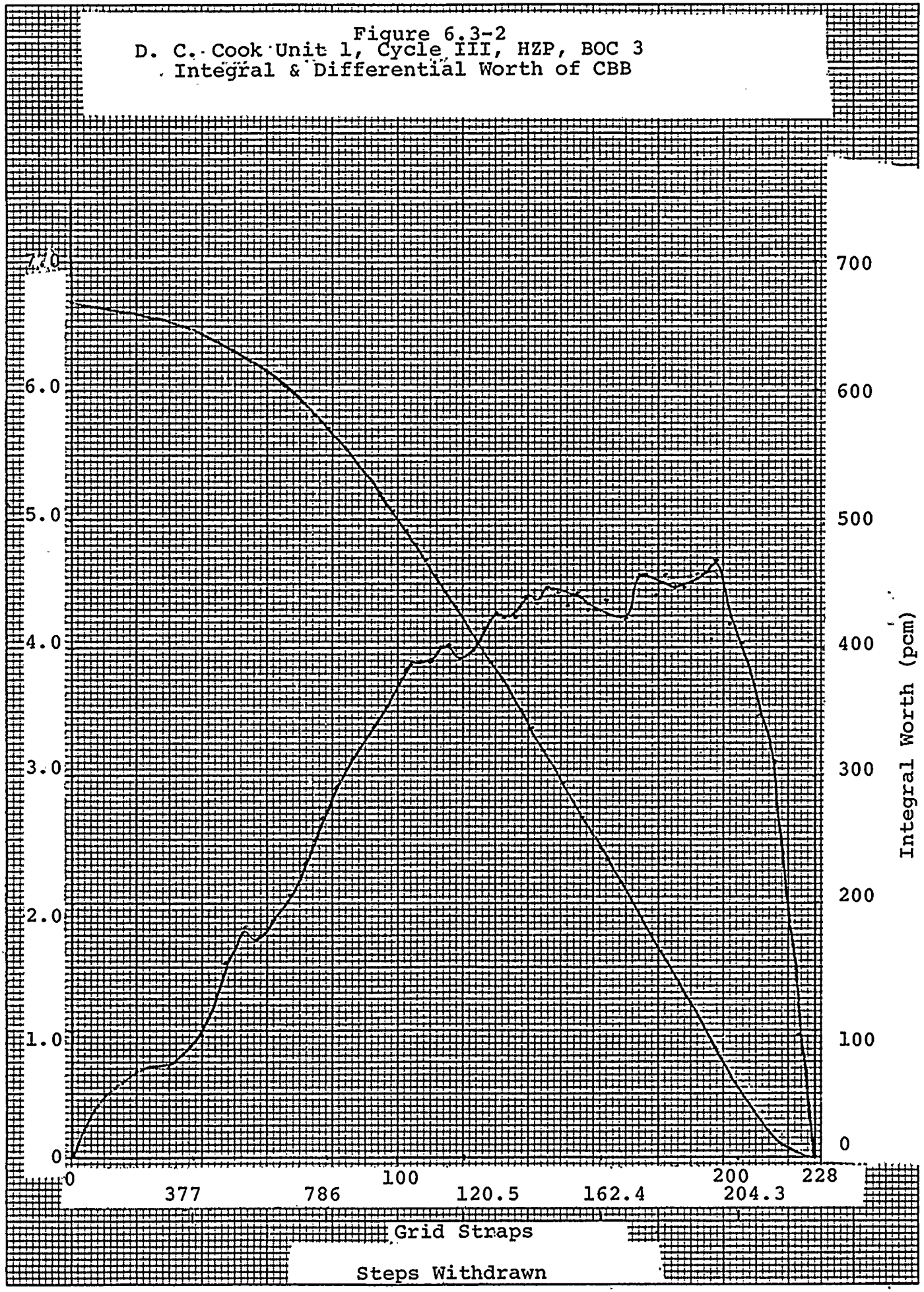

Figure 6.3-3

D. C. Cook Unit 1, Cycle III HZP, BOC 3
Integral & Differential Worth of Bank C

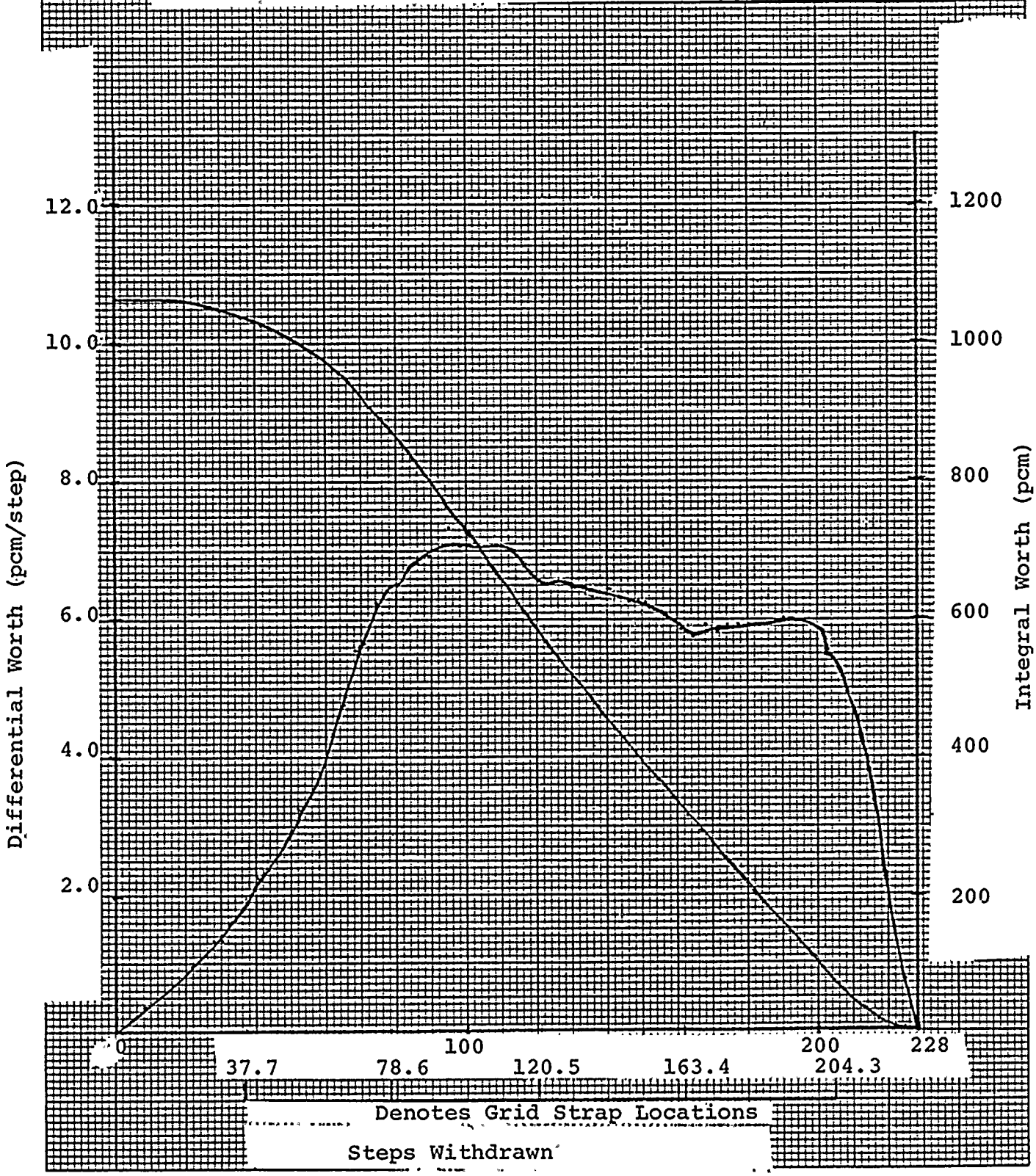

Figure 6.3-4
D. C. Cook Unit 1, Cycle III HZP, BOC 3
Integral & Differential Worth of CBD

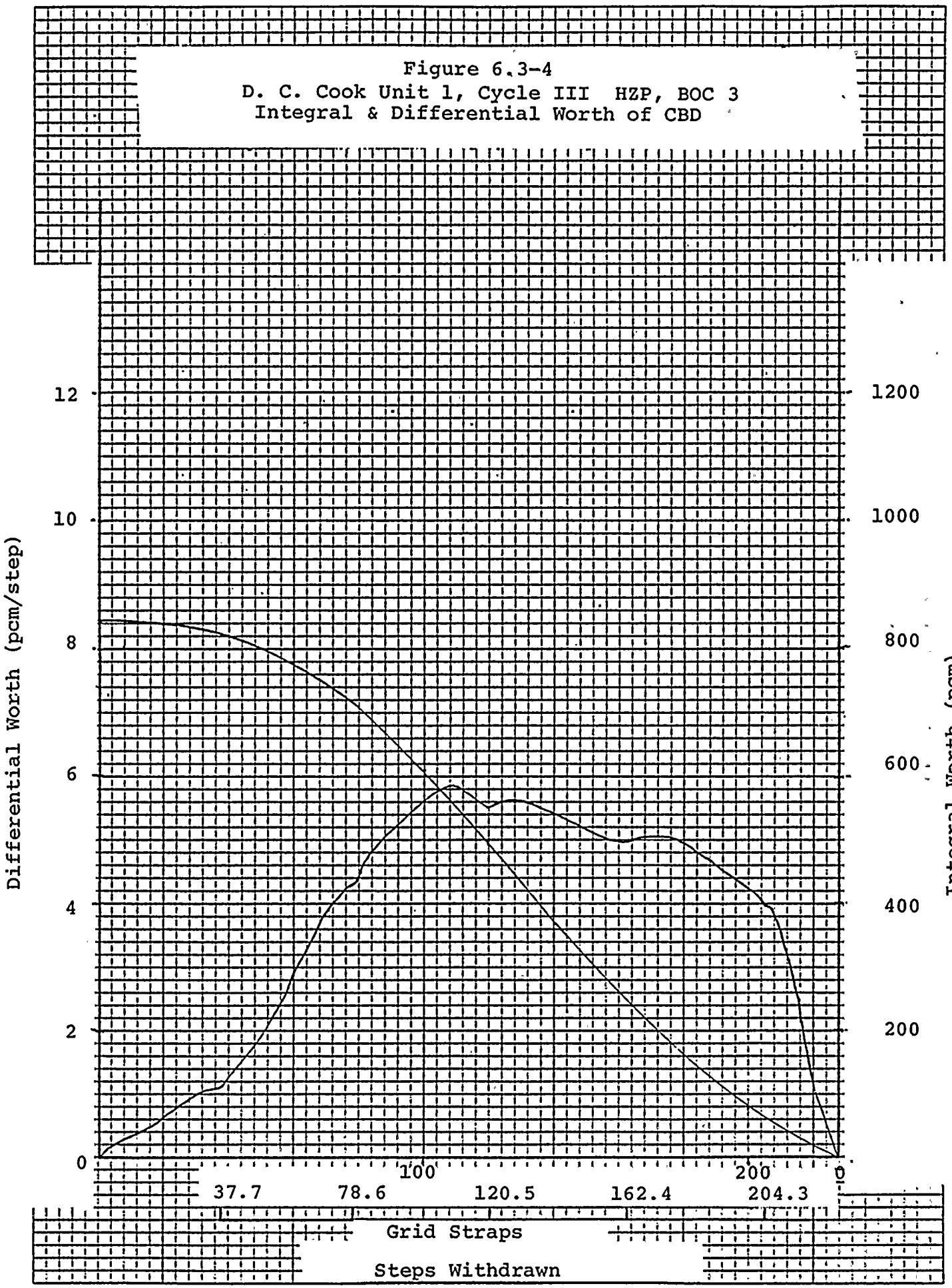

Table 6.3-1 Reactivity Computer Check

Date	Type of Test	ρ Calculated (pcm)	ρ Indicated (pcm)	Error (%)[1]	Average Error (%)	Standard Deviation
6-18-78	Reactor Transient	63.5	62.96	0.86		
6-18-78	Reactor Transient	-39.7	-40.65	-2.34		
6-18-78	Reactor Transient	43.5	43.46	0.09	-0.03	1.616
6-18-78	Reactor Transient	20.0	19.75	1.27		
6-22-78	Exponential	93.04	92.84	0.22		
6-22-78	Exponential	56.14	55.78	0.65		
6-22-78	Exponential	31.70	31.07	2.03	0.88	0.789
6-22-78	Exponential	17.05	16.94	0.65		
6-23-78	Exponential	93.38	93.15	0.25		
6-23-78	Exponential	55.58	56.22	-1.14		
6-23-78	Exponential	31.43	31.76	-1.04	0.59	0.640
6-23-78	Reactor Transient	17.72	17.80	-0.45		

[1] $\text{Error } (\%) = \dfrac{\rho \text{ Calculated} - \rho \text{ Indicated}}{\rho \text{ Indicated}} \times 100$

Figure 6.3-5 D. C. Cook Unit I, Cycle III HZP, BOC
Differential & Integral Rod Worth of A + B + C + D Banks

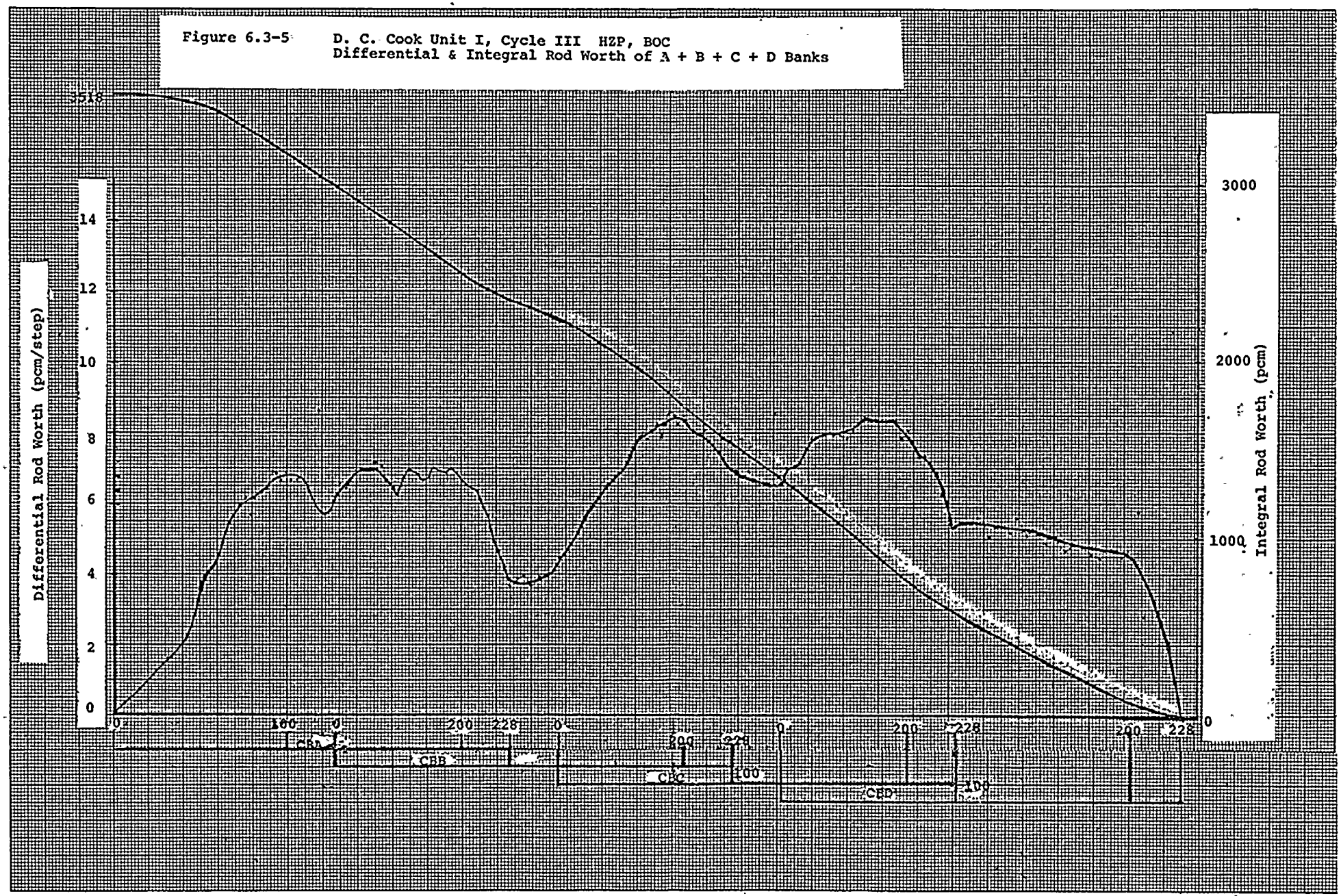

Figure 6.3-6
Typical Rod Worth Trace of CBD ρ=2 pcm/in

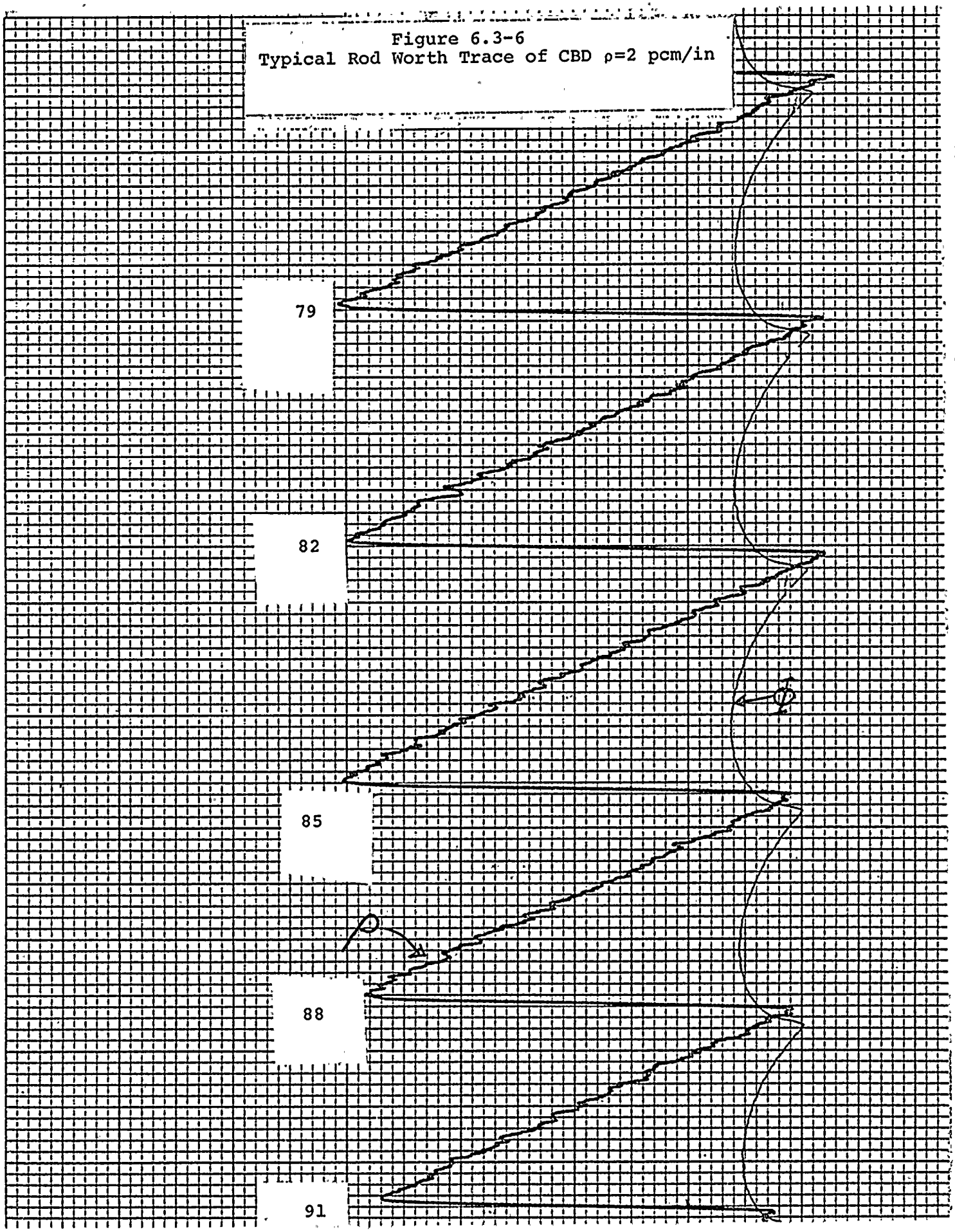

6.4 Power Distribution

During the zero power physics testing program, three full core flux maps were taken. The first was taken with all rods out, the second with control bank D inserted and the third with control banks D and C inserted. Table 6-5 shows the hot channel factors obtained from these maps as well as the design values.

To preclude raising the power level to approx. 4% for the flux maps, a special flux mapping system was developed. This system eliminated much of the noise in the system by substituting battery power supplies for the regular flux mapping AC to DC power supply. Picoammeters were used to monitor the flux levels to ensure proper scale settings for the computer input. This system allowed maps to be taken at < 3% power, which resulted in time savings. An additional benefit of this technique is the smaller Xenon corrections required for boron endpoint data. A block diagram of the system is shown in Figure 6.4-1.

Except for the battery power supplies and picoammeters, the detector output followed its normal path. The output was sampled by the plant process computer (Prodac-250) and was continuously displayed on strip chart recorders. The Prodac computer was used for data collection as well as to punch the data on to a paper tape. The paper tape was read into the AEP DETECTOR code by a remote terminal at the plant. The DETECTOR code compares the detector responses with the predicted responses and calculates peaking factors, power tilts, and core power distribution. Figures 6.4-2 through 6.4-4 show the normalized power for each assembly in the core for the three rodded configurations. Figures 6.4-6 through 6.4-8 show the relative errors between the measured $F_{\Delta H}$ values and those calculated by the fuel vendor. Figure 6.4-5 shows the normalized power for each assembly during map 103-04 and Figure 6.4-9 shows the relative errors between the measured $F_{\Delta H}$ values and the values calculated by the fuel vendor.

Map 103-4 was taken to verify the existence of $F_{\Delta H}$ margin at 50% power with CBC at about 170 steps. The map was taken with CBC at 147 steps and there was a 2.8% margin in $F_{\Delta H}$. Since the control rods were inserted 23 steps deeper than necessary, ample $F_{\Delta H}$ margin existed at 5% power with control bank D at 170 steps.

Figure 6.4-1 Low Power Flux Mapping System

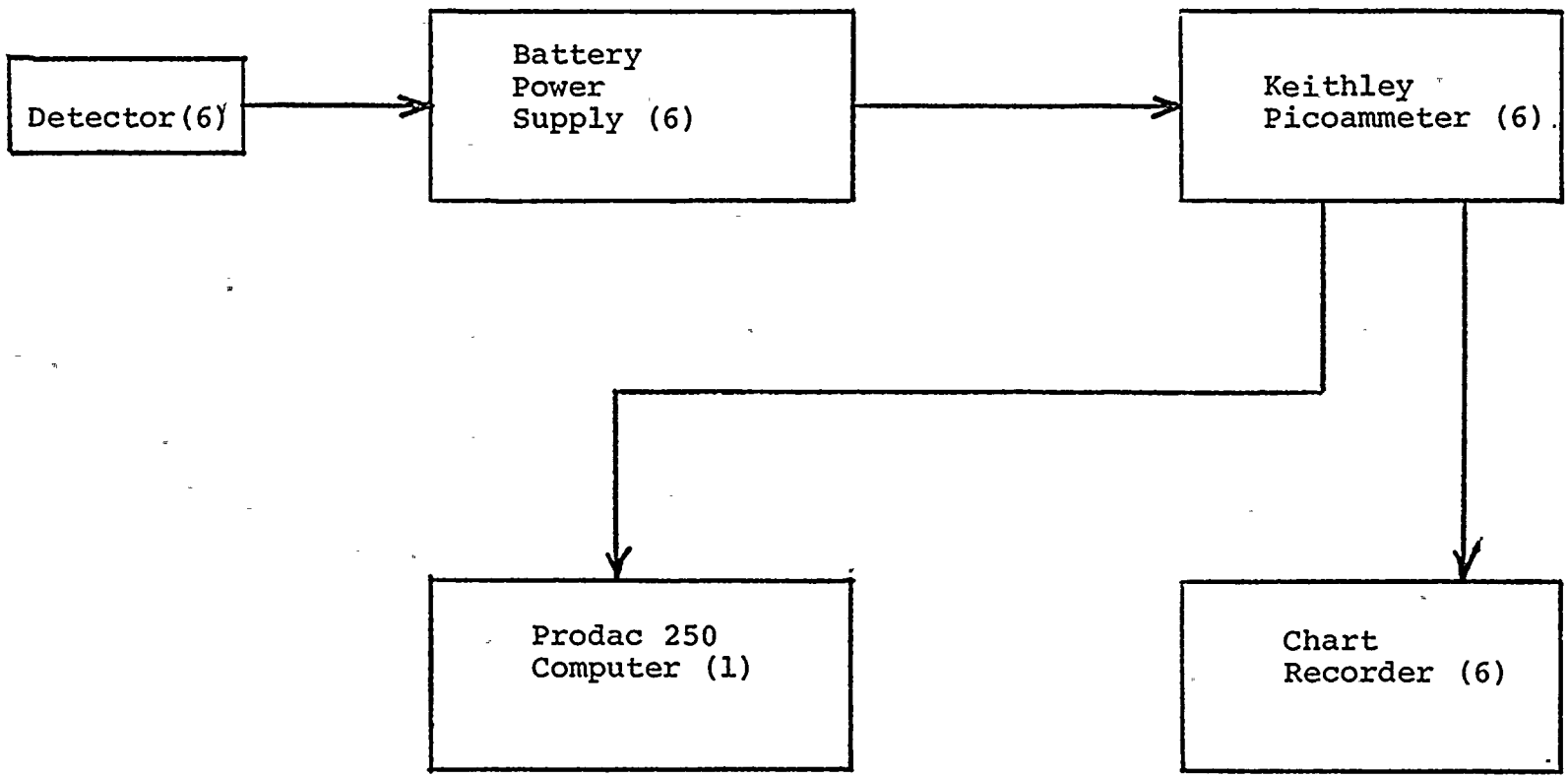

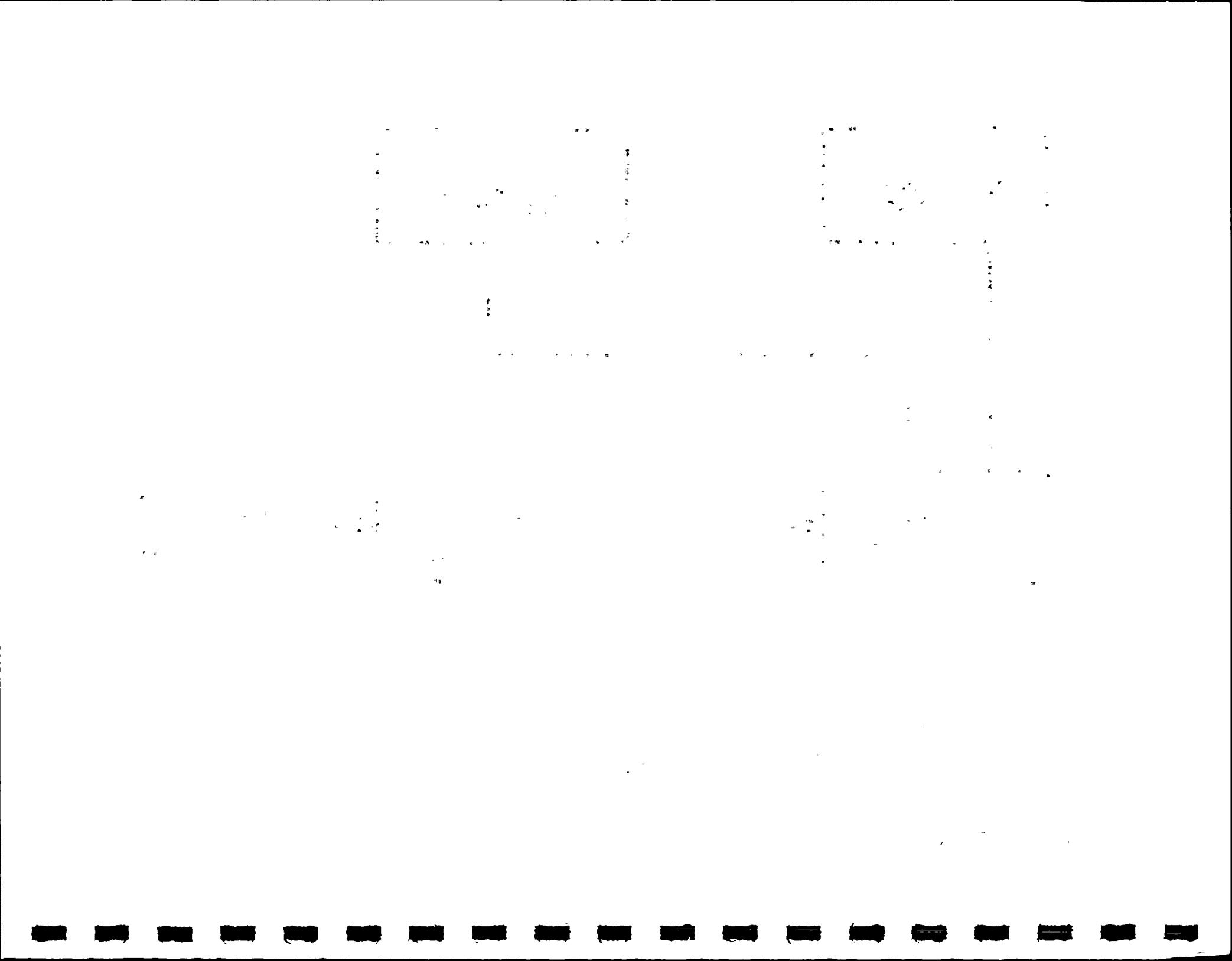

Figure 6.4-2

UNIT1 CYCLE3 HZP ARO MAP 103-01 6/19/78
AEP - THIMBLE DATA

NUCLEAR PEAKING FACTORS FOR ENTHALPY RISE FOR ASSEMBLAGES IN THE POWER NORMALIZATION

	R	P	N	M	L	K	J	H	G	F	E	D	C	B	A
1					0.620	0.813	0.927	0.872	0.881	0.792	0.605				
2			0.644	0.955	1.149	0.970	1.249	0.927	1.211	0.943	1.096	0.840	0.587		
3		0.623	1.083	1.020	1.072	1.132	0.943	0.895	0.937	1.092	1.009	0.949	1.034	0.607	
4		0.942	0.966	1.011	1.250	1.258	1.130	1.106	1.143	1.216	1.173	0.979	0.977	0.880	
5	0.616	1.119	1.011	1.215	1.095	1.254	1.224	1.021	1.219	1.101	1.005	1.162	0.987	1.059	0.571
6	0.793	0.912	1.037	1.201	1.233	1.038	1.174	1.107	1.192	0.997	1.163	1.140	1.011	0.885	0.745
7	0.909	1.215	0.901	1.105	1.191	1.149	0.917	0.890	0.969	1.164	1.154	1.035	0.842	1.119	0.819
8	0.902	0.976	0.864	1.078	1.001	1.045	0.865	0.865	0.878	1.026	0.960	1.036	0.812	0.872	0.804
9	0.915	1.271	0.932	1.126	1.223	1.183	0.968	0.896	0.949	1.134	1.163	1.067	0.855	1.127	0.842
10	0.800	0.955	1.121	1.244	1.277	1.042	1.210	1.091	1.158	0.986	1.177	1.165	1.019	0.892	0.750
11	0.612	1.137	1.050	1.220	1.048	1.235	1.225	1.016	1.203	1.193	1.034	1.172	0.977	1.079	0.580
12		0.908	1.029	1.020	1.206	1.236	1.139	1.102	1.128	1.201	1.178	0.986	0.982	0.891	
13		0.622	1.077	1.012	1.002	1.084	0.947	0.885	0.927	1.092	1.016	0.971	1.050	0.612	
14			0.644	0.922	1.127	0.958	1.271	0.964	1.216	0.932	1.104	0.875	0.598		
15					0.637	0.824	0.913	0.898	0.886	0.779	0.595				

Figure 6.4-3

UNIT1 CYCLE3 HZP D IN MAP I03-02 6/19/78
AEP - THIMBLE DATA
NUCLEAR PEAKING FACTORS FOR ENTHALPY RISE FOR ASSEMBLAGES IN THE POWER NORMALIZATION

	R	P	N	M	L	K	J	H	G	F	E	D	C	B	A
1					0.454	0.524	0.696	0.708	0.675	0.533	0.469				
2			0.686	0.938	0.929	0.473	0.968	0.801	0.947	0.473	0.904	0.834	0.625		
3		0.656	1.161	1.083	1.065	1.040	0.914	0.912	0.907	1.004	1.003	1.015	1.113	0.642	
4		0.902	1.032	1.115	1.339	1.352	1.318	1.300	1.317	1.407	1.374	1.110	1.038	0.865	
5	0.468	0.909	1.004	1.351	1.243	1.465	1.477	1.243	1.484	1.490	1.269	1.344	0.977	0.867	0.429
6	0.542	0.467	0.965	1.365	1.459	1.244	1.419	1.300	1.441	1.244	1.446	1.318	0.943	0.444	0.486
7	0.693	0.946	0.865	1.280	1.451	1.410	1.072	0.936	1.105	1.410	1.416	1.205	0.828	0.867	0.608
8	0.722	0.822	0.854	1.243	1.211	1.281	0.944	0.553	0.926	1.274	1.169	1.197	0.820	0.739	0.652
9	0.669	0.955	0.882	1.247	1.433	1.429	1.122	0.941	1.089	1.387	1.363	1.210	0.821	0.877	0.644
10	0.522	0.469	1.015	1.328	1.440	1.241	1.451	1.294	1.412	1.203	1.410	1.322	0.929	0.448	0.492
11	0.469	0.962	1.055	1.327	1.232	1.458	1.467	1.217	1.475	1.451	1.214	1.292	0.935	0.888	0.432
12		0.925	1.107	1.136	1.335	1.347	1.255	1.258	1.315	1.367	1.278	1.034	0.995	0.879	
13		0.664	1.172	1.069	0.980	0.984	0.895	0.858	0.870	0.983	0.964	0.999	1.107	0.645	
14			0.671	0.905	0.915	0.469	0.975	0.805	0.867	0.451	0.885	0.865	0.636		
15					0.477	0.532	0.672	0.716	0.672	0.492	0.433				

Figure 6.4-4

103003 UNIT 1 CYCLE 3 HZP CONTOOL BANKS C AND D IN JUNE 20 U.M.
AEP - THIMBLE DATA
NUCLEAR PEAKING FACTORS FOR ENTHALPY RISE FOR ASSEMBLAGES IN THE POWER NORMALIZATION

	R	P	N	M	L	K	J	H	G	F	E	D	C	B	A
1					0.498	0.650	0.923	0.969	0.933	0.688	0.534				
2			0.396	0.800	0.954	0.562	1.256	1.076	1.253	0.575	0.948	0.683	0.357		
3		0.374	0.448	0.902	1.098	1.181	1.099	1.112	1.093	1.153	1.047	0.815	0.428	0.376	
4		0.756	0.854	1.099	1.465	1.521	1.433	1.397	1.440	1.532	1.438	1.050	0.834	0.727	
5	0.525	0.965	1.077	1.484	1.362	1.557	1.434	1.088	1.413	1.512	1.304	1.400	0.990	0.881	0.470
6	0.683	0.568	1.142	1.525	1.540	1.199	1.131	0.598	1.122	1.175	1.495	1.426	1.061	0.525	0.604
7	0.941	1.260	1.064	1.398	1.379	1.118	0.781	0.595	0.774	1.116	1.379	1.310	0.977	1.134	0.833
8	1.000	1.113	1.082	1.357	1.042	0.584	0.598	0.369	0.568	0.568	1.029	1.303	0.994	1.017	0.921
9	0.917	1.271	1.093	1.410	1.398	1.122	0.792	0.585	0.753	1.078	1.342	1.336	0.994	1.169	0.885
10	0.678	0.576	1.186	1.546	1.582	1.207	1.137	0.582	1.089	1.143	1.473	1.445	1.057	0.548	0.631
11	0.539	1.033	1.071	1.492	1.380	1.576	1.422	1.060	1.397	1.497	1.306	1.392	0.980	0.942	0.492
12		0.758	0.865	1.102	1.478	1.535	1.375	1.358	1.427	1.506	1.389	1.015	0.809	0.718	
13		0.364	0.426	0.861	1.046	1.138	1.061	1.035	1.042	1.125	1.034	0.824	0.417	0.354	
14			0.381	0.749	0.969	0.562	1.243	1.050	1.127	0.559	0.950	0.729	0.359		
15					0.537	0.673	0.889	0.962	0.889	0.640	0.496				

Figure 6.4-5

103004 UNIT 1 CYCLE 3 HZP CONTOOL BANKS C AND D IN JUNE 20 1978 3% POWER
AEP - THIMBLE DATA

NUCLEAR PEAKING FACTORS FOR ENTHALPY RISE FOR ASSEMBLAGES IN THE POWER NORMALIZATION

	R	P	N	M	L	K	J	H	G	F	E	D	C	B	A
1					0.470	0.577	0.786	0.782	0.778	0.625	0.529				
2			0.618	0.910	0.941	0.517	1.053	0.851	1.038	0.537	0.956	0.824	0.575		
3		0.610	1.013	1.051	1.067	1.072	0.929	0.915	0.925	1.031	1.023	0.994	0.971	0.591	
4		0.923	1.010	1.135	1.409	1.319	1.242	1.221	1.308	1.407	1.355	1.097	0.995	0.843	
5	0.511	0.977	1.062	1.435	1.278	1.481	1.388	1.149	1.481	1.464	1.212	1.325	0.976	0.886	0.454
6	0.609	0.535	1.057	1.404	1.451	1.216	1.302	1.052	1.324	1.204	1.413	1.326	0.981	0.489	0.535
7	0.769	1.057	0.925	1.246	1.372	1.288	0.985	0.811	0.974	1.310	1.351	1.213	0.865	0.960	0.692
8	0.779	0.907	0.930	1.239	1.114	1.032	0.775	0.496	0.787	0.987	1.095	1.199	0.853	0.847	0.766
9	0.741	1.073	0.959	1.278	1.392	1.288	0.970	0.804	0.949	1.247	1.373	1.228	0.865	1.004	0.762
10	0.587	0.530	1.090	1.401	1.477	1.220	1.322	1.065	1.262	1.162	1.407	1.322	0.951	0.524	0.570
11	0.505	1.013	0.988	1.399	1.304	1.494	1.399	1.128	1.417	1.435	1.211	1.312	0.957	0.959	0.478
12		0.869	0.977	1.136	1.437	1.461	1.269	1.268	1.333	1.387	1.313	1.061	0.978	0.870	
13		0.575	0.928	1.026	1.071	1.078	0.951	0.921	0.925	1.024	1.025	0.997	0.974	0.590	
14			0.628	0.890	0.985	0.528	1.061	0.885	0.967	0.527	0.958	0.875	0.593		
15					0.512	0.591	0.741	0.790	0.741	0.569	0.479				

[redacted]

Figure 6.4-6

UNIT1 CYCLE3 HZP ARO MAP I03-01 6/19/78

AEP - THIMBLE DATA

RELATIVE ERRORS IN F SUB DELTA H CALCULATED FROM WEIGHTED THEORETICAL FACTORS. (CALC.-MEAS.)/MEAS.

	R	P	N	M	L	K	J	H	G	F	E	D	C	B	A
1						-0.034	-0.033	-0.040	0.000	0.009	-0.007	-0.011			
2					-0.087	-0.085	-0.037	-0.023	-0.011	0.045	0.021	0.005	0.010	0.040	0.001
3				-0.058	-0.045	-0.035	-0.046	-0.042	0.002	0.025	0.009	-0.007	0.014	0.037	0.000	-0.033	
4				-0.078	0.023	0.003	-0.033	-0.033	0.006	0.006	-0.006	0.001	0.030	0.036	0.011	-0.012	
5			-0.046	-0.026	0.000	-0.009	-0.036	-0.035	-0.019	-0.013	-0.015	0.016	0.050	0.036	0.025	0.029	0.029
6			-0.030	0.009	0.022	-0.001	-0.028	-0.034	-0.003	-0.026	-0.018	0.006	0.031	0.052	0.047	0.040	0.033
7			-0.042	-0.005	0.022	0.004	-0.012	0.010	0.061	0.026	0.004	-0.003	0.019	0.071	0.094	0.080	0.063
8			-0.053	-0.024	0.035	0.006	-0.015	0.020	0.047	0.068	0.031	0.039	0.026	0.047	0.101	0.093	0.062
9			-0.049	-0.049	-0.012	-0.015	-0.039	-0.019	0.005	0.020	0.025	0.024	0.012	0.039	0.077	0.073	0.033
10			-0.038	-0.035	-0.055	-0.036	-0.061	-0.037	-0.033	-0.012	0.011	0.017	0.019	0.030	0.039	0.032	0.027
11			-0.039	-0.042	-0.037	-0.013	0.007	-0.020	-0.020	-0.009	-0.003	0.015	0.021	0.027	0.035	0.010	0.013
12				-0.043	-0.039	-0.006	0.003	-0.015	-0.003	0.009	0.008	0.013	0.026	0.029	0.006	-0.025	
13				-0.056	-0.040	-0.028	0.021	0.000	-0.002	0.035	0.020	0.002	0.007	0.013	-0.016	-0.041	
14					-0.088	-0.053	-0.018	-0.010	-0.028	0.005	0.017	0.016	0.002	-0.002	-0.017		
15							-0.060	-0.045	-0.026	-0.029	0.004	0.009	0.006				

THE MEAN VALUE = 0.0000 AND THE STANDARD DEVIATION = 0.0349 FOR THE ABOVE 193 VALUES

THE MEAN OF THE ABSOLUTE VALUES = 0.0275 . THE MAXIMUM MAGNITUDE = 0.1007 AT R -C

Figure 6.4-7

UNIT1 CYCLE3 H7P.D IN MAP I03-02 6/19/78
AEP - THIMBLE DATA

RELATIVE ERRORS IN F SUB DELTA H-CALCULATED FROM WEIGHTED THEORETICAL FACTORS. (CALC.-MEAS.)/MEAS.

	R	P	N	M	L	K	J	H	G	F	E	D	C	B	A
1						-0.058	-0.072	-0.089	-0.046	-0.060	-0.087	-0.089			
2					-0.093	-0.093	-0.060	-0.051	-0.050	0.002	-0.029	-0.051	-0.034	0.021	-0.005
3				-0.050	-0.045	-0.044	-0.062	-0.062	-0.025	-0.006	-0.017	-0.028	-0.005	0.020	-0.004	-0.030
4				-0.056	0.011	0.013	0.019	0.019	-0.012	-0.012	-0.012	-0.021	-0.007	0.018	0.005	-0.015
5			-0.095	-0.045	-0.011	0.009	0.019	0.015	0.003	-0.001	-0.002	-0.002	-0.002	0.015	0.017	0.002	-0.014
6			-0.113	-0.056	-0.007	-0.002	0.011	0.013	0.024	0.013	0.008	0.013	0.020	0.034	0.017	-0.006	-0.012
7		-0.097	-0.043	0.009	-0.005	0.002	0.023	0.051	0.028	0.020	0.023	0.027	0.057	0.054	0.044	0.029	
8		-0.079	-0.034	0.038	0.011	0.005	0.017	0.008	0.033	0.029	0.023	0.041	0.050	0.080	0.074	0.020	
9		-0.065	-0.053	-0.011	0.021	0.014	0.010	0.005	0.021	0.035	0.040	0.067	0.053	0.063	0.033	-0.028	
10		-0.080	-0.060	-0.055	0.026	0.024	0.016	0.001	0.018	0.029	0.047	0.046	0.030	0.033	-0.017	-0.022	
11		-0.097	-0.098	-0.058	0.027	0.028	0.020	0.010	0.021	0.005	0.025	0.044	0.055	0.062	-0.023	-0.021	
12			-0.079	-0.057	-0.006	0.022	0.022	0.038	0.021	-0.010	0.008	0.068	0.093	0.048	-0.031		
13			-0.062	-0.055	-0.032	0.018	-0.009	-0.005	0.057	0.024	-0.008	0.036	0.036	0.001	-0.034		
14				-0.073	-0.060	-0.046	-0.042	-0.057	-0.003	0.060	-0.005	-0.014	-0.016	-0.022			
15						-0.104	-0.086	-0.056	-0.057	-0.056	-0.010	-0.012					

THE MEAN VALUE = -0.0065 AND THE STANDARD DEVIATION = 0.0424 FOR THE ABOVE 193 VALUES

THE MEAN OF THE ABSOLUTE VALUES = 0.0339 . THE MAXIMUM MAGNITUDE = 0.1134 AT 6 -P

Figure 6.4-8

103003 UNIT 1 CYCLE 3 HZP CONTOOL BANKS C AND D IN JUNE 20 U.M,
AEP - THIMBLE DATA
RELATIVE ERRORS IN F SUB DELTA H CALCULATED FROM WEIGHTED THEORETICAL FACTORS. (CALC.-MEAS.)/MEAS.

	R	P	N	M	L	K	J	H	G	F	E	D	C	B	A
1						-0.036	-0.047	-0.060	-0.031	-0.070	-0.100	-0.100			
2					-0.111	-0.115	-0.036	-0.034	-0.033	-0.001	-0.031	-0.057	-0.029	0.036	-0.015
3				-0.060	-0.052	-0.063	-0.037	-0.037	-0.011	0.002	-0.006	-0.014	0.010	0.036	-0.007	-0.065	
4				-0.067	-0.005	0.001	0.015	0.015	0.006	0.006	0.001	0.008	0.034	0.047	0.019	-0.030	
5			-0.094	-0.055	-0.026	-0.001	0.015	0.002	-0.010	-0.004	0.005	0.032	0.060	0.059	0.059	0.035	0.011
6			-0.107	-0.064	-0.024	-0.001	0.005	-0.010	-0.016	-0.014	-0.008	0.010	0.035	0.069	0.051	0.013	-0.011
7			-0.091	-0.051	-0.000	0.016	0.010	-0.013	-0.015	-0.020	-0.006	-0.011	0.010	0.076	0.089	0.054	0.028
8			-0.074	-0.043	0.008	0.012	0.015	-0.006	-0.036	-0.012	0.015	0.021	0.028	0.055	0.097	0.046	-0.005
9			-0.067	-0.059	-0.027	-0.001	-0.004	-0.016	-0.029	-0.002	0.022	0.024	0.037	0.055	0.070	0.022	-0.033
10			-0.099	-0.077	-0.059	-0.014	-0.022	-0.017	-0.021	0.012	0.022	0.038	0.050	0.055	0.056	-0.030	-0.033
11			-0.118	-0.118	-0.021	-0.006	0.002	-0.010	-0.001	0.023	0.017	0.042	0.059	0.065	0.069	-0.033	-0.033
12				-0.070	-0.018	-0.002	0.006	0.006	0.049	0.035	0.010	0.026	0.070	0.083	0.051	-0.018	
13				-0.035	-0.004	-0.019	0.011	-0.001	0.024	0.077	0.042	0.010	0.022	0.024	0.019	-0.006	
14					-0.075	-0.056	-0.050	-0.034	-0.023	0.024	0.077	-0.029	-0.031	-0.030	-0.019		
15						-0.106	-0.080	-0.024	-0.024	-0.024	-0.031	-0.031					

THE MEAN VALUE = -0.0065 . AND THE STANDARD DEVIATION = 0.0443 FOR THE ABOVE 193 VALUES

THE MEAN OF THE ABSOLUTE VALUES = 0.0345 . THE MAXIMUM MAGNITUDE = 0.1178 AT 11-R

Figure 6.4-9

103004 UNIT 1 CYCLE 3 HZP CONTOOL BANKS C AND D IN JUNE 20, 1978 3% POWER
AEP - THIMBLE DATA
RELATIVE ERRORS IN F SUB DELTA H CALCULATED FROM WEIGHTED THEORETICAL FACTORS. (CALC.-MEAS.)/MEAS.

	R	P	N	M	L	K	J	H	G	F	E	D	C	B	A
1					-0.065	-0.106	-0.135	-0.073	-0.126	-0.175	-0.168				
2				-0.072	-0.092	-0.058	-0.082	-0.072	0.002	-0.059	-0.117	-0.073	0.003	-0.001	
3			-0.058	-0.026	-0.048	-0.054	-0.062	-0.003	0.031	0.001	-0.024	-0.014	0.007	0.015	-0.027
4				-0.104	-0.002	-0.011	-0.018	0.064	0.066	0.067	0.012	-0.002	0.021	0.024	0.013	-0.020	
5		-0.148	-0.100	-0.056	-0.037	0.004	0.010	0.056	0.053	-0.010	0.021	0.059	0.043	0.028	-0.007	-0.040	
6		-0.166	-0.130	-0.065	-0.012	0.022	0.022	0.067	0.126	0.048	0.032	0.049	0.047	0.008	-0.049	-0.049	
7		-0.128	-0.090	-0.019	0.040	0.048	0.070	0.078	0.102	0.090	0.052	0.064	0.068	0.049	0.002	-0.031	
8		-0.083	-0.069	-0.008	0.029	0.063	0.135	0.142	0.090	0.125	0.186	0.082	0.063	0.081	-0.003	-0.067	
9		-0.095	-0.104	-0.054	0.013	0.033	0.070	0.094	0.112	0.118	0.105	0.048	0.055	0.049	-0.042	-0.120	
10		-0.134	-0.123	-0.093	-0.009	0.004	0.019	0.050	0.111	0.100	0.069	0.054	0.050	0.039	-0.112	-0.108	
11		-0.137	-0.132	0.016	-0.012	-0.015	0.001	0.048	0.073	0.035	0.042	0.060	0.053	0.049	-0.083	-0.088	
12			-0.049	0.032	-0.012	-0.037	-0.039	0.043	0.027	-0.007	0.012	0.053	0.058	0.031	-0.050		
13			-0.000	0.062	-0.025	-0.058	-0.068	-0.026	0.025	0.001	-0.018	-0.015	0.004	0.012	-0.025		
14				-0.086	-0.071	-0.101	-0.101	-0.079	-0.036	0.010	-0.100	-0.075	-0.056	-0.032			
15						-0.141	-0.128	-0.082	-0.082	-0.082	-0.094	-0.082					

THE MEAN VALUE = -0.0104 AND THE STANDARD DEVIATION = 0.0710 FOR THE ABOVE 193 VALUES

THE MEAN OF THE ABSOLUTE VALUES = 0.0593 . THE MAXIMUM MAGNITUDE = 0.1861 AT H -F

6.5 Shutdown Margin Verification

After the control rod banks were measured individually, the shutdown margin was verified. The results of the verification are shown in Table 6.5-1. As can be seen from the table, there was ample (1810 pcm) excess shutdown margin.

ravishingly,
the
seen from
down

Table 6.5-1

Shutdown Margin Verification

(1)	The measured rod worth of measured banks (pcm)	3600
(2)	The predicted rod worth of measured banks (pcm)	3579
(3)	R; the ratio of the measured to the predicted rod worth [=(1)/(2)]	1.006
(4)	The predicted worth of remaining banks (unmeasured) (pcm)	3570
(5)	The adjusted worth of remaining banks (unmeasured) = R*(4) (pcm)	3591
(6)	Total adjusted rod worth =[(1) + (5)] (pcm)	7191
(7)	F14 (the most reactive rod) worth (pcm)	701
(8)	Total control bank requirement (pcm) (2)	2930
(9)	All rods inserted less most reactive stuck rod (pcm) [(6)-(7)]	6490
(10)	Calculated shutdown margin [(9)-(8)](pcm)	3560
(11)	Required shutdown margin (pcm)	1750
(12)	Excess shutdown margin (pcm)	1810

SECTION 7.0

POWER ASCENSION TESTING

SECTION 7.1

PLANT CHEMISTRY HISTORY DURING POWER ASCENSION

PURPOSE

The chemical monitoring program for Reactor Coolant System, Steam Generators and auxiliary systems was developed to:

1. Establish base activity levels for Cycle III to aid in determination of future corrosion problems or fuel defects,
2. Determine that there are no defective or excessively contaminated fuel elements,
3. Insure that no new or unusual corrosion mechanisms had taken place during refueling,
4. Determine that there is negligible primary to secondary leakage,
5. Insure all chemical specifications were maintained.

To accomplish these ends, primary and secondary sampling schedules were implemented to monitor fission and corrosion product activities, contaminants and control chemicals. Complete primary and secondary analyses were performed at a maximum 8 hour time interval with increased frequencies during power transients, reactor trips or other unusual circumstances.

SUMMARY OF RESULTS

The unit was shut down for refueling with a 100% generator trip. The iodine spike following this transient was a maximum of 2.026μCi/gm dose equivalent iodine 131. Prior to refueling the coolant system was treated with hydrogen peroxide to solubilize Co^{58}. Maximum CVCS purification then reduced the coolant gross β-γ activity to 0.05 μCi/cc with Co^{58} at 0.078 μCi/cc prior to refueling. Gross activity in the coolant has stabilized with constant power operation at 0.60 μCi/cc, slightly lower than before the shut down. Isotopic analysis, since refueling, has indicated a reduction in activity of all isotopes detected as indicated in Table 7.1-2. Iodine -131 average activity was reduced from 1.22×10^{-2} μCi/cc prior to refueling to 1.36×10^{-3} μCi/cc. During startup the CVCS mixed bed demineralizer was inadvertently put in service with high reactor coolant ammonia concentrations and the resin was exhausted. The demineralizer released chlorides which contaminated the coolant to a maximum of 1.0 PPM chlorides. Chlorides were reduced to less than 0.15 PPM in 26 hours by dilution of the coolant system and diverting letdown to waste. Lithium in the reactor coolant

was increasing rapidly (figure 7.1-6) and the CVCS cation bed was found to be in service. This bed also exhausted because of contact with the reactor coolant containing ammonia. Lithium was out of specification at 2.4 PPM. A reactor trip on the same day and it's associated dilution reduced the coolant lithium concentration to 1.8 PPM during startup. Both the CVCS mixed bed and cation resin have been replaced and no further problems have been encountered. Once at constant power operation the coolant system chemistry has been stable and in specification during Cycle III operation.

DISCUSSION OF TEST

PRIMARY SYSTEM

All samples were collected from either or both hot leg sample points each eight hours throughout initial operation. Additional samples were also collected following each reactor trip, power transient or any time a coolant chemistry parameter is exceeded or approached.

Dose equivalent iodine -131 spiked following the 100% trip and a maximum concentration of 2.026 μCi/gm was recorded. Prior to refueling the coolant system was treated with hydrogen peroxide to solubilize the Co^{58} at 1.37 x 10^{-3}μCi/cc. Five gallons of 30% hydrogen peroxide were added and Co^{58} activity peaked at 6.68 x 10^{-1}μCi/cc. Throughout this operation the CVCS cation and mixed bed demineralizers were in service at maximum purification flow >120 GPM letdown; whenever possible. The coolant system activities were reduced to 0.05 μCi/cc gross beta-gamma and 0.078 μCi/cc Co^{58} in 48 hours. Refueling operations were then started and no chemistry problems were encountered.

During the startup, hydrazine was added to the coolant to scavenge oxygen prior to heatup. The CVCS letdown flow during this operation is diverted around the demineralizers. The coolant was then monitored for ammonia to determine when the demineralizers could be put back in service. Due to a procedural deficiency, an erroneous ammonia concentration of less than 0.05 PPM was obtained. Based on this analysis the CVCS mixed bed was placed in service. Followup analysis five hours later showed the coolant ammonia concentration to be 12 PPM. At this time the CVCS mixed bed was removed from service. Analysis of the coolant indicated chloride concentrations had jumped to 1.0 PPM. In an effort to reduce the chloride concentration the coolant system was diluted by using the RWST as a charging source and diverting all letdown to the CVCS Holdup Tanks. Following this action the chloride concentration was reduced to 0.15 PPM, see Figure 7.1-8. Faced with the inability to further reduce the chloride concentration quickly the coolant system was degassed and drained to ½ loop. The coolant system was refilled and the chloride concentration was found to be less than detectable (0.05 PPM) and has remained in specification since.

The CVCS cation demineralizer was requested to be put in service on 7-13-78 to reduce the increasing lithium concentration, It was found to be still in service. Analysis indicated 1.8 PPM entering the cation demineralizer and 2.5 PPM exiting. The cation resin had apparently also exhausted because of contact with reactor coolant with high ammonia concentrations. Lithium continued to increase and peaked at 2.4 PPM on 7-14-78. A reactor trip that day and it's associated boration/dilution cycle lowered the coolant lithium concentration to 1.8 PPM. The cation resin was replaced and has been used to reduce lithium concentrations as necessary in the coolant with no further problems.

Since the startup iodine concentrations in the coolant have been monitored carefully. Iodine -131 activity in the coolant rose initially (Figure 7.1-2) until CVCS purification was re-established. Since that time, with the exception of an iodine -131 spike of 3.89×10^{-2} µCi/cc following a 100% trip on 7-14-78, the iodine activity has steadily decreased to it's present average value of 1.3×10^{-3}µCi/cc. The detected iodine activities are lower than noted in Cycle II (Table 7.1-2) at a comparable core life. The iodine 131/133 ratio is also lower than determined in Cycle II. Gross beta-gamma activity also showed an initial increase (Figure 7.1-1) caused by lack of CVCS purification and has, since power operation, stabilized at approximately 0.60 µCi/cc. Table 7.1-2 shows a comparison between predicted values, equilibrium values for Cycle II at 98% power and equilibrium values for Cycle III at 100% power.

SECONDARY SYSTEM

Samples for all data were obtained from the individual steam generator sample line. Samples were taken on at least an 8 hr. frequency with increased sampling during periods of power increase or system cycle contamination.

During startup the steam generators showed a rapid cleanup in sodium contamination (Figure 7.1-7). Steam generator cation conductivities were also reduced quickly initially but have yet to remain below 2 µmho during power operation. Several small condenser leaks have been identified and plugged during operation. Problems with blowdown system valves has limited blowdown of the steam generators on occasions. Throughout these minor, expected problems secondary chemistry has been monitored carefully and no problems were detected.

Throughout the Cycle III operation the specifications listed in Table 7.1-4 were maintained with the exception of steam generator cation conductivity. This is to be expected during a startup following a long outage. Chemistry control has been maintained during power operation by chemical feed and steam generator blowdown. No secondary system chemistry problems are present, and no primary-to-secondary leaks are suspected.

TABLE 7.1-1

REACTOR COOLANT WATER QUALITY

	SPECIFICATION	POWER OPERATION AVERAGE VALUE
pH at 25°C	4.2 - 10.5	6.4
Oxygen (PPM)	0.10 MAX	0.010
Chloride (PPM)	0.15 MAX	<0.05
Flouride (PPM)	0.15 MAX	<0.05
Hydrogen cc(STP)/Kg H_2O	25 - 50	35
Suspended Solids (PPM)	1.0	0.5
Li^7 (PPM)	0.70 - 2.20	1.50

TABLE 7.1-2

ACTUAL VS. PREDICTED ISOTOPES IN COOLANT (μCi/cc)

ISOTOPE	EQUILIBRIUM VALUES 1% FUEL DEFECT FSAR	ACTUAL LEVELS CYCLE II 98% Power*	ACTUAL LEVELS CYCLE III - 100% Power*
I-131	1.78	2.5×10^{-2}	1.38×10^{-3}
I-133	2.75	4.4×10^{-2}	8.59×10^{-3}
I-134	0.385	1.9×10^{-2}	1.52×10^{-2}
I-135	1.39	2.5×10^{-2}	1.25×10^{-2}
Cs-138	0.639	5.9×10^{-2}	1.91×10^{-2}
Kr-85M	1.62	1.2×10^{-2}	1.72×10^{-3}
Kr-87	0.898	1.7×10^{-2}	1.43×10^{-3}
Kr-88	2.54	2.1×10^{-2}	3.78×10^{-3}
Xe-133	185.6	1.4×10^{-1}	2.17×10^{-2}
Xe-135	5.19	7.8×10^{-2}	1.08×10^{-2}

* At a comparable cycle time.

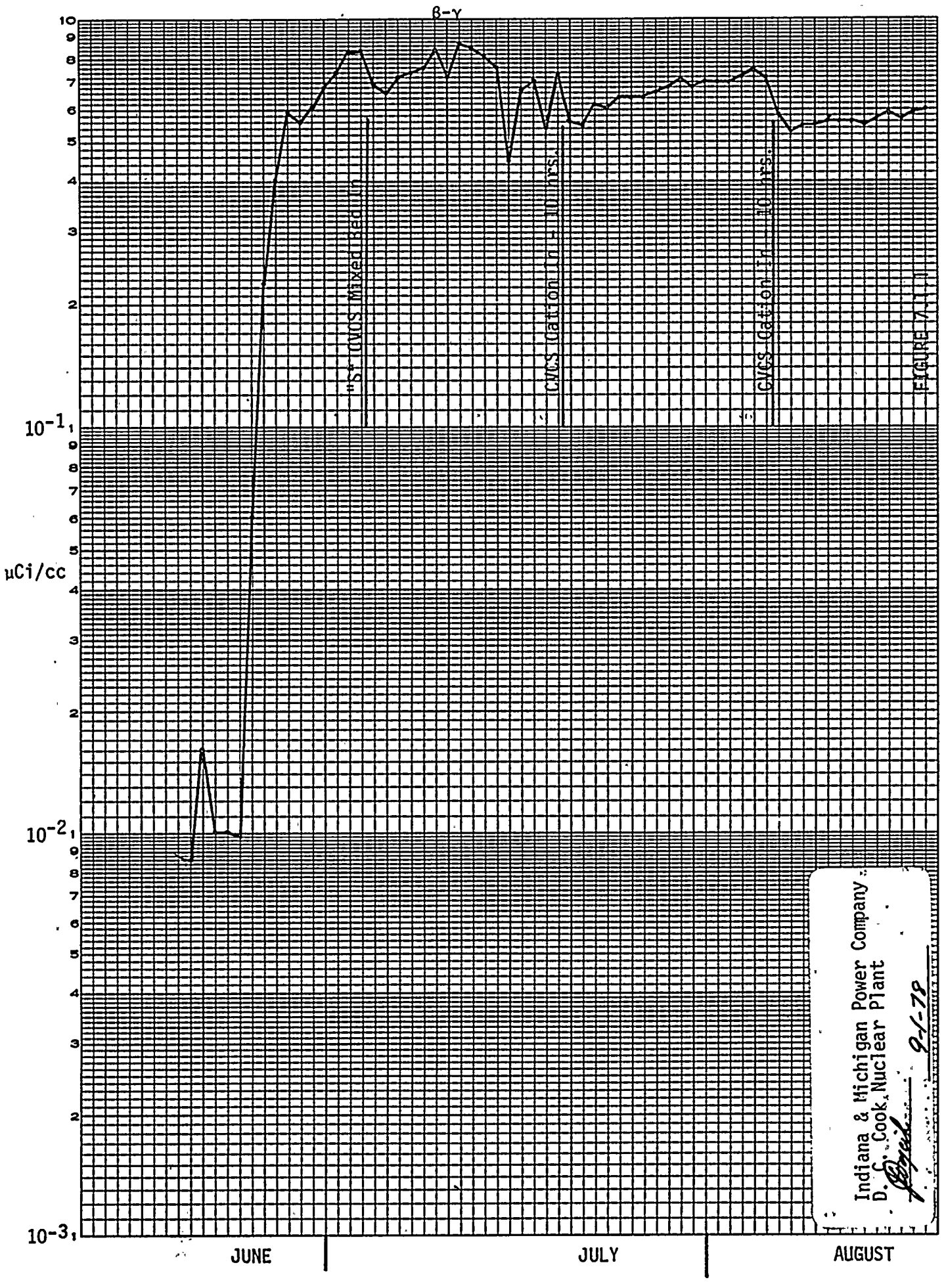
β-γ
μCi/cc
10
9
8
7
6
5
4
3
2
10^{-1}
10^{-2}
10^{-3}
"S" CVCS Mixed Bed In
CVCS Cation In - 10 hrs.
CVCS Cation In - 10 hrs.
JUNE
JULY
AUGUST
Indiana & Michigan Power Company
D. C. Cook Nuclear Plant
9-1-78

FIGURE 7.1.1

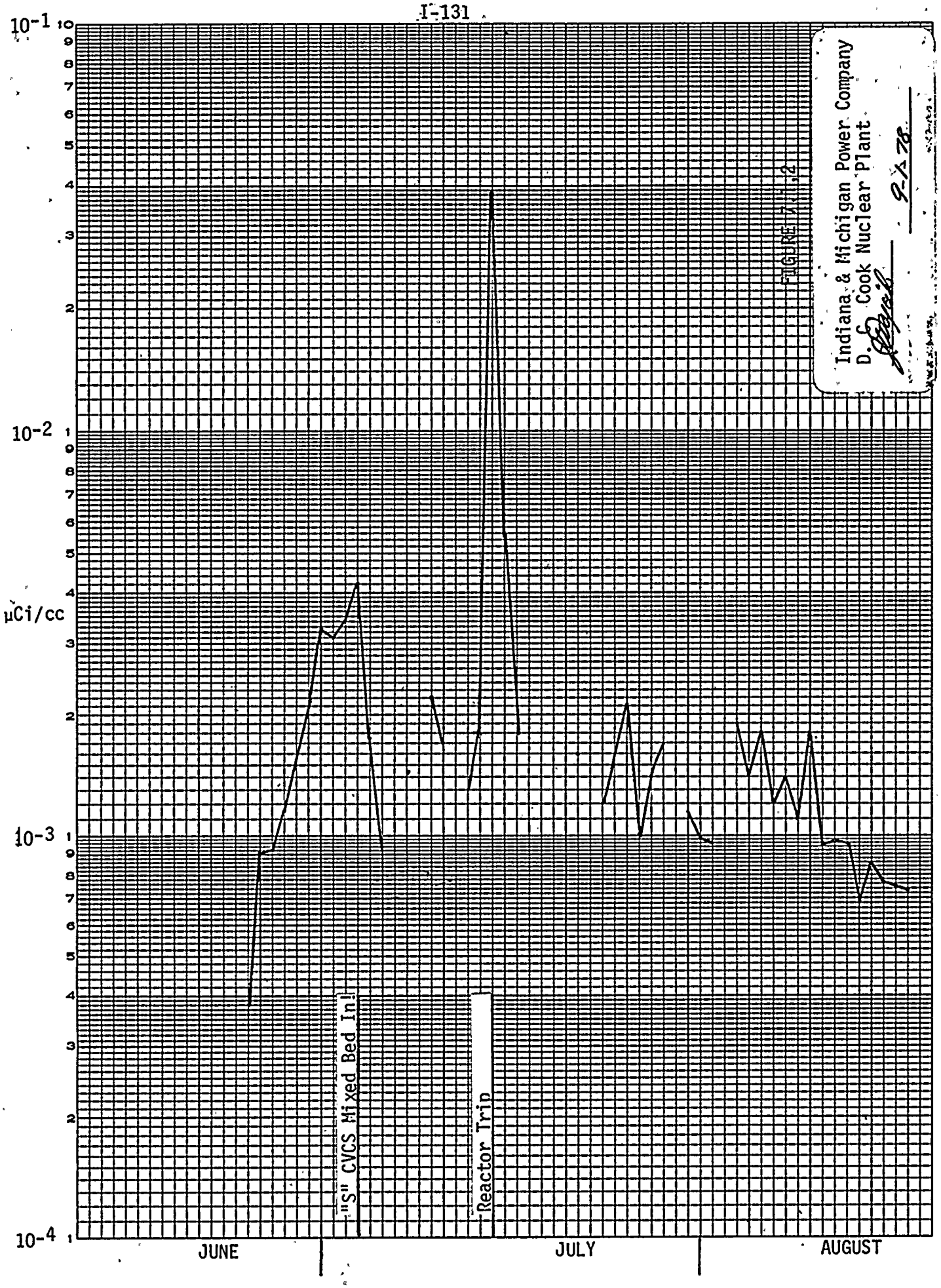
I-131
10-1
10-2
10-3
10-4
µCi/cc
"S" CVCS Mixed Bed In!
Reactor Trip
JUNE
JULY
AUGUST
FIGURE 7.4-1.2
Indiana & Michigan Power Company
D. C. Cook Nuclear Plant
9-A 78

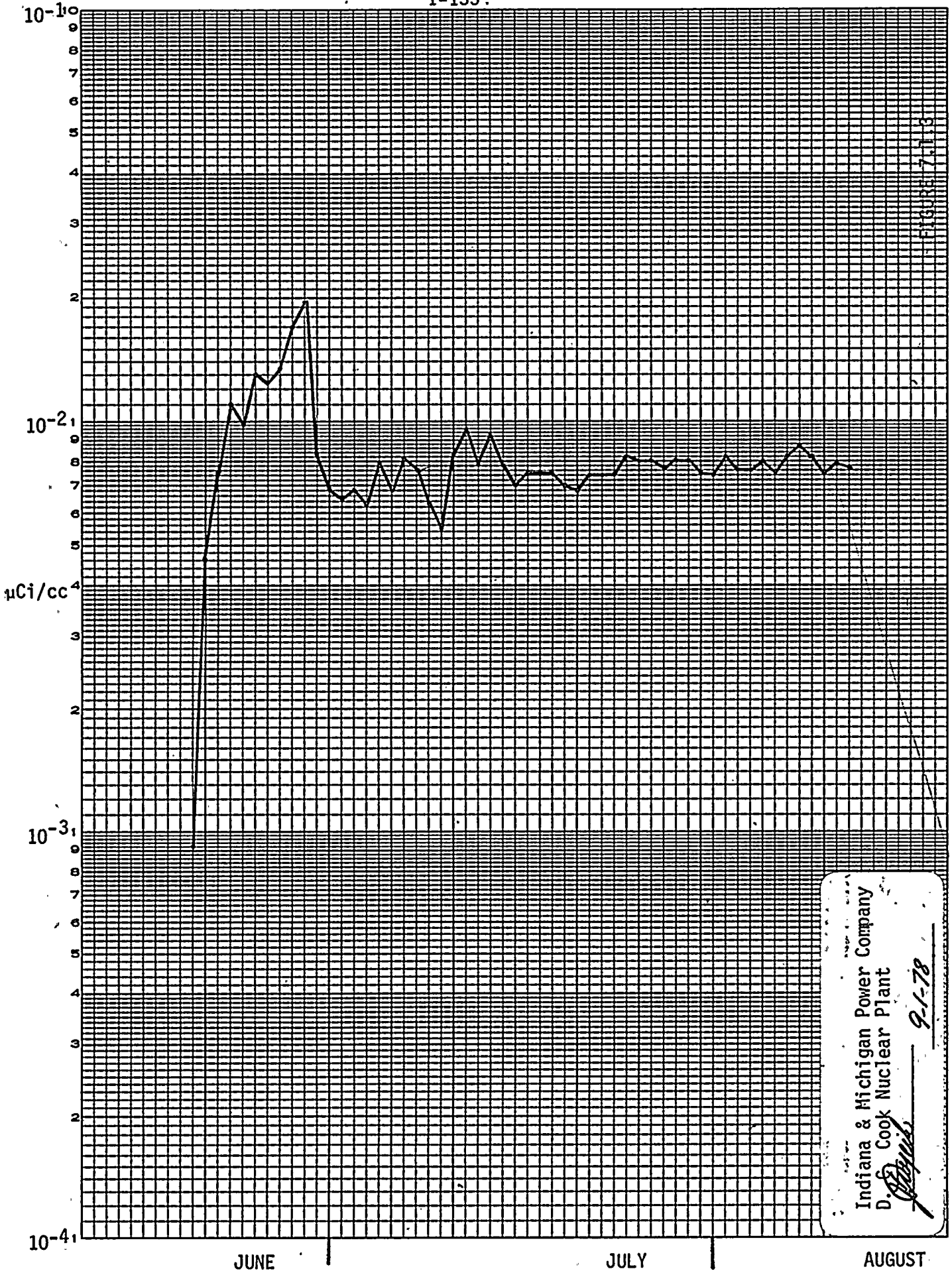
10-1
10-2
10-3
10-4
µCi/cc
JUNE
JULY
AUGUST
Indiana & Michigan Power Company
D. C. Cook Nuclear Plant
9-1-78

FIGURE 7.1.3

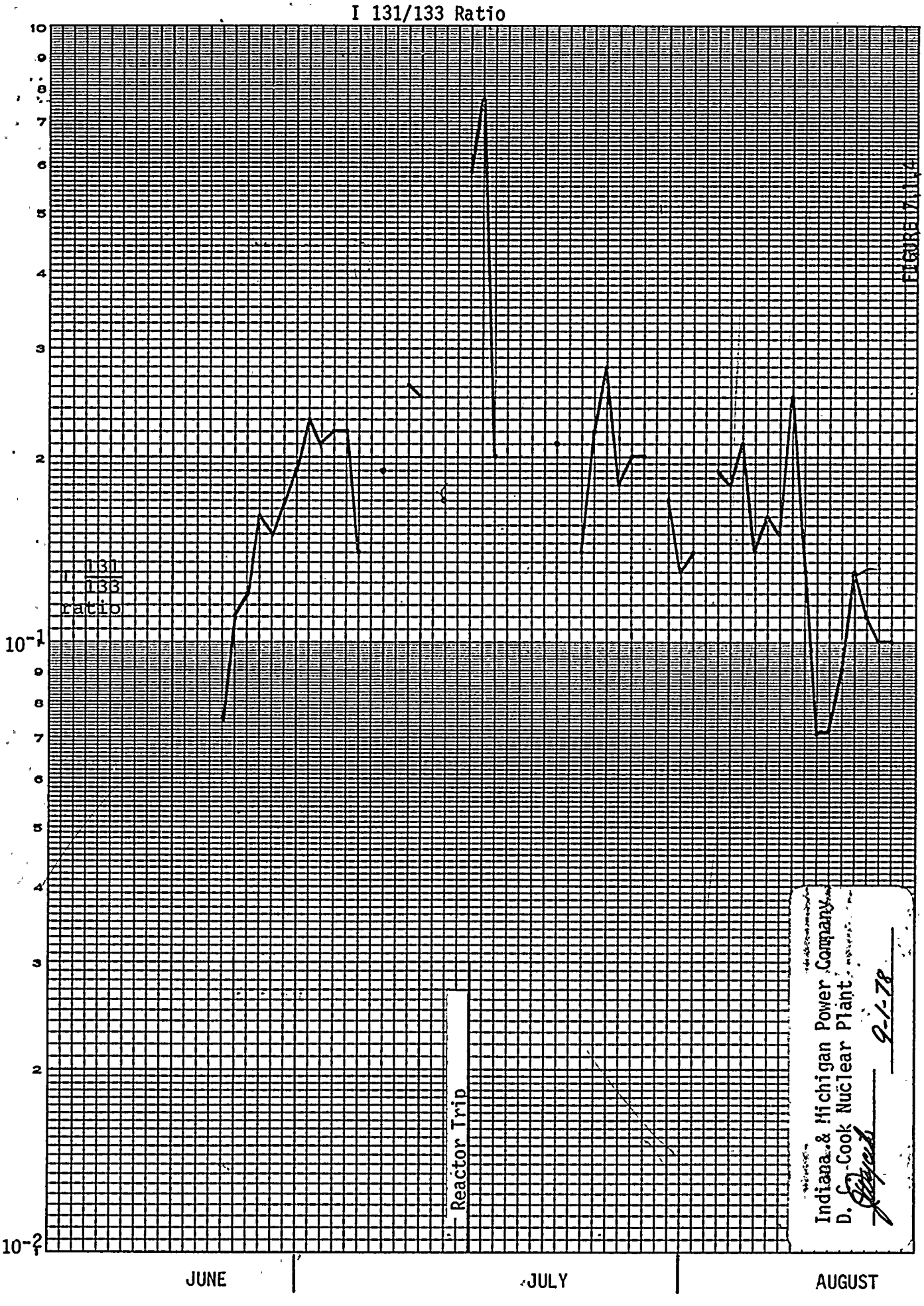
I 131/133 Ratio
10
9
8
7
6
5
4
3
2
I 131/133 ratio
10⁻¹
9
8
7
6
5
4
3
2
10⁻²
Reactor Trip
JUNE
JULY
AUGUST
Indiana & Michigan Power Company
D. C. Cook Nuclear Plant
9-1-78

FIGURE 7.1-5
REACTOR POWER

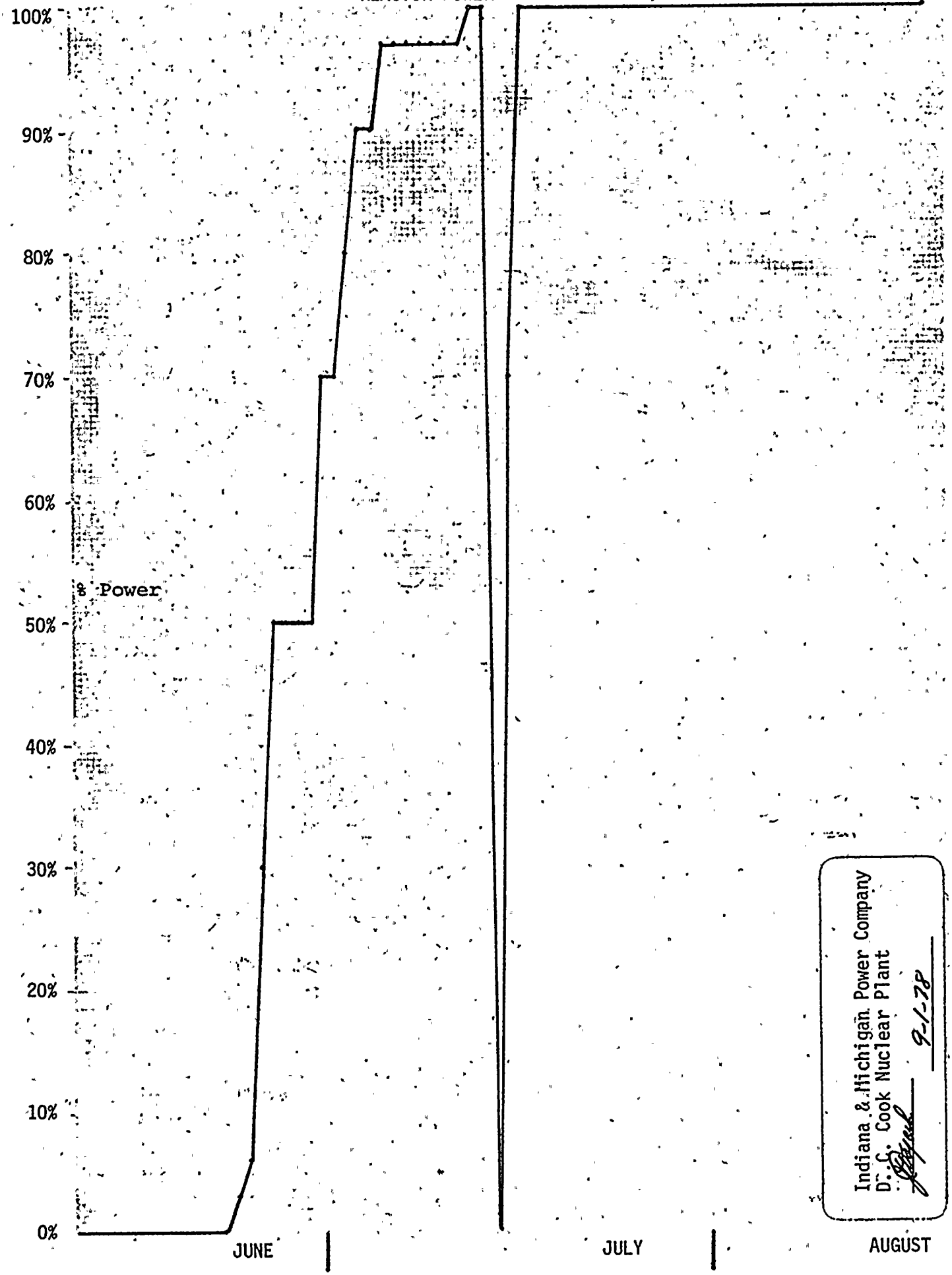

Indiana & Michigan Power Company
D. C. Cook Nuclear Plant
9-1-78

AUGUST

Cook Inlet
9 & 11 Fish

FIGURE 7.1-6
Li^7 PPM

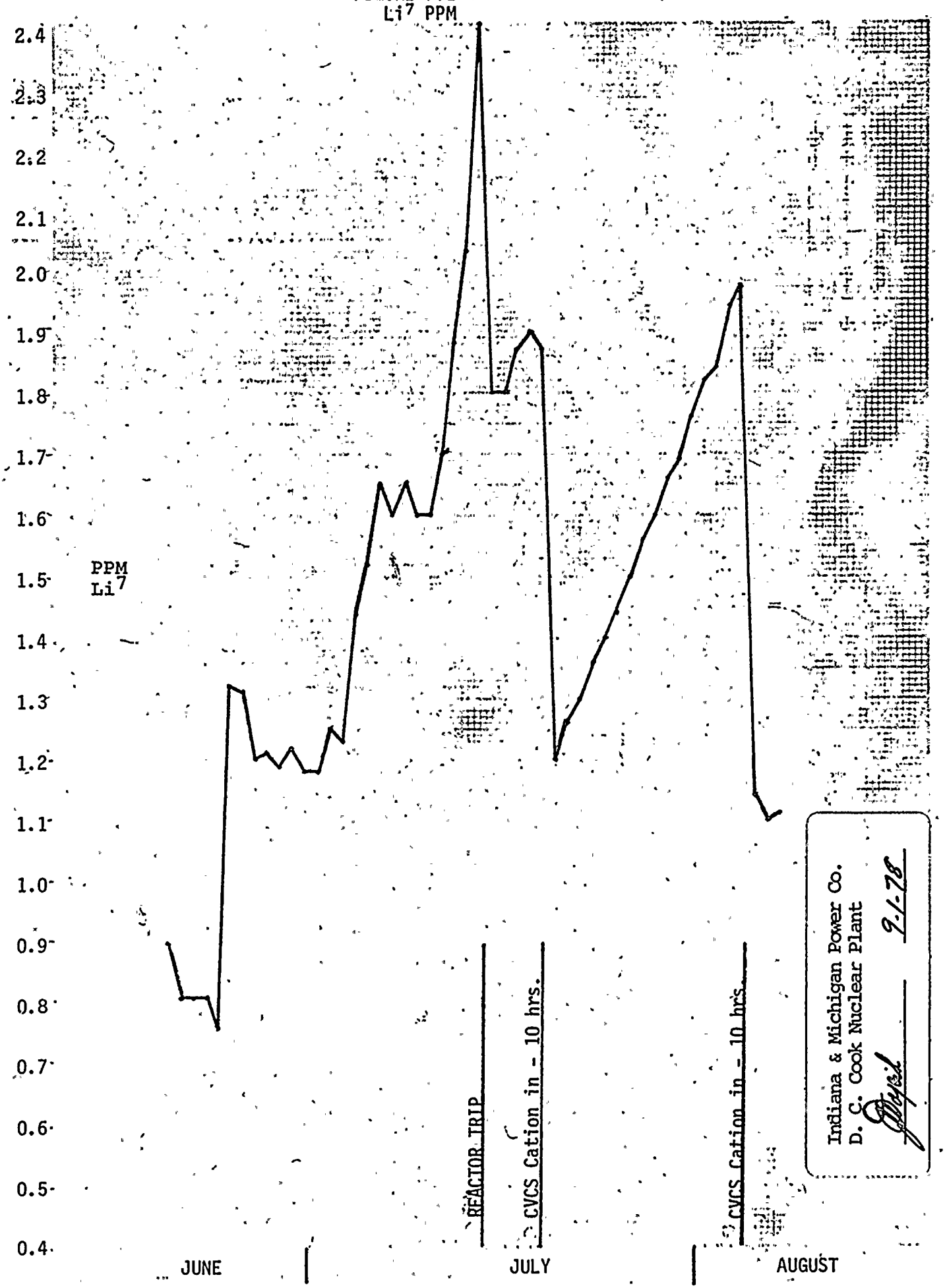

Indiana & Michigan Power Co.
D. C. Cook Nuclear Plant
9-1-78

FIGURE 7.1-7
STEAM GENERATOR SODIUM AVERAGE

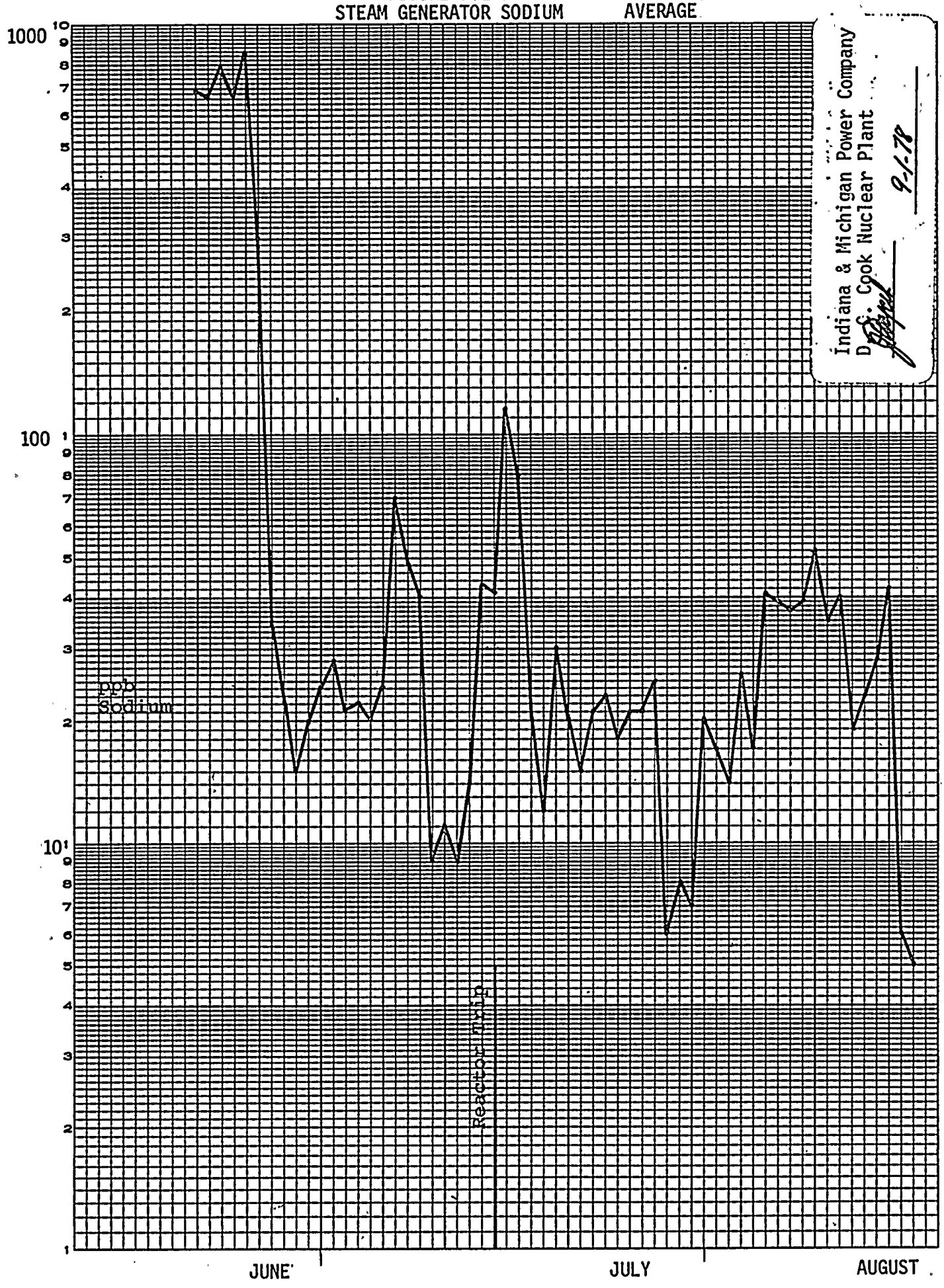

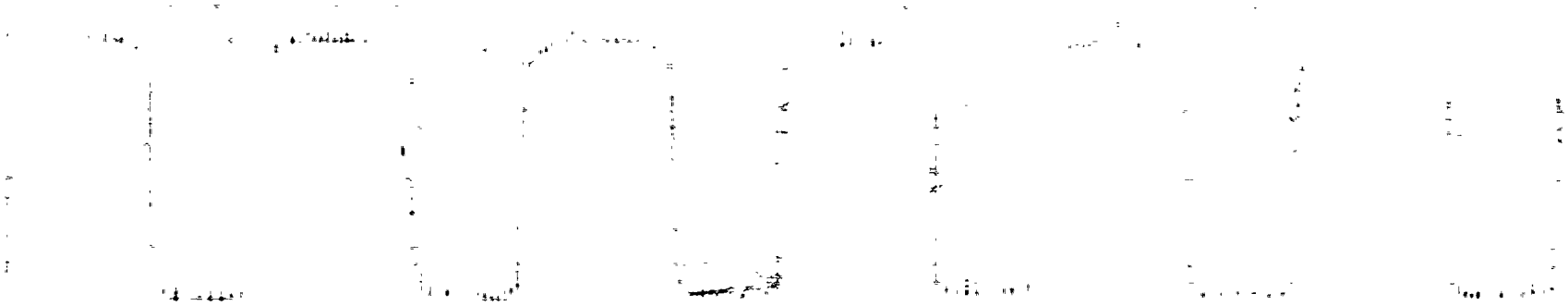

REACTOR COOLANT TEMP (^{o}F) + CHLORIDE (PPM) VS TIME Figure 7.1-8

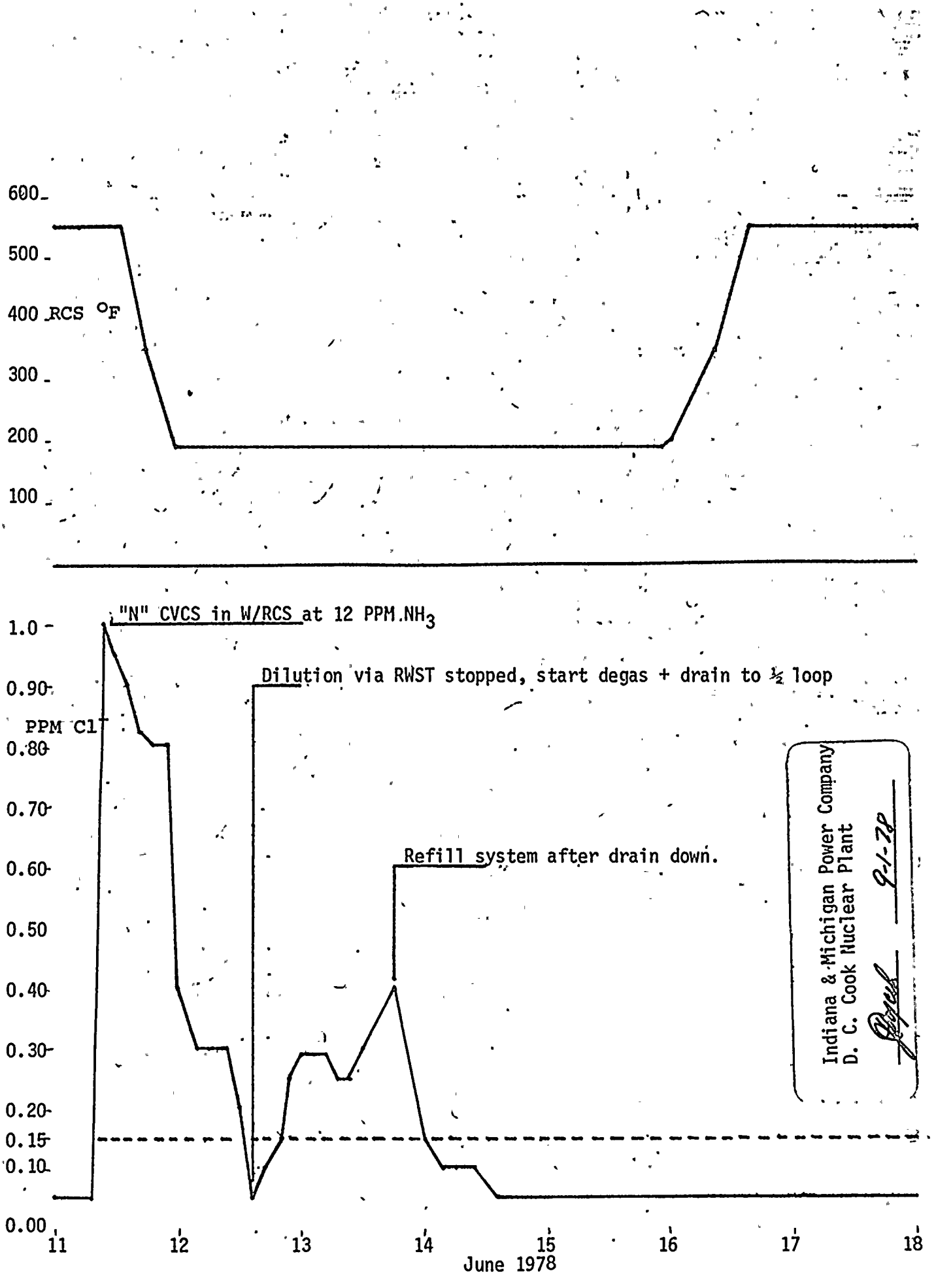

TABLE 7.1-3

REACTOR COOLANT SYSTEM CORROSION PRODUCTS

ISOTOPE	RESAR - 41	ACTUAL VALUE CYCLE II - 98% Power*	ACTUAL VALUE CYCLE III - 100% Power*
Cr-51	9.5×10^{-4}	1.9×10^{-4}	8.15×10^{-5}
Mn-54	7.9×10^{-4}	1.5×10^{-5}	1.59×10^{-5}
Mn-56	3.0×10^{-2}	4.5×10^{-4}	NOT DETECTED
Fe-59	1.1×10^{-3}	1.1×10^{-5}	1.0×10^{-5}
Co-58	2.6×10^{-2}	2.9×10^{-4}	2.02×10^{-4}
Co-60	7.7×10^{-4}	3.0×10^{-5}	8.14×10^{-5}

* At a comparable cycle time.

TABLE 7.1-4

STEAM GENERATOR WATER QUALITY

PARAMETER	SPECIFICATION	STEAM GENERATOR NO. 1	2	3	4
pH at 25°C	8.5 - 9.0	8.8	8.85	8.8	8.9
Cation Conductivity (μmho's)	<2.0	1.8	1.9	2.4	1.76
Sodium (ppb)	<100	6	7	7	7
Cl^- (PPM)	<0.15	<0.15	<0.15	<0.15	<0.15
SiO_2 (PPM)	<1.0	0.30	0.30	0.30	0.30
Free Hydroxide (PPM) (as OH^-)	<0.05	<0.05	<0.05	<0.05	<0.05
Suspended Solids (PPM)	<1.0	0.75	0.60	0.70	0.86

SECTION 7.2

PLANT RADIATION SURVEYS

PURPOSE

The adequacy of the shielding design for the reactor and associated primary coolant system was verified during the initial plant startup. Surveys during subsequent startups are performed for the following purposes.

1. Verify the adequacy of any radiation shielding that has been significantly modified since the last startup.

2. Verify the adequacy of radiation shielding for systems that have been significantly modified such that the source term may have changed, thus changing the shielding adequacy.

3. Verify that general plant radiation levels have not significantly changed due to variations in sources that may have been affected by feed changes.

SUMMARY OF RESULTS

No significant modifications were made to primary shielding or the primary coolant systems such that the source term for existing shielding would have been changed.

Table 7.2-1 presents a summary of results of the surveys taken for gamma radiation. The summary lists the average reading (not truly a statistical average but level of the general area) and the maximum level found.

The Cycle III survey shows an apparent decrease in radiation levels of the RHR Hx, and pipe annulus. This is best explained by noting that the Cycle II survey of these areas was performed after 100% power operation and subsequent reactor trip and startup. The decrease in maximum radiation level of the Volume Control Tank may have been caused by varying liquid levels.

The increase in radiation levels of the Refueling Cavity and Transfer Tube (Containment side) were caused by additional contamination deposited in the cavity after refueling operations. The average radiation levels of the Letdown Hx almost doubled from Cycle II to Cycle III. Buildup of "crud" is suspected for this increase.

Routine surveys of the plant taken during startup, power ascension and subsequent containment entries, have failed to yield any results showing either significant increases or decreases of radiation levels beyond those previously noted.

DISCUSSION OF TEST

Surveys were performed as per procedure 12 THP 6010.RAD.201 (Radiation Surveys) and routine surveys as per Technical Department Standing Order TSO-010 (Routine Radiation/Conatmination Surveys) and associated attachments.

TABLE 7.2-1

GAMMA RADIATION LEVELS

Cycle Power Level Units of Measure Area Surveyed	II 100% mR/Hr Avg.	Max.	III 100% mR/Hr Avg.	Max.
Spent Fuel Pit	1-2	5	2-4	7
Spent Fuel Pit Hx	1.5	2	2	4
Letdown Hx	150	380	275	500
Volume Control Tank	400	3000	350	800
Nuclear Sampling Room	2-4	6	2-8	10
Charging Pump Rooms	15-20	25	10-20	25
Safety Injection Pump Rooms	0.4	0.7	1	3
591 El. Vestibule	10-25	60	15-30	80
RHR Pumps	15-35	50	10-40	70
RHR Hx	40-75	300	40	80
Pipe Annulus	10-50	120	10-25	80
Upper Containment	4-20	35	5-20	40
Refueling Cavity*	10-30	50	30-70	90
Transfer Tube (Cont. Side)*	NS	55	NS	100

NS - Not Surveyed

* Performed at zero power level

SECTION 7.3

LOOSE PARTS MONITORING SYSTEM

PURPOSE

The purpose of obtaining loose parts data is to compare the spectral traces obtained to previously collected data at similar conditions. This is done in an effort to detect any significant changes in the vibration characteristics of the equipment being monitored. These changes could be the result of a loose part existing on/in the piece of equipment being monitored from work conducted during refueling and primary system maintenance. Periodic collection of such data is also a useful reference to allow early detection and evaluation of changes which may occur during plant life.

SUMMARY OF RESULTS

In evaluating the signals obtained during data collection the amplitudes at the following frequencies are the most predominate.

19.7 cps	Reactor coolant pump rotational speed
138 cps	The first harmonic of reactor coolant pump impeller vane passing frequency (pump impellers have seven vanes, thus, 7 x 19.7 = 138 cps
276 cps	Second harmonic of reactor coolant pump impeller vane passing frequency (138 cps x 2)
414 cps	Third harmonic of 138 cps
552 cps	Fourth harmonic of 138 cps
690 cps	Fifth harmonic of 138 cps

When comparing the data obtained to previous spectral traces, it was found that no significant abnormal vibration peaks were noted. The only exception is a .15G signal at 1420 cps from the steam generator #2 mounted accelermotor.

DISCUSSION OF TEST

Spectral traces were obtained on 6-19-78 at 0% reactor power and on 7-18-78 at 99% reactor power. The data collected was compared to data taken prior to refueling (11-9-77), 100% reactor power).

When examining the traces taken from the accelerometers located on the reactor vessel, it can be seen that the signal amplitude at 552 cps decreased by approx. 55% during the power ascension from 0 to 99% reactor power. The signals present at 276 cps, however, rose approximately 35%. Figures 7.3.1, 7.3.2 and 7.3.3 are representative of these trends. These levels are

quite low and probably relate to pump/vessel interactions, rather than core interactions. The parameter to observe with regard to pump operation is the 276/552 ratio, which in this case was four times greater at 99% than at 0%.

The 276 cps steam generator mounted accelerometer signals seemed to decrease as reactor power rises in all steam generators except number 1, which rose 110% from 0 to 100% reactor power. The amplitude of this peak at 99% however, corresponds to the other steam generator 276 cps signals at this power level. When comparing 276 cps 100% data to traces obtained prior to refueling it can be seen that the new data is approximately of the same magnitude with the exception of the steam generator #1 trace which decreased by an order of ten. See Figures 7.3.4, 7.3.5 and 7.3.6.

The other predominant steam generator vibration peak occurred at 552 cps. This signal also decreased as reactor power increased. At 99% reactor power, all amplitudes corresponded to pre-refueling 100% data except for the steam generator #1 peak which decreased by approximately 94%.

All loops except #4 have a history of a somewhat wandering high frequency vibration. Spectral traces of the steam generator #1 mounted accelerometer reflected a vibration at 1370 cps of approximately .06 G's. On 6-19-78, a 1190 cps .0069 signal was noted. Again on 7-18-78, yet another vibration is apparent at 1210 cps with a magnitude of .0082 G's. This peak is typical of both loop 1 & 3 and is illustrated on Figures 7.3.4, 7.3.5 and 7.3.6. The steam generator #2 mounted accelerometer shows a higher frequency signal at 1420 cps. The frequency remained constant during power ascension, but the amplitude dropped 21% from .19 G's at 0% reactor power to .15 G's at 99% reactor power. See Figures 7.3.8 and 7.3.9.

Reactor coolant pump mounted accelerometer traces reflected the predominant pump frequencies of 276, 414, 552 and 690 cps. Traces obtained reflected consistant amplitude data when compared to past monitoring programs. Figure 7.3.7 illustrates typical reactor coolant pump spectral traces.

[redacted]

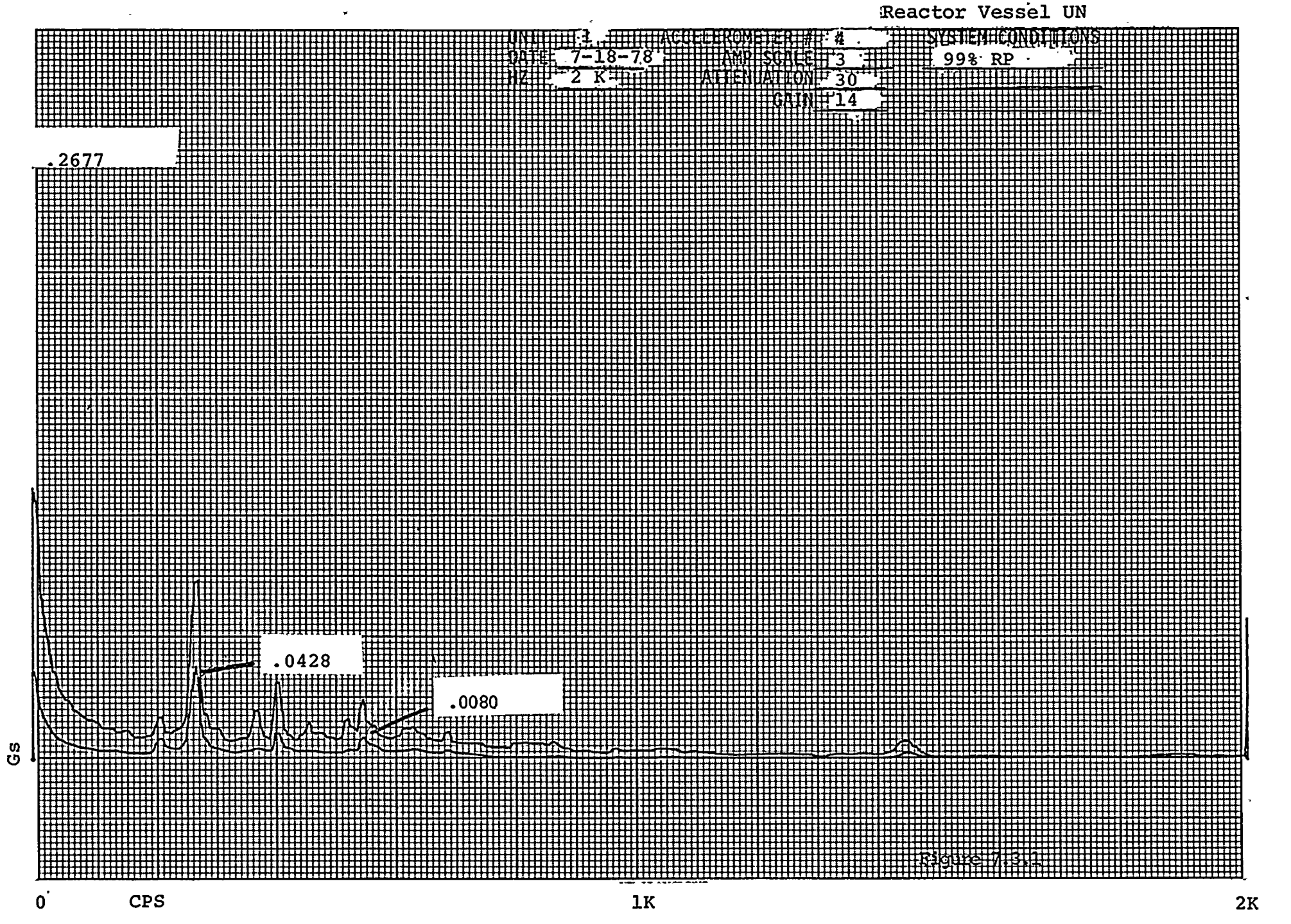
Reactor Vessel UN
UNIT 1
DATE 7-18-78
HZ 2 K
ACCELEROMETER # 4
AMP SCALE 3
ATTENUATION 30
GAIN 14
SYSTEM CONDITIONS
99% RP
.2677
.0428
.0080
Gs
0
CPS
1K
2K

Figure 7.3.1

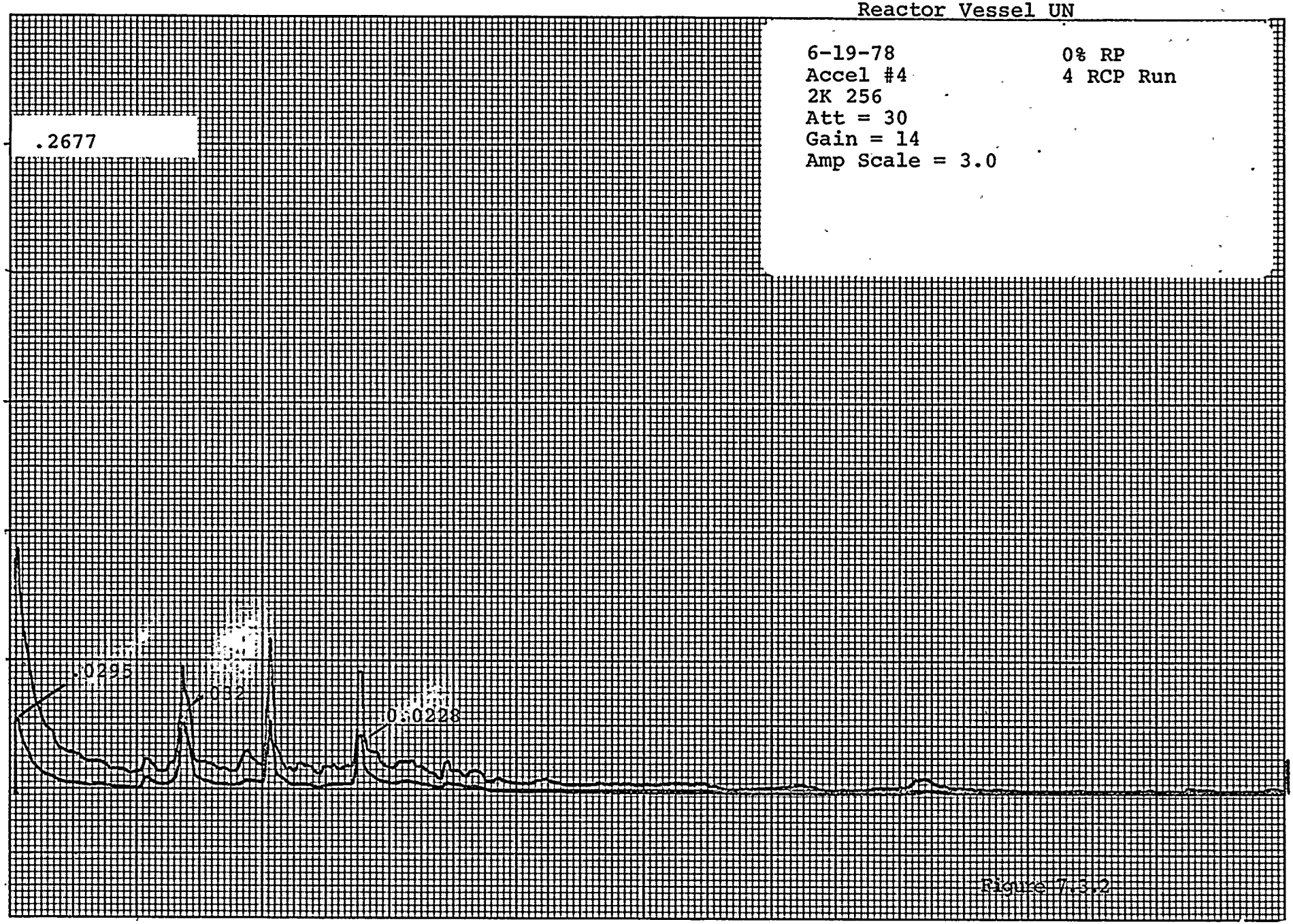
Reactor Vessel UN
6-19-78
Accel #4
2K 256
Att = 30
Gain = 14
Amp Scale = 3.0
0% RP
4 RCP Run
.2677
.0295
.0228
Gs
0
CPS
1K
2K

Figure 7.3.2

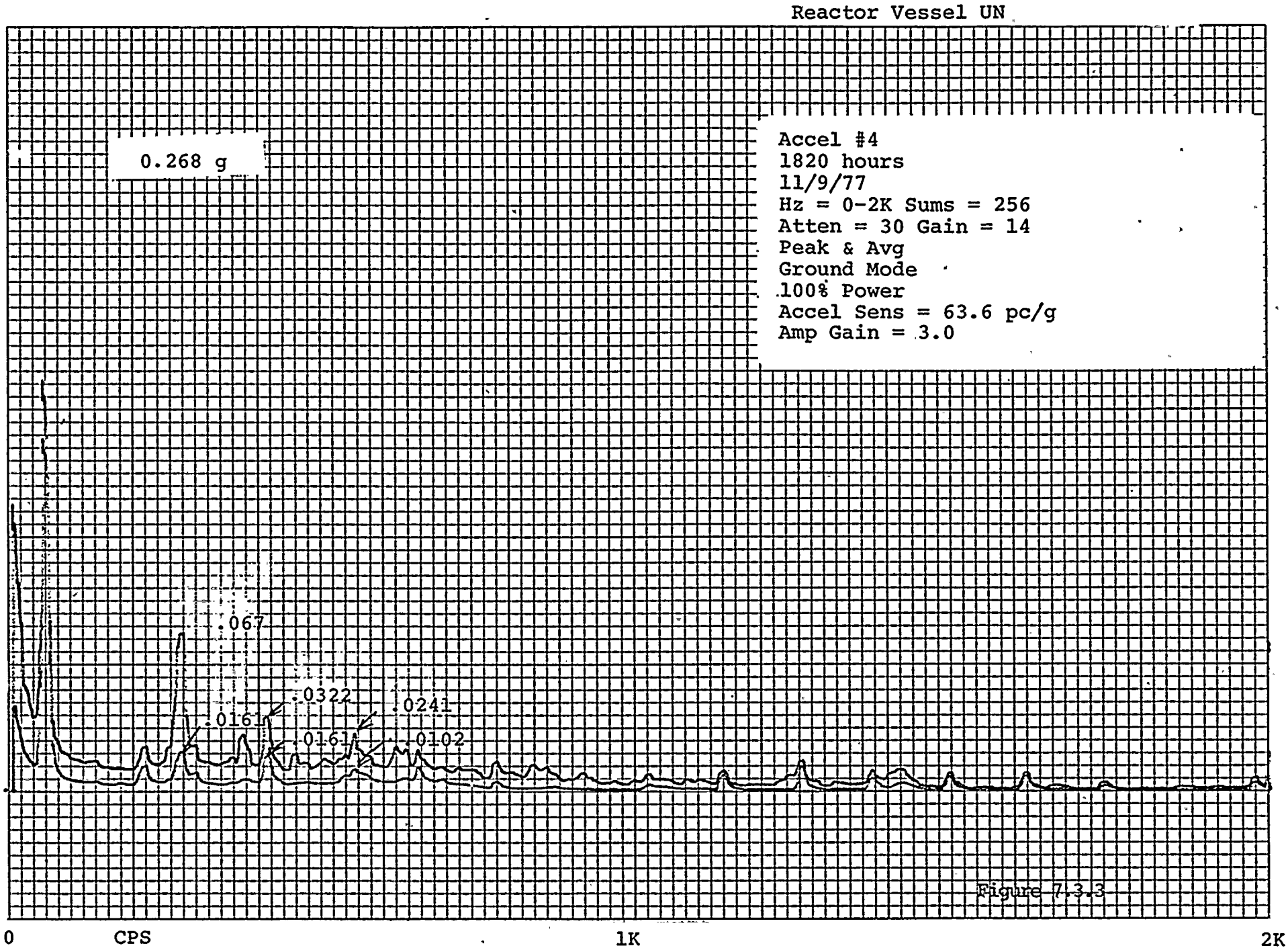
Reactor Vessel UN
0.268 g
Accel #4
1820 hours
11/9/77
Hz = 0-2K Sums = 256
Atten = 30 Gain = 14
Peak & Avg
Ground Mode
100% Power
Accel Sens = 63.6 pc/g
Amp Gain = 3.0
Gs
.067
.0322
.0241
.016
.0161
.0102
0
CPS
1K
2K

Figure 7.3.3

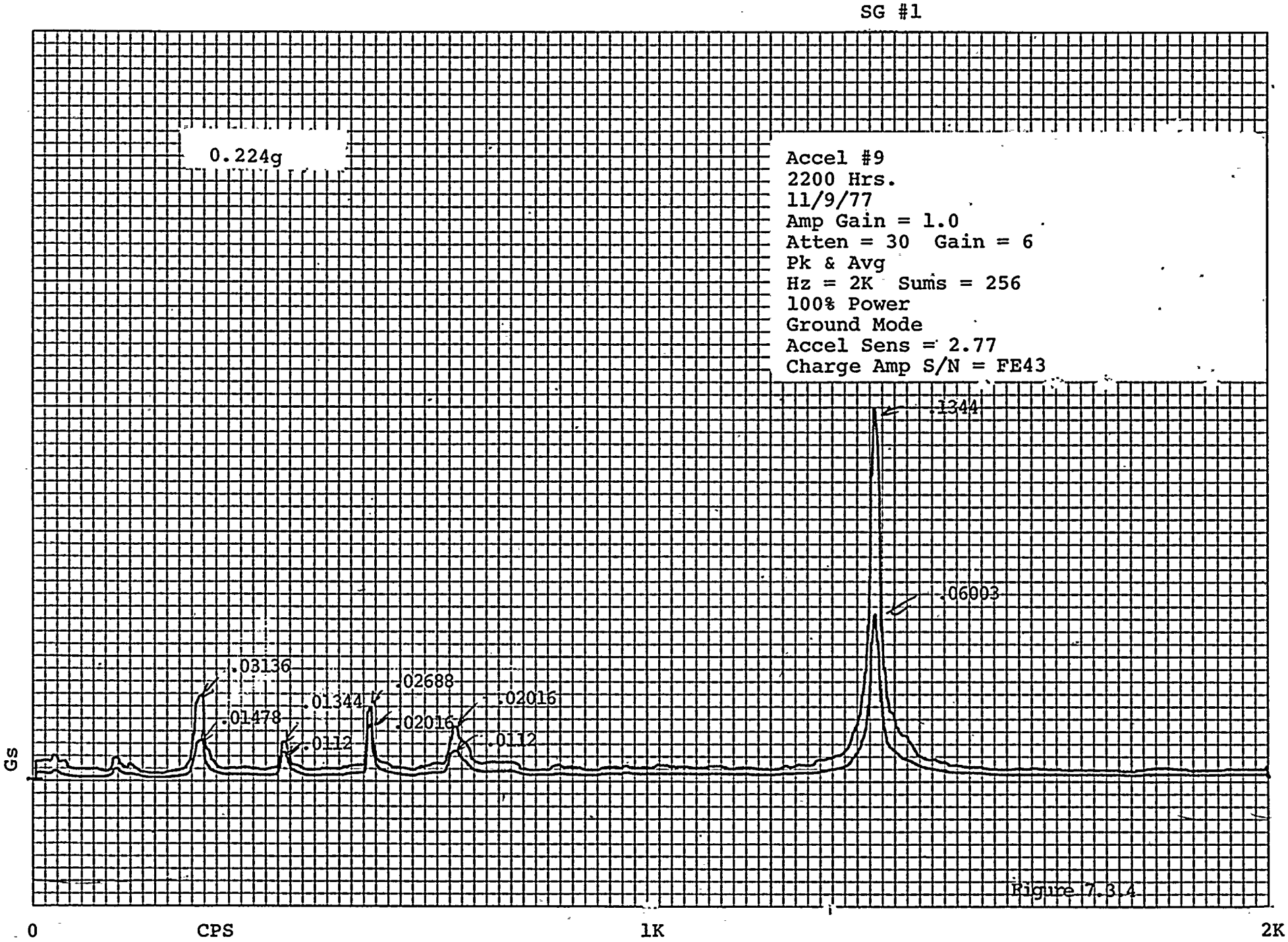
SG #1
0.224g
Accel #9
2200 Hrs.
11/9/77
Amp Gain = 1.0
Atten = 30 Gain = 6
Pk & Avg
Hz = 2K Sums = 256
100% Power
Ground Mode
Accel Sens = 2.77
Charge Amp S/N = FE43
.1344
.06003
.03136
.01478
.01344
.0112
.02688
.02016
.02016
.0112
Gs
0
CPS
1K
2K

Figure 7.3.4

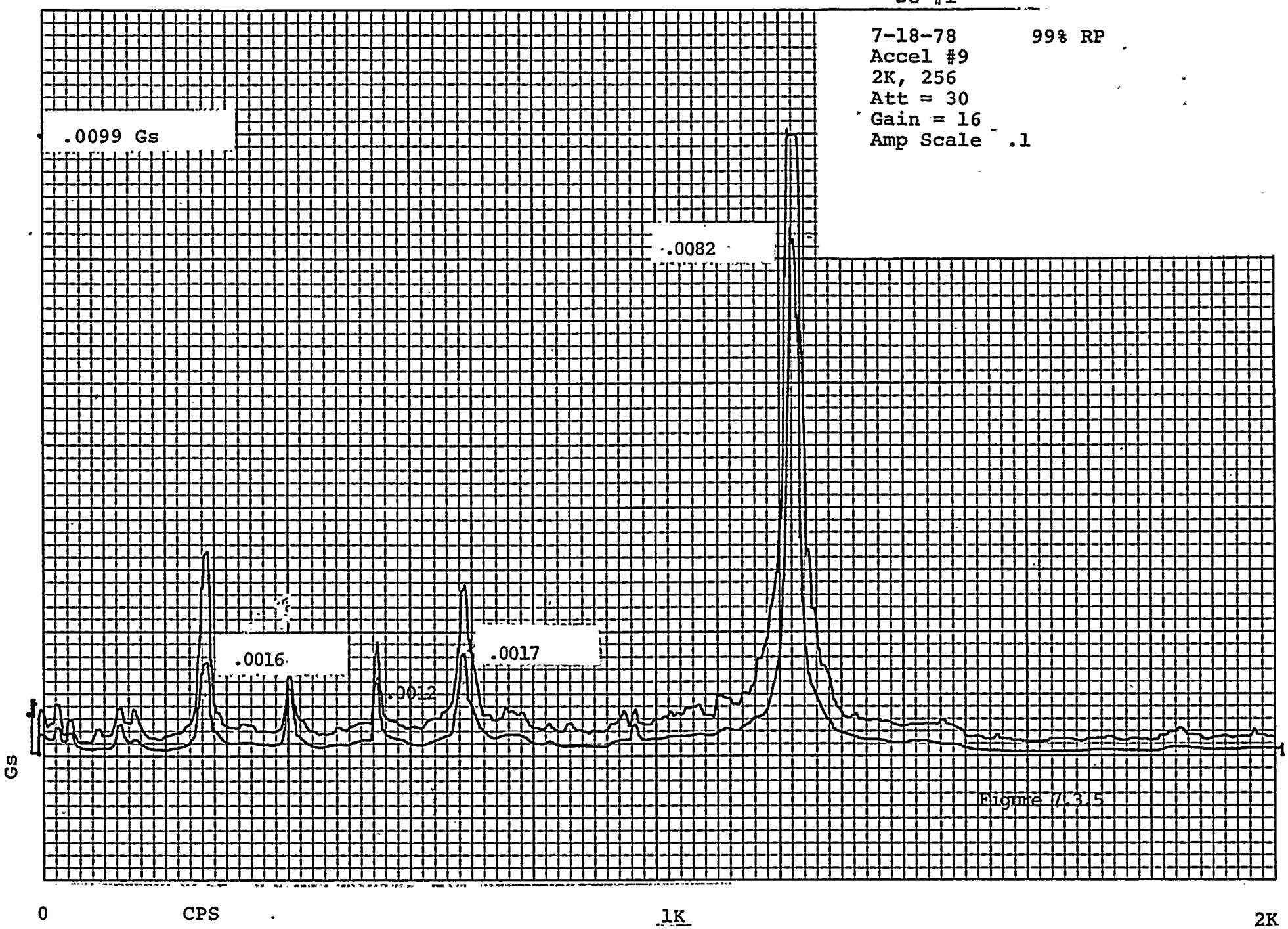
SG #1
7-18-78 99% RP
Accel #9
2K, 256
Att = 30
Gain = 16
Amp Scale .1
.0099 Gs
.0082
.0016
.0012
.0017
Gs
0
CPS
1K
2K

Figure 7.3.5

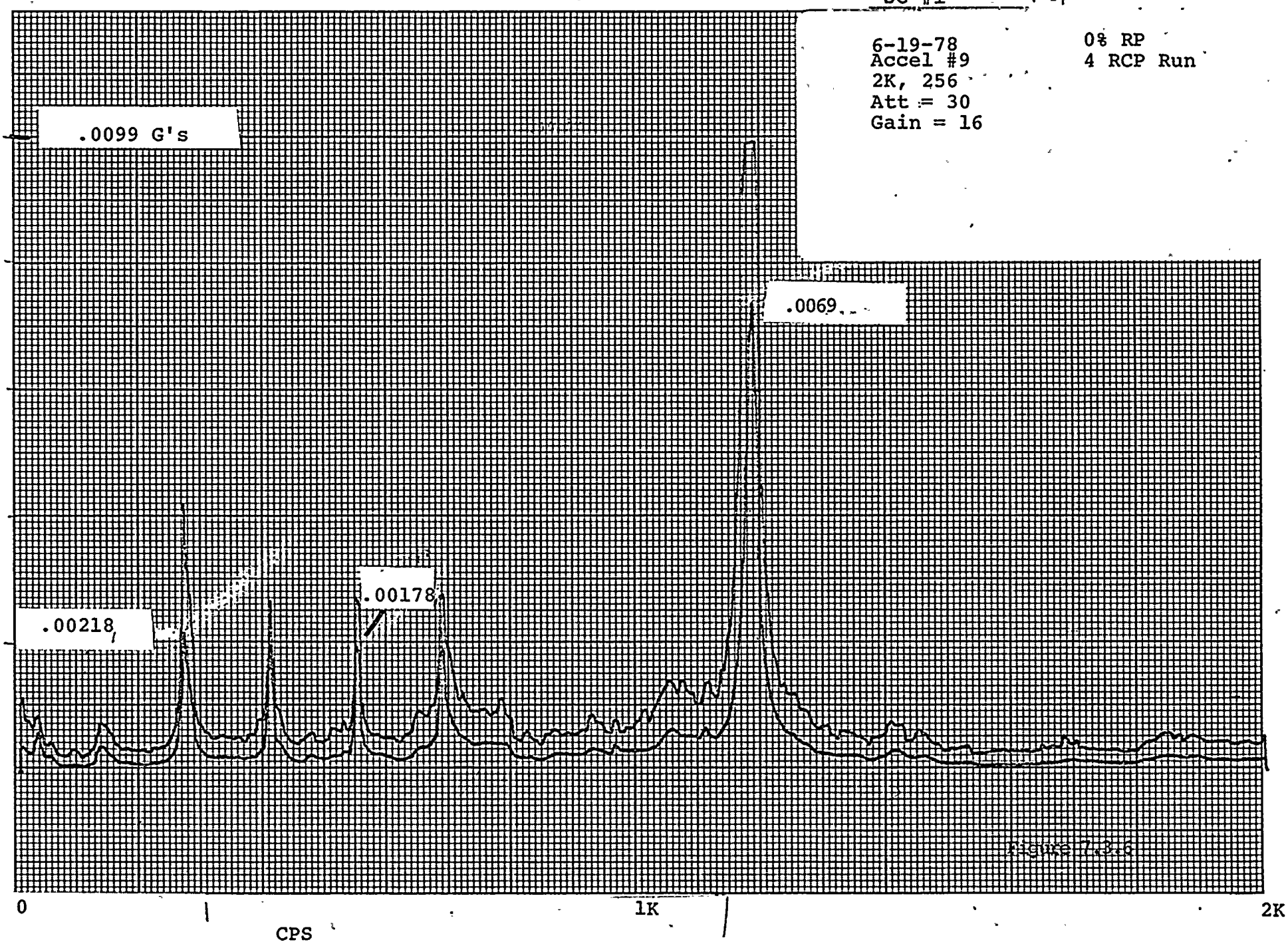
SG #1
6-19-78
Accel #9
2K, 256
Att = 30
Gain = 16
0% RP
4 RCP Run
.0099 G's
.0069
.00178
.00218
G's
0
1K
2K
CPS

Figure 7.3.6

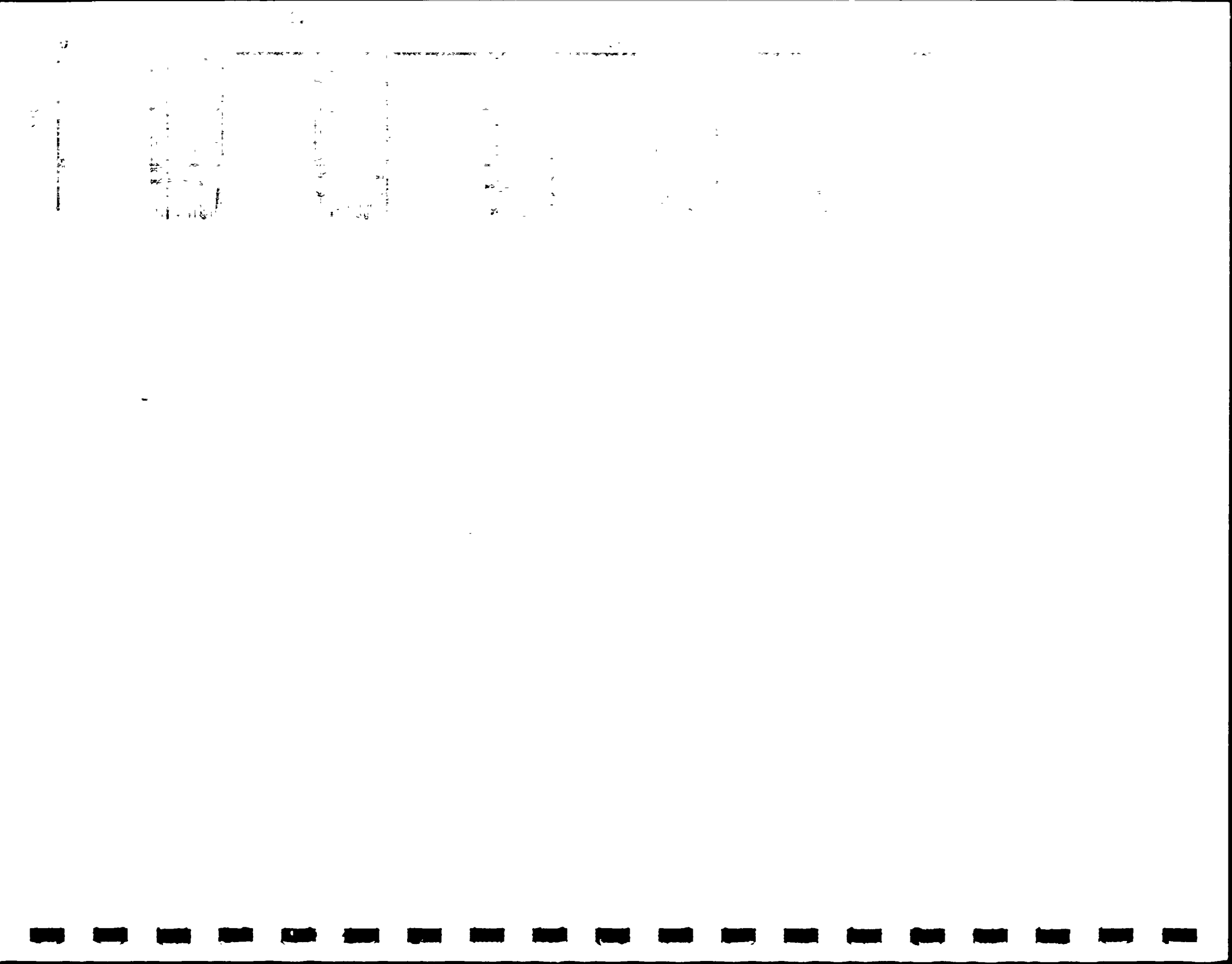

RCP #3

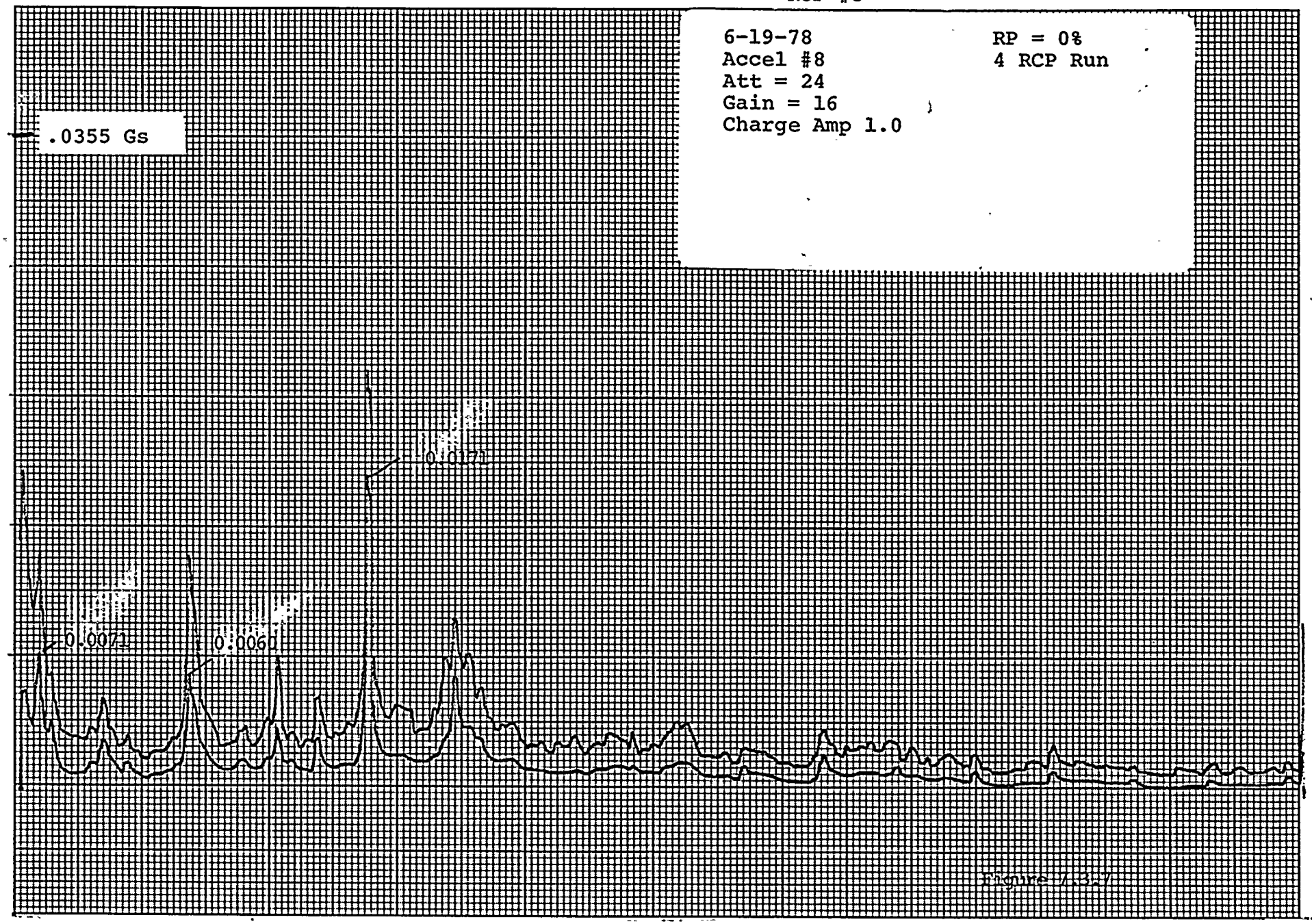

Figure 4.3-7

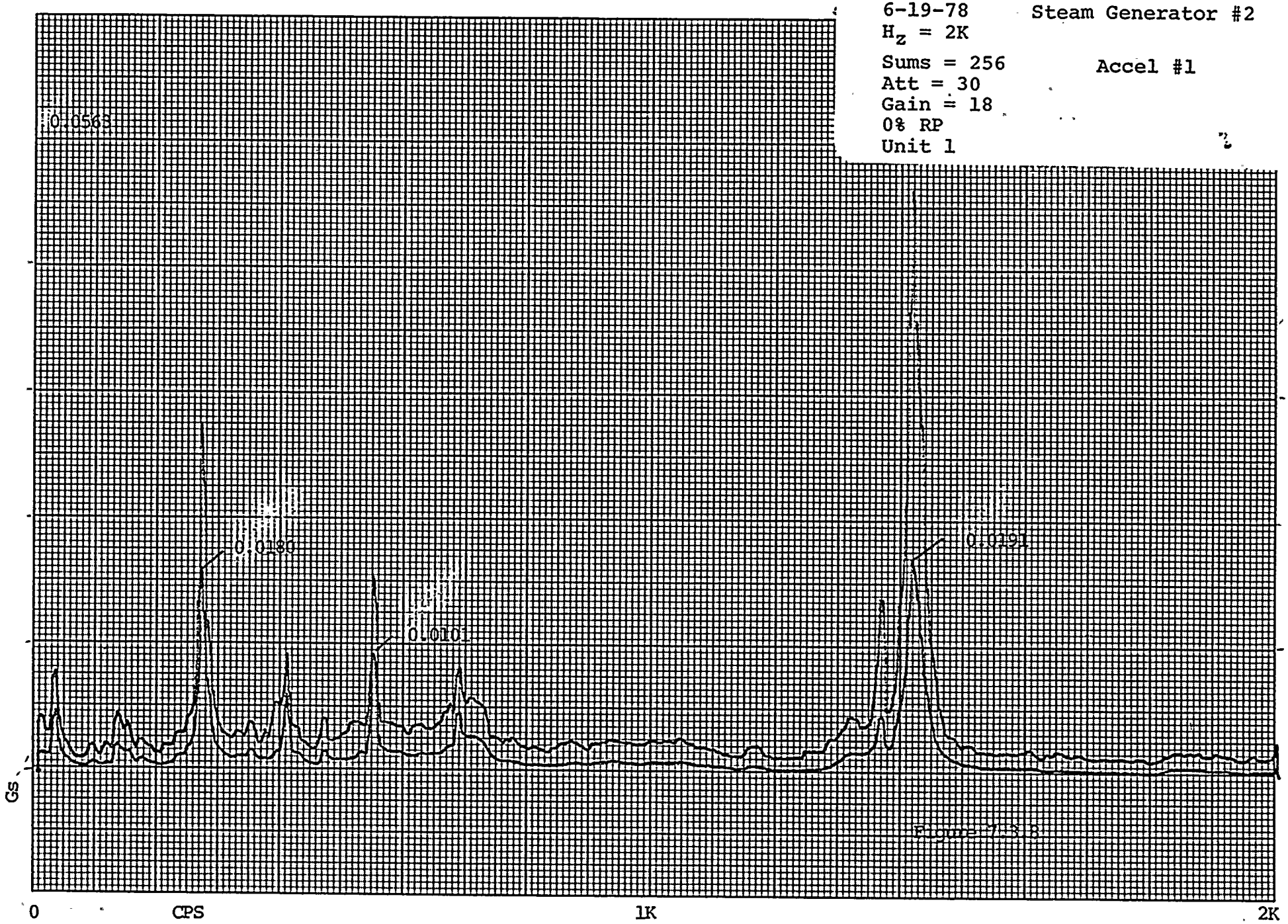
6-19-78
Steam Generator #2
H_Z = 2K
Sums = 256
Accel #1
Att = 30
Gain = 18
0% RP
Unit 1
0.0563
0.0380
0.0101
0.0491
Gs
0
CPS
1K
2K

Figure 7-3.8

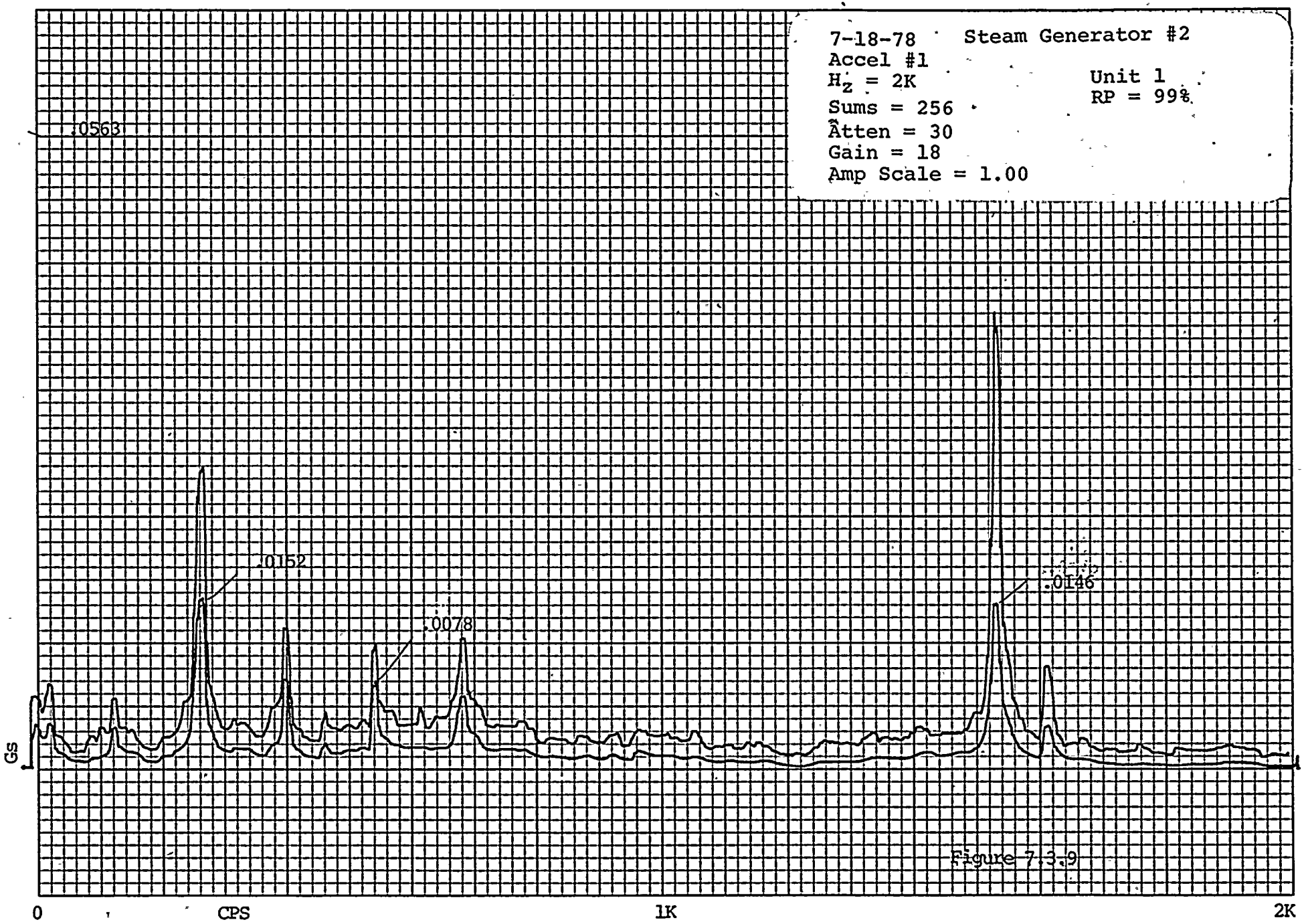
7-18-78 Steam Generator #2
Accel #1
H_z = 2K
Sums = 256
Atten = 30
Gain = 18
Amp Scale = 1.00
Unit 1
RP = 99%
.0563
.0152
.0078
.0146
Gs
0
CPS
1K
2K

Figure 7.3-9

SECTION 7.4

POWER RANGE NOISE MEASUREMENTS

PURPOSE

The purpose in obtaining power range noise measurements is to provide a relative indication of core barrel motion. Variations in neutron flux, as seen by the power range excore detectors, are recorded at various intervals throughout the life of the plant to determine whether the magnitude of core barrel motion is changing over time.

SUMMARY OF RESULTS

Core barrel motion has increased by at least 16% since the last measurements were made approximately 19 months ago on 12/16/76. Previously, it was observed that core motion had increased by approximately 39% over a 6 month period from 6/9/76 to 12/16/76.

Since the baseline set of measurements were made in April of 1975, core barrel motion appears to be continuously increasing with time at an approximate rate of 6 mils/per year.

DISCUSSION OF TEST

Brush recordings of the power range excore detector outputs (voltage signals proportional to neutron flux levels) were obtained on 7/19/78 while the unit was at 98% power. Since the excore detectors do not move with the core internals, variations in neutron flux seen by the detectors are indicative of core barrel motion. Each power range subchannel detector signal was recorded using a Brush 260 recorder run at speeds of 125 mm/min and 125 mm/sec. Recording the detector output at these speeds allows neutron flux variations at 0.3 Hz, 6.8 Hz and 60 Hz to be clearly displayed. In the past, the magnitude of core barrel motion has been greatest at 0.3 Hz and 6.8 Hz. An indication of 60 Hz noise is helpful in determining component malfunctions due to short circuits.

The excore detector output signal presents itself as a composite waveform consisting of an AC variation, representing changes in neutron flux, superimposed on a steady state carrier that is proportional to reactor power level. When obtaining the brush recording, the DC carrier level is suppressed such that only the AC variation appears on the strip chart. The suppressed signal, however, is recorded for future calculations.

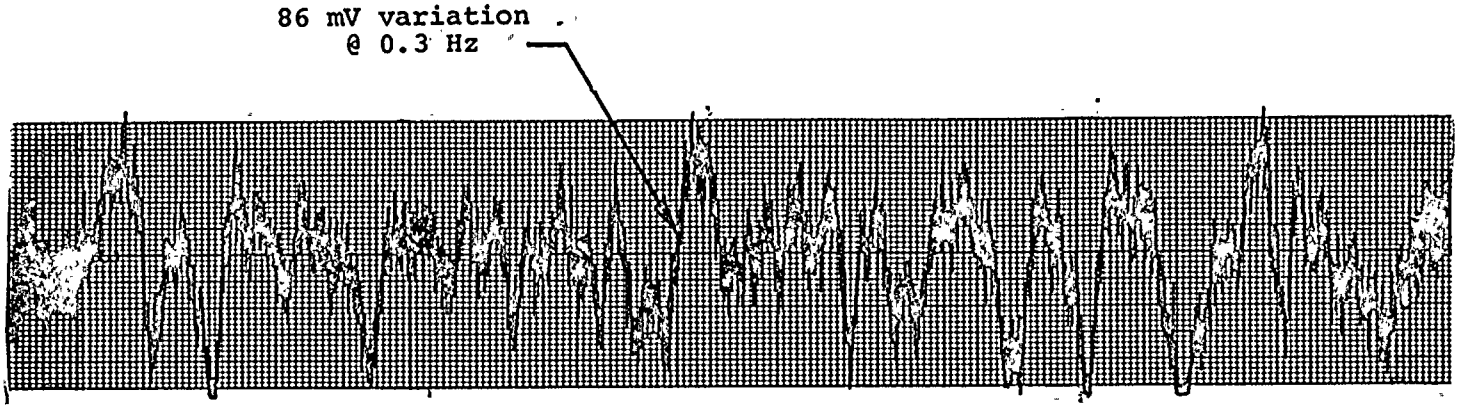

N42 Upper
125 mm/min
2 mV/div

Trace #1

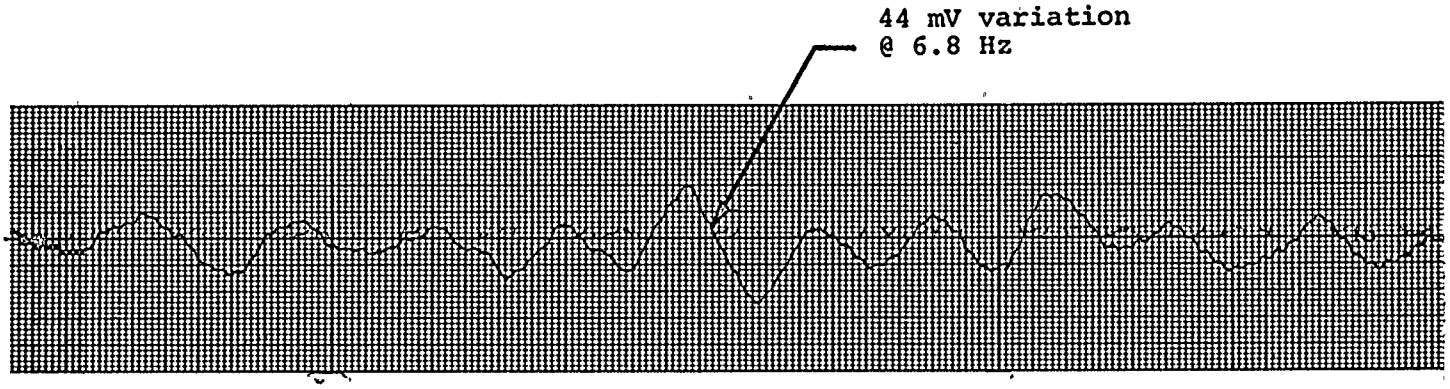

N44 Lower
125 mm/sec
2 mV/div

Trace #2

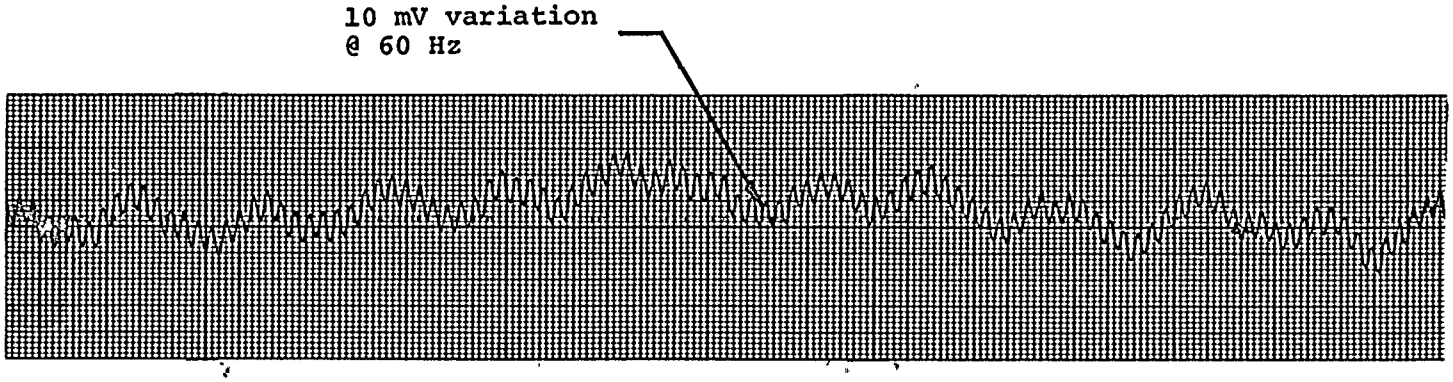

Trace #3

N43 Upper
125 mm/sec
2 mV/div

Figure 7.4-1

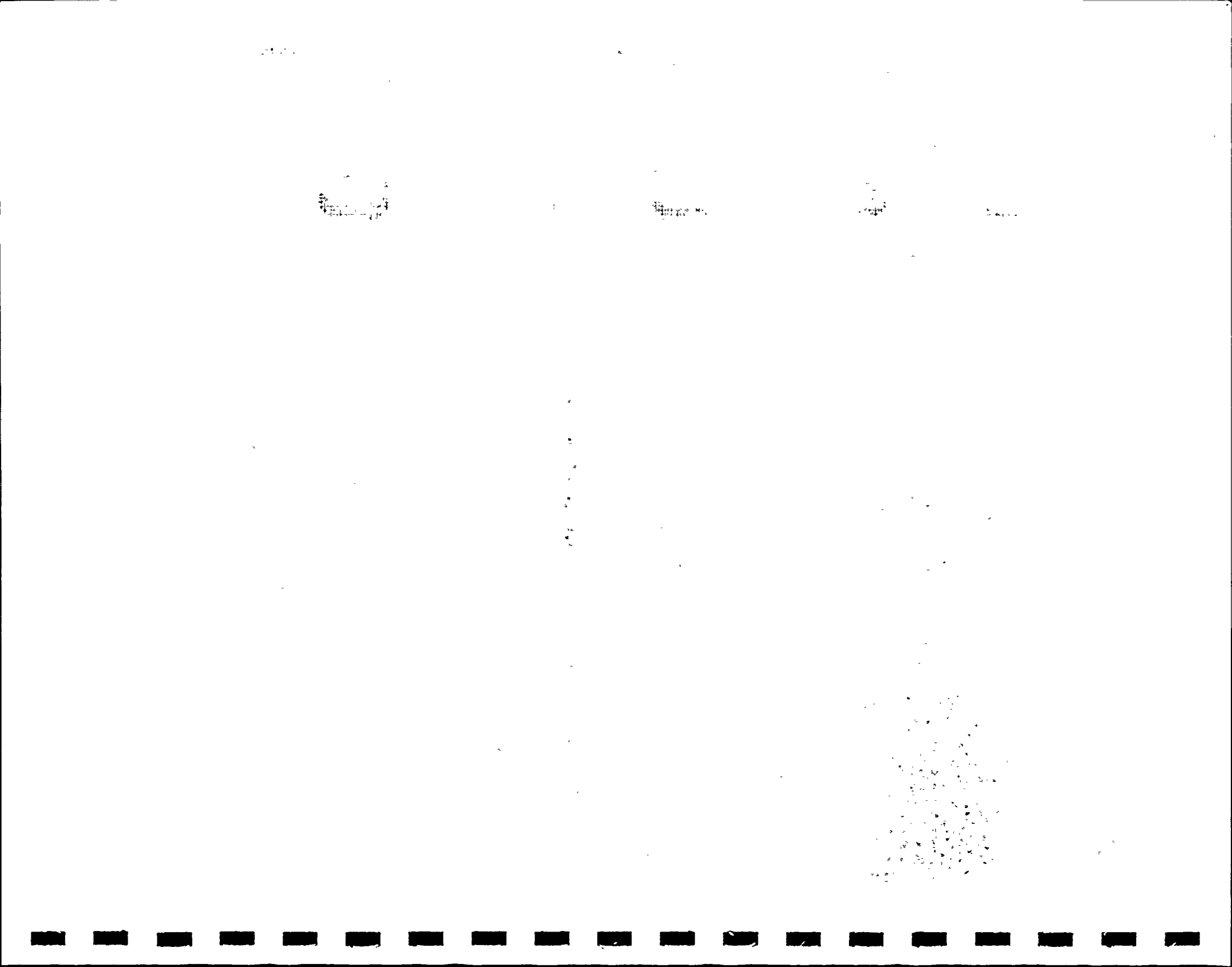

Figure 7.4-1 traces 1 through 3, reveal the largest peak to peak variations found from the detector signals at 0.3 Hz, 6.8 Hz, and 60 Hz respectively.

A noise to signal ratio (NSR), indicative of the magnitude of core barrel motion at a given power level, is obtained by dividing the peak to peak AC variation by the DC carrier magnitude. As shown below, the noise to signal ratios, computed from data collected on 7/19/78, are compared to those computed from data of 12/16/76 and 6/9/76 while the unit was at 97% and 100% power, respectively.

Noise to Signal Ratios

Freq. (Hz)	7/19/78 - 98% Pwr. Ratio (mv)	%	Displ.* (mil)	12/16/76 - 97% Pwr. Ratio (mv)	%	Displ.* (mil)	6/9/76 - 100% Pwr. Ratio (mv)	%	Displ.* (mil)
0.3	(86/4187)	2.09	--	(74/4120)	1.80	--	(50/4120)	1.21	--
6.8	(44/4187)	1.05	38.9	(36/4120)	0.87	33.2	(26/4120)	0.63	23.8
60	(10/4187)	0.24	--	(11/4120)	0.27	--	(10/4120)	0.24	--

* It should be noted that empirical evidence has shown that at a frequency of 6.8 Hz,approx. 1 mil displacement corresponds to a NSR of 0.027%.

From the above computations, it can be seen that core barrel motion has increased by at least 16% at 6.8 Hz since 12/16/76. It should be noted, however, that the increase in signal magnitude observed from 12/16/76 to 7/19/78 is smaller than the increase from 6/9/76 to 12/16/76 of 39%. It should be kept in mind that the recent 16% increase in magnitude is over a 19 month period whereas the 39% increase was over a 6 month period.

In addition, it appears that core barrel motion at 6.8 Hz, is increasing with time at a rate of approximately 6 mils per year. As is shown in the table below, the magnitude of vibration at 6.8 Hz has increased from 20 mils to 39 mils over a 39 month period.

Month/Year	Mils (peak - to - peak)
4-75	20 (baseline meas.)
6-76	24
12-76	33
7-78	39

Figure 7.4-2 displays the noise to signal ratios obtained from each detector on 7/19/78. Figure 7.4-3 shows the excore detector layout. As can be seen from these figures, predominant core barrel motion is being experienced in the east-west direction in the southern portion of the reactor since the largest magnitude of flux variation is being witnessed by detectors N42 and N43 (based on noise to signal ratios).

Figure 7.4-2

"Noise To Signal Ratios For Excore Detectors"
7/19/78 - 98% Power

Detector	Noise to Signal Ratio (%) @ 0.3 Hz	6.8 Hz	60 Hz
41 Upper	1.67	0.81	0.10
41 Lower	1.38	0.76	0.10
42 Upper	2.05	0.81	0.14
42 Lower	2.01	0.95	0.14
43 Upper	1.72	0.86	0.24
43 Lower	2.05	0.91	0.24
44 Upper	1.19	0.96	0.10
44 Lower	1.53	1.05	0.10

Figure 7.4-3

"Excore Detector Layout"

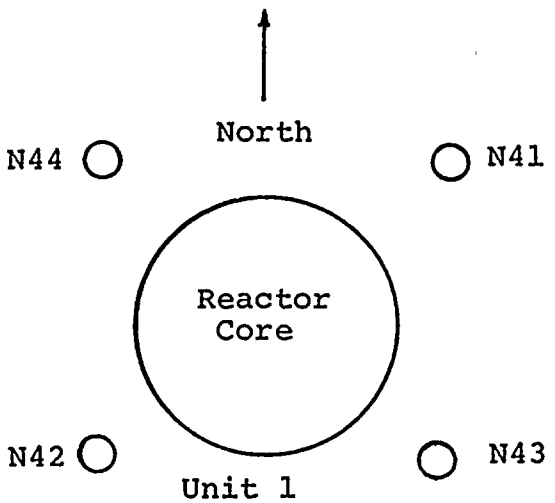

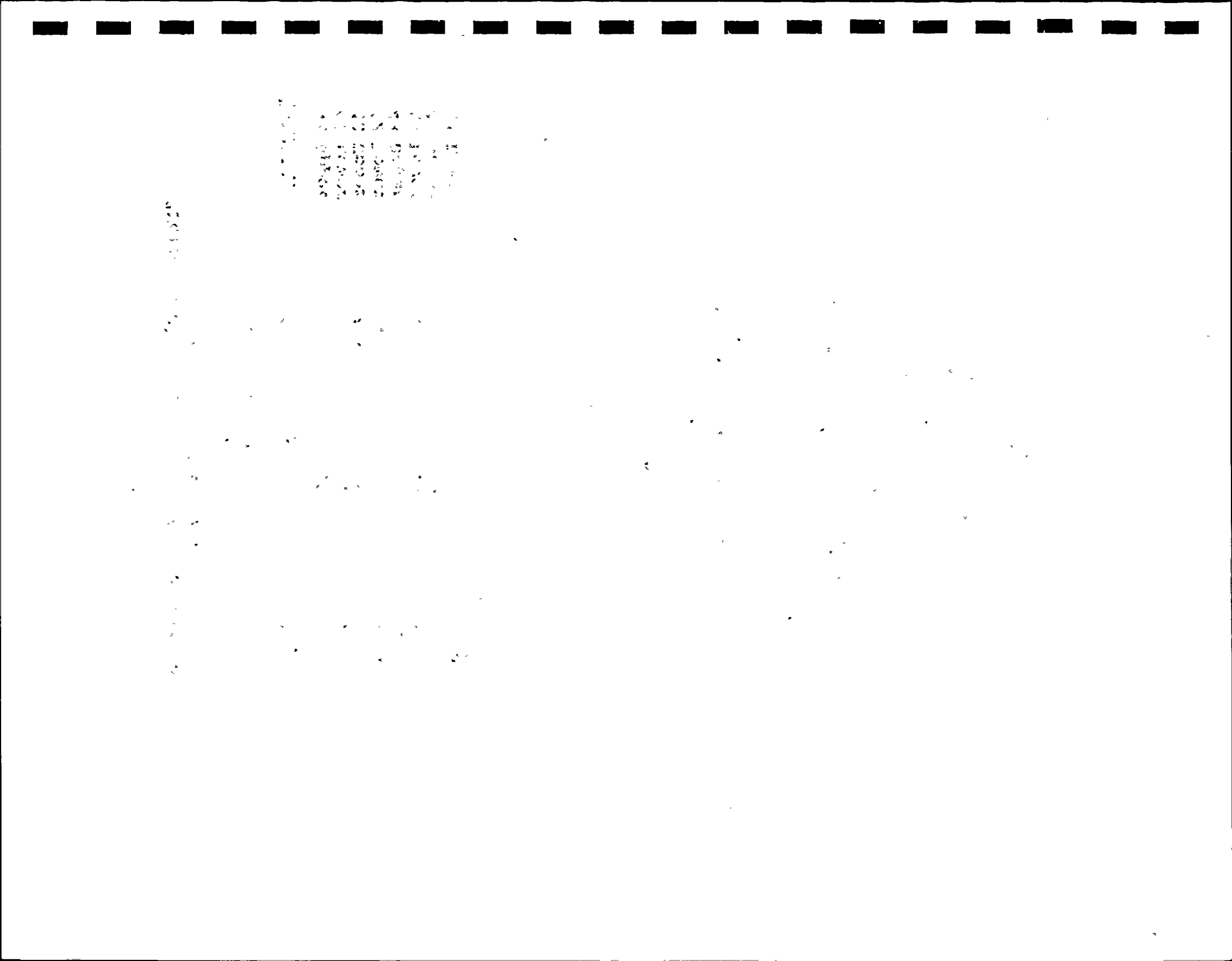

SECTION 7.5

POWER ASCENSION TESTS

PURPOSE

The purpose of this test was to determine the power coefficient of reactivity at various power levels, to verify that the moderator temperature coefficient was within Technical Specification limits, and to perform the incore and excore calibration prior to escalation above 70% reactor thermal power.

SUMMARY OF RESULTS

Power coefficient measurements were performed using two different techniques. One technique used small changes in power level with reactivity measured by boron substitution. The other technique used the data from combining Doppler and moderator coefficients which were measured by rod substitution. During the power ascension testing program, power coefficient data was collected at 50, 70 and 90% of rated thermal power. Table 7.5.1.1 summarizes the power coefficient and moderator temperature coefficient data obtained during the testing program. The moderator temperature coefficient was found to be negative and within the Technical Specification limits at the testing power levels.

Both the power coefficient data measured by using the boron substitution technique, and the data obtained from combining Doppler and moderator coefficient measurements, were compared to review criteria. All the measurements satisfied the review criteria. Figure 7.5.1.1 shows the power coefficient data compared to design prediction. Figure 7.5.1.2 illustrates the design and measured moderator temperature coefficients versus RCS boron concentration. The average deviation between the measured and design moderator temperature coefficient is 5 pcm/%. This suggests that the data obtained in these tests are consistent with HZP MTC data and also confirms that the positive MTC at HZP was real.

Table 7.5.1.2 shows the results of measuring the parameter R. R is defined as the ratio of Doppler coefficient to isothermal temperature coefficient. The measurements were compared to the same ratio, R', calculated by using the Doppler and isothermal temperature coefficient measurements by rod substitution. The largest deviation between R and R' is -19.5% with an average deviation of -12.2%. This suggests that the data obtained in these tests are consistent.

Table 7.5.1.1

Summary of Unit 1 Cycle 3, BOC Power Coefficient Data

Moderator Temperature Coefficient (MTC)

MTC (pcm/°F)	Power Level (%)	Tavg (°F)	Boron Concentration (ppm)
-1.834	50.4	544.7	984.5
-3.923	70.3	554.9	935.0
-4.464	89.5	560.6	887.0

Power Coefficient By Boron Substitution $\frac{\Delta\rho}{\Delta p}$

$\frac{\Delta\rho}{\Delta p}$ (pcm/%)	Power Level (%)	Boron Concentration (ppm)
-13.06	41.7	989.1
-13.31	64.1	929.4
-15.53	81.1	894.8

Power Coefficient By Rod Substitution $\frac{\Delta\rho}{\Delta P}$

$\frac{\Delta\rho}{\Delta p}$ (pcm/%)	MTC*0.208	Doppler Power Coefficient (pcm/%)	Power Level (%)	Boron (ppm) Concentration
-12.46	-0.38	-12.08	48.9	984.5
-12.88	-0.85	-12.03	66.9	935.0
-12.31	-0.93	-11.31	87.7	887.0

Figure 7.S.1.1

Comparison of Power Coefficients
Based on Rod Substitution and Boron Substitution

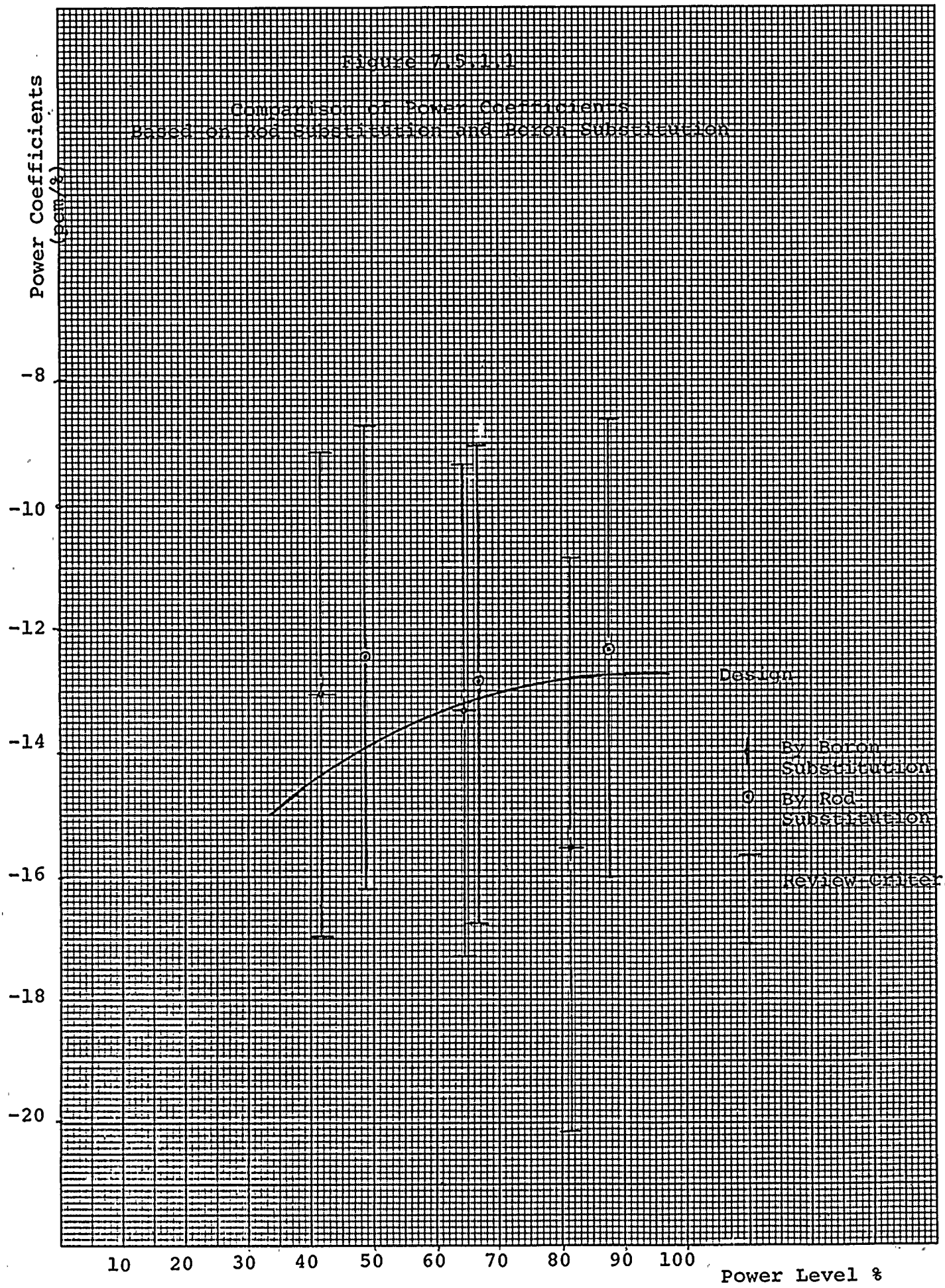

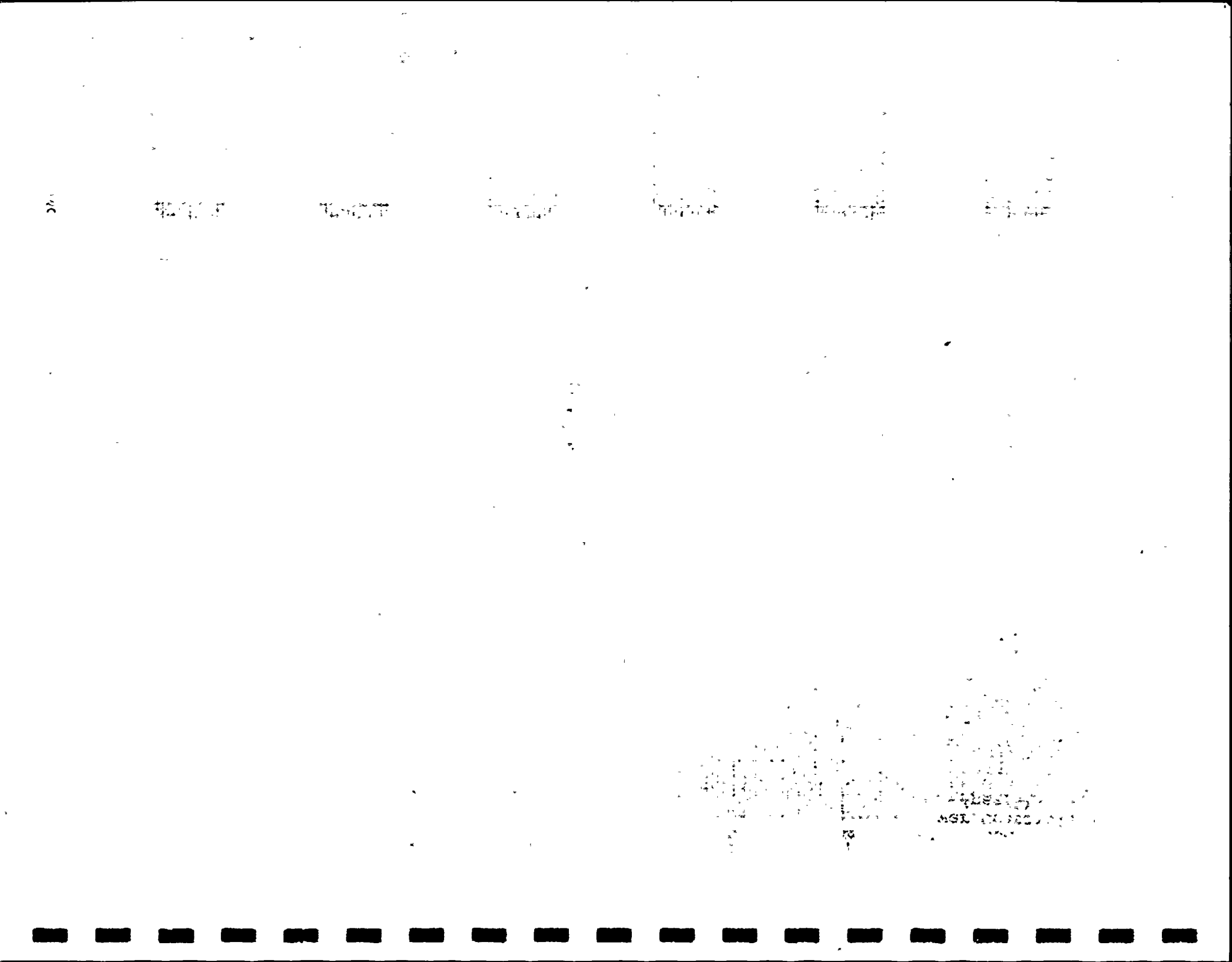

Figure 7.5.1.2

Moderator Temperature Coefficient vs. Boron Concentration Cycle 3, BOC

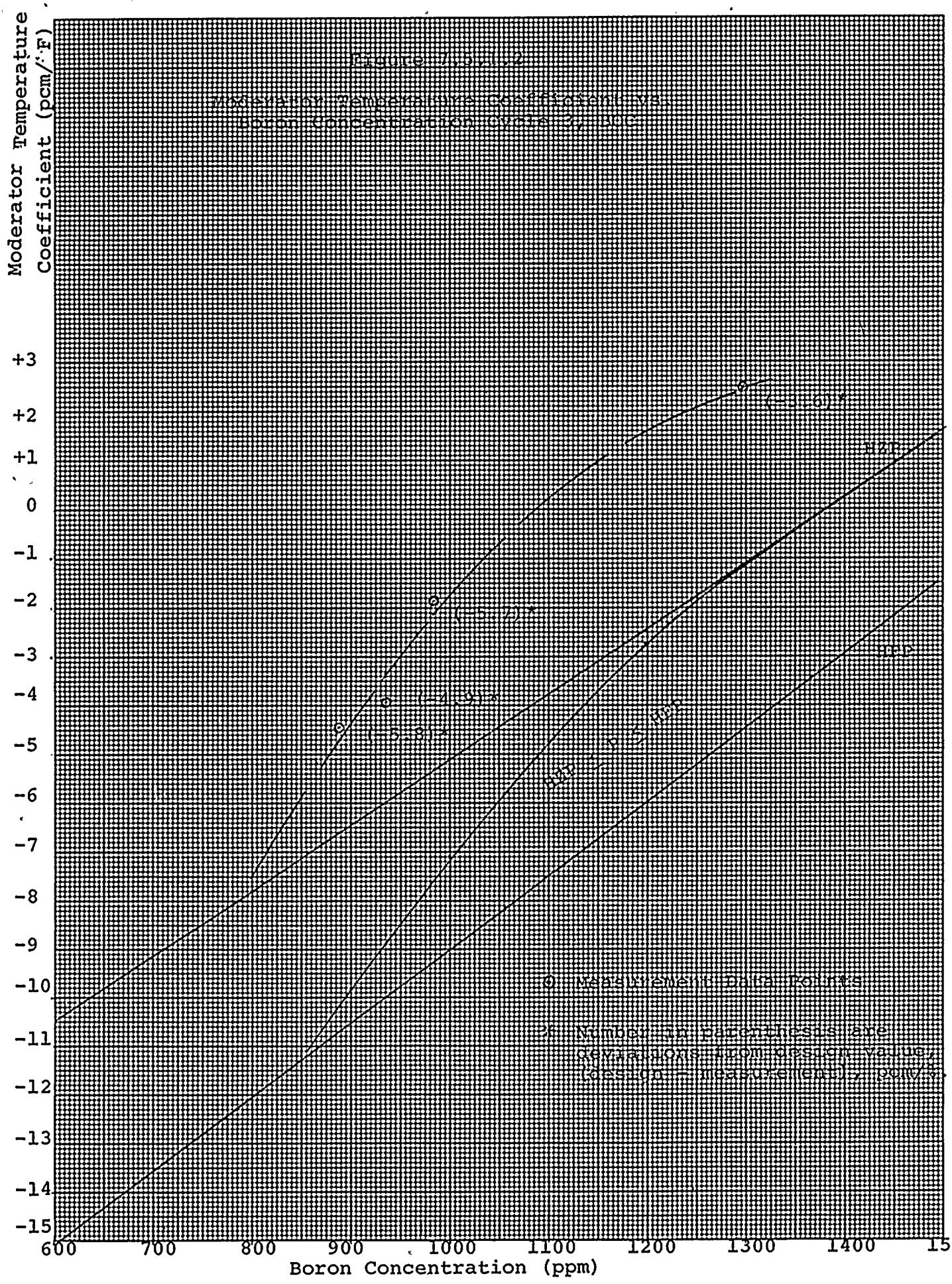

Table 7.5.1.2

Comparison of R and R'

R (°F/%)		R'* (°F/%)	$\frac{\Delta\rho}{\Delta T}$ Isoe. (pcm/°F)	$\frac{\Delta\rho}{\Delta P}$ Dop. (pcm/%)	Deviation $\frac{R-R'}{R'} \times 100$	(%) Power Level	Boron (ppm) Concentration
**	Average						
-2.860							
-3.287	-3.073	-3.816	-3.165	-12.08	-19.5	48.8	984.5
-2.114							
-2.131	-2.123	-2.327	-5.168	-12.03	-8.8	66.6	935.0
-1.174							
-2.327	-1.751	-1.909	-5.664	-10.81	-8.3	86.4	887.0

$$*R' = -\left[\left(\frac{\Delta\rho}{\Delta P}\right)_{Dop} / \left(\frac{\Delta\rho}{\Delta T}\right)_{Iso}\right]$$

** Two measurements were obtained, one data set was obtained by power reduction during the test and the other was obtained by power ascension. The former data was followed by the latter one in column one of Table 7.5.1.2.

DISCUSSION

Since the nuclear instrumentation system has rod shadowing and temperature decalibration effects, the change in power level was monitored by ΔT measurements. A comparison between the actual thermal power and the indicated ΔT power was made. The largest deviation is 2.62% and the mean average is 1.94%. The use of ΔT power was satisfactorily justified.

All parameters of interest (e.g. Tav, power level, etc.) were recorded via the plant process computer (P-250) except reactivity, which was recorded on the reactivity computer. The P-250 allowed rapid data collection for minimizing data taking and human error.

The first power coefficient test, at 50%, was commenced at 2138 hours on June 28, 1978 and completed at 0641 hours on June 29, 1978. The power coefficient test at 70% was started at 1100 hours on July 1, 1978 and completed 2143 hours on July 1, 1978. The last power coefficient test, at 90%, was initiated at 1020 hours on July 4, 1978 and completed at 1755 hours on July 4, 1978.

The ratio of Doppler coefficient to isothermal temperature coefficient, obtained from power coefficient data, R', was compared to the measured ratio of Doppler coefficient to isothermal temperature coefficient measurement, R, in an additional test which will be discussed in detail in the $\Delta T/\Delta P$ Measurement Section.

The techniques used to measure power coefficient moderator temperature coefficient and Doppler coefficient will be discussed in detail in the following sections.

Doppler Coefficient

The Doppler power coefficient was measured by inserting and later withdrawing the control rods. After monitoring parameters associated with reactivity insertion (e.g. Tav, power level, rod position, C_B, etc.), the control rods were inserted a predetermined amount. The amount of reactivity inserted by control rod movement was measured with the reactivity computer. While inserting the control rods, generator load was reduced to keep Tav as constant as possible. A period of approximately 15 min. at the reduced load was again used to monitor reactivity parameters. The control rods were then withdrawn to restore Tav and load to near their original values. Another steady period of data acquisition then commenced.

The following equation was used to calculate the Doppler power coefficient:

$$\text{Doppler Power Coeff. pcm/\%} = \frac{\partial \rho}{\partial Tf}\frac{\partial Tf}{\partial p} = \frac{\left[\frac{\partial \rho}{\partial T}(Tav_2 - Tav_1) + \Delta\rho\ \text{rods} + \Delta\rho xe\right]}{(P_2 - P_1)} + \frac{\partial \rho}{\partial Tf}\ [.208°F/\%]$$

where:

$\frac{\partial \rho}{\partial T}$ = the measured isothermal temp coefficient (pcm/°F)

Tav_2 = final RCS temperature, °F,

Tav_1 = initial RCS temperature, °F,

$\Delta\rho_{rods}$ = change in reactivity due to control rod movement, pcm,

$\Delta\rho_{xe}$ = change in reactivity due to Xe, pcm,

P_2 = final reactor power, %,

P_1 = initial reactor power, %

Figure 7.5.2.1 shows the Doppler coefficient vs. power level compared to design calculations. Table 7.5.2.1 summarizes the review criteria which is given in the following form:

Measured Doppler Power Coeff. + 30% $\leq$ Design Doppler Power Coeff $\leq$ Measured Doppler Coefficient - 30%

All the measured data in Table 7.5.2.1 met the review criteria.

Table 7.5.2.1

Summary of Doppler Coefficients Data

Avg Pwr Lvl %	Measured Doppler* Coefficient (pcm/%)	Average	Measured Doppler Coeff + 30% pcm/%	≤	Design Doppler Coefficient pcm/%	≤	Measured Doppler Coefficient - 30% pcm/%
48.9	-11.87 -12.29	-12.08	-15.70		-12.50		-8.46
66.9	-11.36 -12.69	-12.03	-15.64		-11.40		-8.42
87.7	-10.92 -10.70	-10.81	-14.05		-10.70		-7.57

*Note: Two measurements were obtained, one was obtained by power reduction during the test and the other was obtained by power ascension. The former data was followed by the latter one in column two of Table 8.2.1.

Figure 7.5.2.1

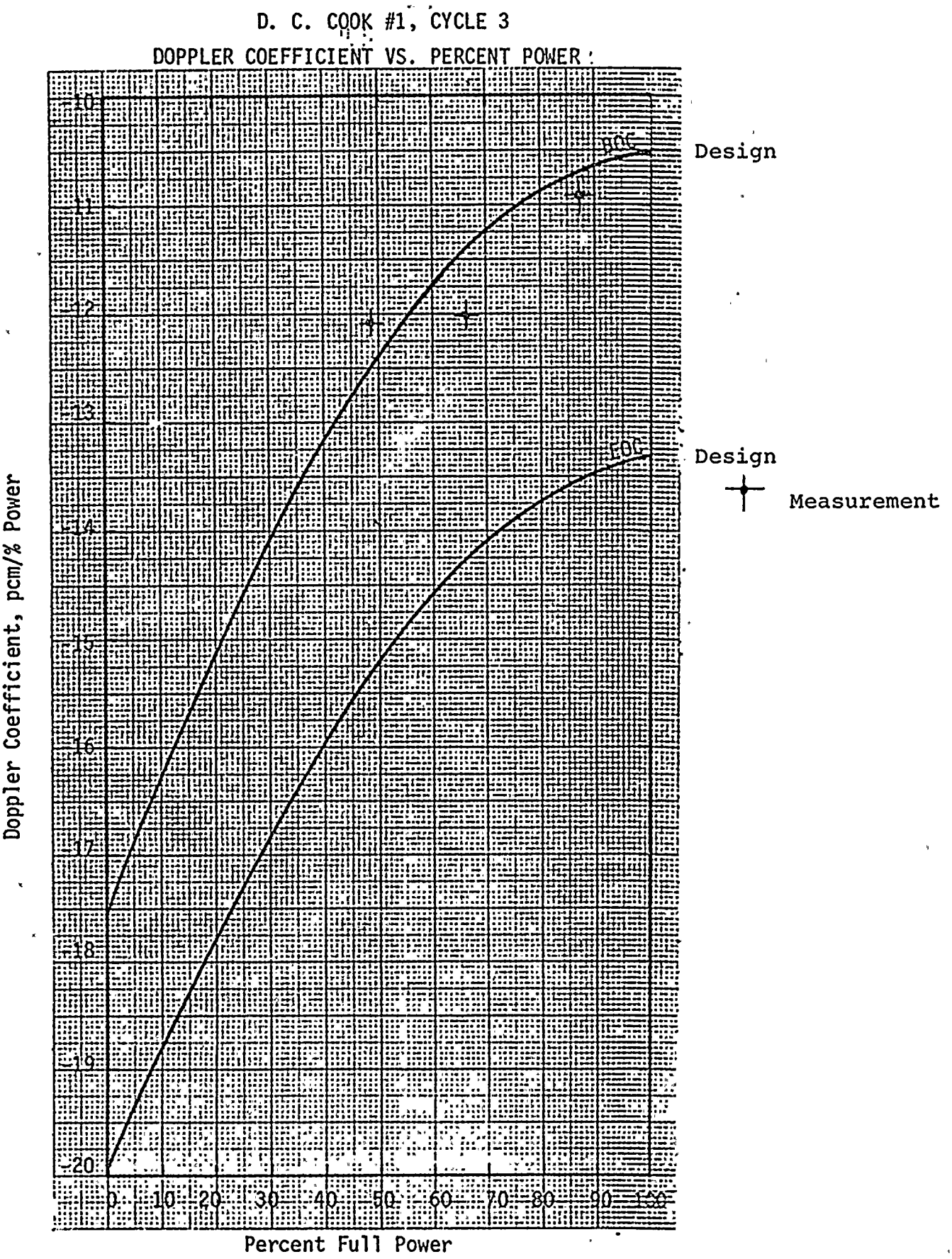
D. C. COOK #1, CYCLE 3
DOPPLER COEFFICIENT VS. PERCENT POWER
Doppler Coefficient, pcm/% Power
-10
-11
-12
-13
-14
-15
-16
-17
-18
-19
-20
0
10
20
30
40
50
60
70
80
90
100
Percent Full Power
BOC
EOC
Design
Design
Measurement

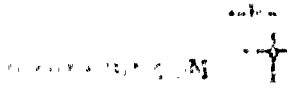

Moderator Temperature Coefficient

The moderator temperature coefficient (MTC) was measured by a technique similar to that described in the Doppler power coefficient discussion. The difference between the two measurements is that in the MTC test, the load (power level) is held constant and Tav allowed to change due to the reactivity insertion from the control rods.

The data was then analyzed by the utilization of the following formula:

$$MTC = \frac{\partial \rho}{\partial Tav} = -\frac{\left(\frac{\partial \rho}{\partial Tf}\ \frac{\partial Tf}{\partial P}\ (P_2 - P_1) + \Delta\rho_{xe} + \Delta\rho\ rods\right)}{(Tav_2 - Tav_1)} - \frac{\partial \rho}{\partial Tf}$$

where:

$\frac{\partial \rho}{\partial Tf}\ \frac{\partial Tf}{\partial p}$ = Doppler power coefficient (measured value), pcm/%,

P_2 = final power level, %,

P_1 = initial power level, %,

$\Delta\rho_{xe}$ = change in reactivity due to Xe, pcm,

$\Delta\rho_{rods}$ = change in reactivity due to control rod motion, pcm,

Tav_2 = final RCS average temperature, °F,

Tav_1 = initial RCS average temperature, °F, and

$\frac{\partial \rho}{\partial Tf}$ = Doppler temperature coefficient (assumed from design calculations), pcm/°F.

Table 7.5.3.1 summarizes the results of measured MTC compared to design MTC. The design moderator temperature coefficient in Table 7.5.3.1 were read from the MTC curve in Figure 7.5.1.2. This curve was plotted between HZP MTC and HFP MTC lines and represents the change of moderator temperature coefficient versus the measured critical boron concentration at various power levels during the power ascension tests. The curve above the design HZP MTC line was plotted based on the measured data. It shows the change of the measured MTC versus critical boron concentrations at various power levels.

From comparison of these two curves, it can be seen that the measured MTC was consistently higher than the design data. The average deviation was 5 pcm/°F.

As discussed in Section 6.1, operating limitations were instituted during power ascension to comply with the Technical Specification limit on the moderator temperature coefficient. These limitations were put into effect at 1130 on June 23, 1978. By 1300 on June 25, 1978, the boron concentration was sufficiently low that the moderator coefficient was negative for any rod configuration. On August 23, 1978, with a burnup of 2100 MWD/MT, sufficient boron letdown had occurred that a positive moderator coefficient could not be attained even in the absence of xenon poison.

Table 7.5.3.1

Summary of Unit 1, Cycle 3
BOC Moderator Temperature Coefficient Data

Average Boron Conc (ppm)	Measured MTC* (pcm/°F)	Average	Design MTC (pcm/°F)	Deviation Design-Meas. (pcm/°F)	Average Tav (°F)
984.5	-1.284 -2.384	-1.835	-7.50	-5.7	549.7
935.0	-3.092 -4.754	-3.923	-8.85	-4.9	554.9
887.0	-3.895 -5.033	-4.464	-10.25	-5.8	560.6

*Note: Two measurements were obtained, one was obtained by decreasing reactor coolant temperature and the other was obtained by increasing reactor coolant temperature. The former data was followed by the latter one in column two of Table 7.5.3.1.

ΔT/ΔP Measurement

The ΔT/ΔP measurement was designed to find the ratio, R, of the Doppler power coefficient to isothermal temperature coefficient. It was used as a consistency test to verify the measured values described in the Doppler coefficient and the Moderator Temperature Coefficient Sections.

The measurement technique was to monitor reactivity parameters for approximately 15 minutes, then the load was reduced. Tav then increased inserting negative reactivity which in turn reduced reactor power. At the reduced load, a steady state was established. Load was then increased to near its original value and another steady state was established. Reactivity parameters were monitored for 15 minutes at these steady states.

The measured value of R was obtained from the following relationship.

$$R = \left(\frac{Tav_2 - Tav_1}{P_2 - P_1}\right) + \frac{\rho_{xe}}{\left(\frac{\partial \rho}{\partial Tav} + \frac{\partial \rho}{\partial Tf}\right)(P_2 - P_1)} - \frac{\frac{\partial \rho}{\partial Tf}\frac{\partial Tavg}{\partial P}\Big|_{prog.}}{\left(\frac{\partial \rho}{\partial Tav} + \frac{\partial \rho}{\partial Tf}\right)}$$

where:

Tav = RCS average temperature, °F,

P_2 = final thermal power level, %,

P_1 = initial thermal power level, %,

Tf = average fuel temperature, °F,

$\frac{\partial \rho}{\partial Tf}$ = Doppler temperature coefficient from design calculation, (pcm/°F)

$\frac{\partial \rho}{\partial Tav} + \frac{\partial \rho}{\partial Tf}$ = isothermal temperature coefficient from measured data (pcm/°F)

$\frac{\partial Tf}{\partial p}$ = programmed ration of change of fuel temperature to thermal power level $\left(\frac{°F}{\%}\right)$

ρ_{xe} = change in reactivity due to Xe (pcm),

$$\frac{\partial Tav}{\partial P}_{prog.} = 0.208 \ (°F/\%)$$

R' is defined as the ratio of the Doppler power coefficient to isothermal temperature coefficient calculated by rod substitution. Figure 7.5.4.1 illustrates the results of the comparison between R and R'. This suggests that the data obtained in these tests are satisfactorily consistent.

Figure 7.5-4.1

Comparison of R and R' Unit 1, Cycle 3 - BOC

Ratio of Doppler Coefficient to Isothermal Temperature Coefficient

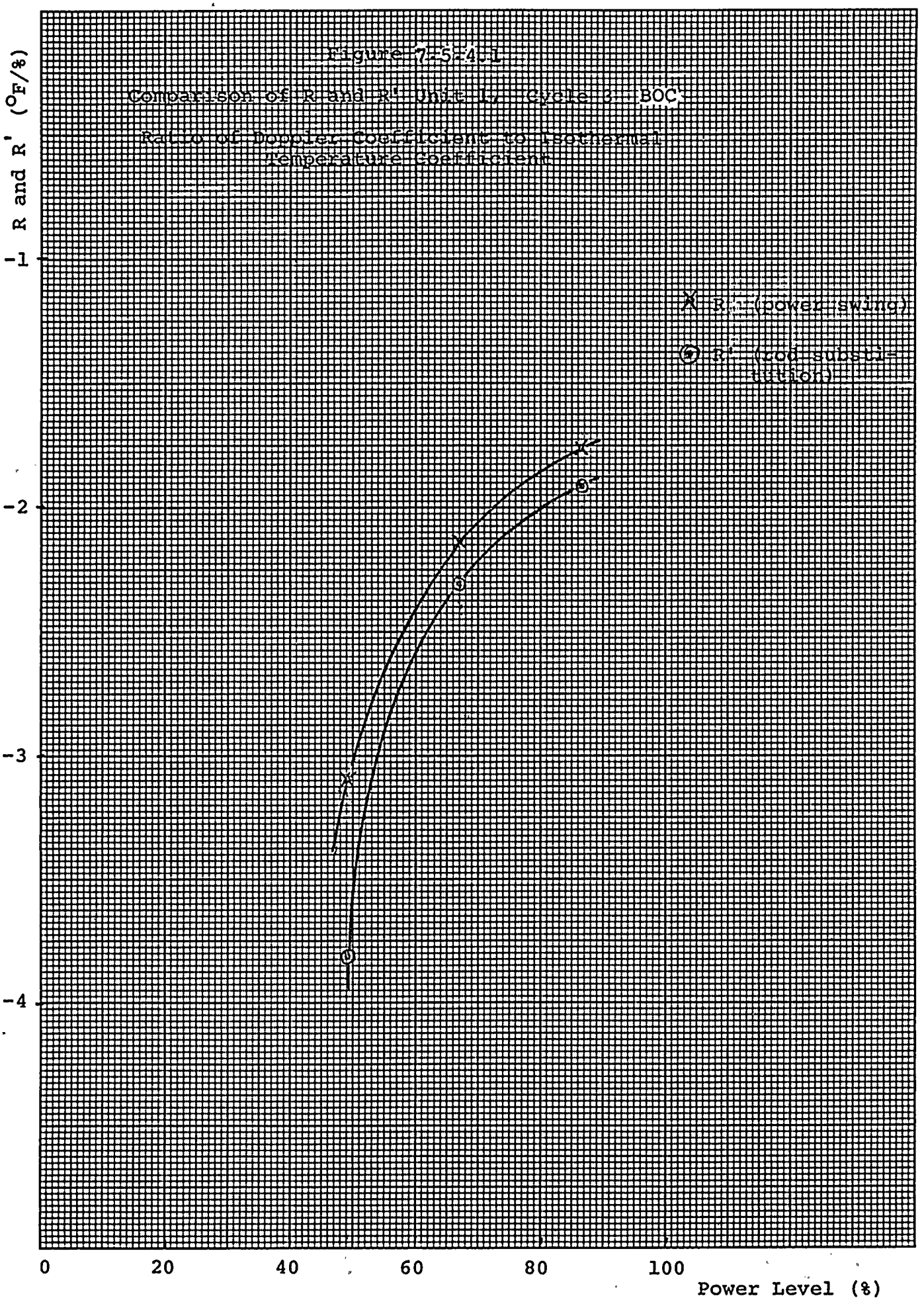

Power Coefficient

The power coefficient was measured by boron substitution. After a fifteen minute monitoring period as in the other tests, a predetermined amount of boric acid was injected into the RCS. As power level dropped, the load was reduced to keep Tav on the programmed value. At the reduced power level, another 15 minute monitoring period was used. However, due to a xenon buildup a steady period was nearly unattainable. Later the reactor was diluted to its original power level and another monitoring period was used. Again, the xenon transient caused difficulty in attaining a steady period for data gathering.

The data was analyzed using the following formula:

$$\text{power coefficient} = \left[\frac{\Delta\rho C_B + \Delta\rho_{xe}}{P_2 - P_1}\right] - \left[\frac{Tav_2 - Tav_1}{P_2 - P_1} - 0.208°F/\%\right] \frac{\partial\rho}{\partial T}$$

where,

$\Delta\rho_{CB}$ = change in reactivity due to a change in boron concentration, pcm,

$\Delta\rho_{xe}$ = change in reactivity due to Xe, pcm,

P_2 = final power level, %,

P_1 = initial power level, %,

Tav_2 = final RCS average temperature, °F,

Tav_1 = initial RCS average temperature, °F,

$\frac{\partial\rho}{\partial T}$ = isothermal temperature coefficient from measured data, pcm/°F,

$.208°F/\%$ = programmed Tav.

Table 7.5.5.1 summarizes the power coefficient data obtained in these tests. Figure 7.5.1.1 illustrates the test results and its comparison with the design data. The data shows some degree of scatter. It is believed that this is due to one or both of the following reasons.

a. Difficulty in obtaining an accurate estimate of the change in boron concentration used, therefore it was obtained by carefully monitoring the amount of boric acid and primary water added to the RCS. However, the primary water and boric acid integrator are also subject to error.

b. The electrical noise is high resulting in errors in the reactivity change during rod movement.

The design data was prepared based on the information from the design report; D. C. Cook Cycle 3 Start-Up Predictions and Nuclear Data for Operations, NX-NF-78-9, March 1978. Doppler coefficients are converted to power coefficients by adding 0.208°F/% times the moderator temperature coefficient. The design power coefficients were compared to the measured power coefficients obtained both from rod substitution and boron substitution.[1]

The results are summarized in Table 7.5.5.1 with the design data, and review criteria of the following form:

Measured Power Coefficient + 30%	$\leq$	Design Power Coefficient	$\leq$	Measured Power Coefficient - 30%

All data meet the review criteria.

[1] It must be noted that there may be systematic differences between rod subsitution and boron substitution data since the flux redistribution is opposite in the two experiments.

TABLE 7.5.5.1

COMPARISON OF POWER COEFFICIENTS

METHOD	POWER LEVEL (%)	MEASURED PWR COEFF. (pcm/%) AVERAGE	MEASURED PWR COEFF. +30%	$\leq$ DESIGN* $\leq$ PWR COEFF. (pcm/%)	MEASURED PWR COEFF. -30%	BORON CONCENTRATION (ppm)	MEASURED PWR** COEFFICIENT (pcm/%)
BY BORON SUBSTIT.	41.7	-13.06	-16.98	-14.30	-9.14	989.1	-11.50 -14.62
	64.1	-13.31	-17.30	-13.00	-9.32	929.4	-12.25 -14.36
	81.1	-15.53	-20.19	-12.85	-10.87	894.8	-14.88 -16.18
BY ROD SUBSTIT.	48.9	-12.46	-16.20	-13.91	-8.72	984.5	
	66.9	-12.88	-16.74	-13.19	-9.02	935.0	Note***
	87.7	-12.31	-16.00	-12.78	-8.62	887.0	

* Design data was obtained by interpolation.

**Two measurements were obtained, one was obtained by power reduction during the test and the other was obtained by power ascension. The former data was followed by the latter one in column seven of Table 7.5.5.1.

***See Tables 7.5.2.1 and 7.5.3.1 for consistency information in rod substitution tests.

Incore-Excore Detector Calibration

The other data obtained in the power ascension tests was the excore-incore calibration. It was done at 50% power level. A total of five full core flux maps were taken for this purpose. The first map was initiated at 0544 hours on June 27, 1978. The last map was completed 0847 hours, June 28, 1978. The results of this work was displayed in Figures 7.5.6.1 through 7.5.6.5. Table 7.5.6.2 summarizes the linear least square fitting equations to correlate the incore axial offset and excore detector current and axial offset data.

Data taking during the maps, consisting of simultaneous readings of power range upper and lower detector current readings and the axial offset generated from the maps was then processed by computer. The computer program calculated a least squares fit of the incore axial offset vs. excore detector current and then scaled the results to 100% RTP using calorimetric data taken during the maps. The incore and excore correlation data is listed in Table 7.5.6.1. This data was used to calibrate the nuclear instrumentation system. Figure 7.5.6.6 is the history plot of power level, flux difference and control bank D position versus time during the period of Incore-Excore Detector Calibration Test.

Table 7.5.6.1

Detector Currents Calculated From The Least Squares Fit Axial Offsets

Upper Currents For Det. 41	195.7645	210.4246	225.0847	239.7449	257.3369	269.0649	283.7251
Lower Currents For Det. 41	371.1333	350.1372	329.1411	308.1450	282.9495	266.1526	245.1567
Upper Currents For Det. 42	261.4087	280.0757	298.7424	317.4894	339.8096	354.7429	373.4099
Lower Currents For Det. 42	404.4536	382.7422	361.0305	339.3191	313.2651	295.8958	274.1843
Upper Currents For Det. 43	285.5188	306.2156	326.9121	347.6689	372.4448	389.0020	409.6987
Lower Currents For Det. 43	487.9353	460.6987	433.4624	406.2261	373.5422	351.7532	324.5166
Upper Currents For Det. 44	219.0677	237.4917	255.9156	274.3396	296.4482	311.1875	329.6113
Lower Currents For Det. 44	365.0652	345.0554	325.0457	305.0359	281.0239	265.0161	256.0005
Axial Offset %	-30	-20	-10	0	+10	+20	+30

Table 7.5.6.2

Correlations Between Incore Axial Offset and Excore Detector Current And Excore Axial Offset Data

Upper Currents For Det. 41	Upper Current = 1.4660 *(Incore A.O.) + 239.7449
Lower Currents For Det. 41	Lower Current =-2.0996 *(Incore A.O.) + 308.1450
Upper Currents For Det. 42	Upper Current = 1.8667 *(Incore A.O.) + 317.4094
Lower Currents For Det. 42	Lower Current = -2.1712 *(Incore A.O.) + 339.3191
Upper Currents For Det. 43	Upper Current = 2.0697 *(Incore A.O.) + 347.6089
Lower Currents For Det. 43	Lower Current = -2.7236 *(Incore A.O.) + 406.226
Upper Currents For Det. 44	Upper Current = 1.8424 *(Incore A.O.) + 274.3396
Lower Currents For Det. 44	Lower Current =-2.0010 *(Incore A.O.) + 305.0359
Incore Axial Offset Det. 41	Incore A.O. = 1.5314 *(Excore A.O.) + 18.8284
Incore Axial Offset Det. 42	Incore A.O. = 1.6062 *(Excore A.O.) + 5.2680
Incore Axial Offset Det. 43	Incore A.O. = 1.5570 *(Excore A.O.) + 11.8963
Incore Axial Offset Det. 44	Incore A.O. = 1.4969 *(Excore A.O.) + 7.8588

Figure 7.5.6.1 Incore A.O. vs. Excore A.O.

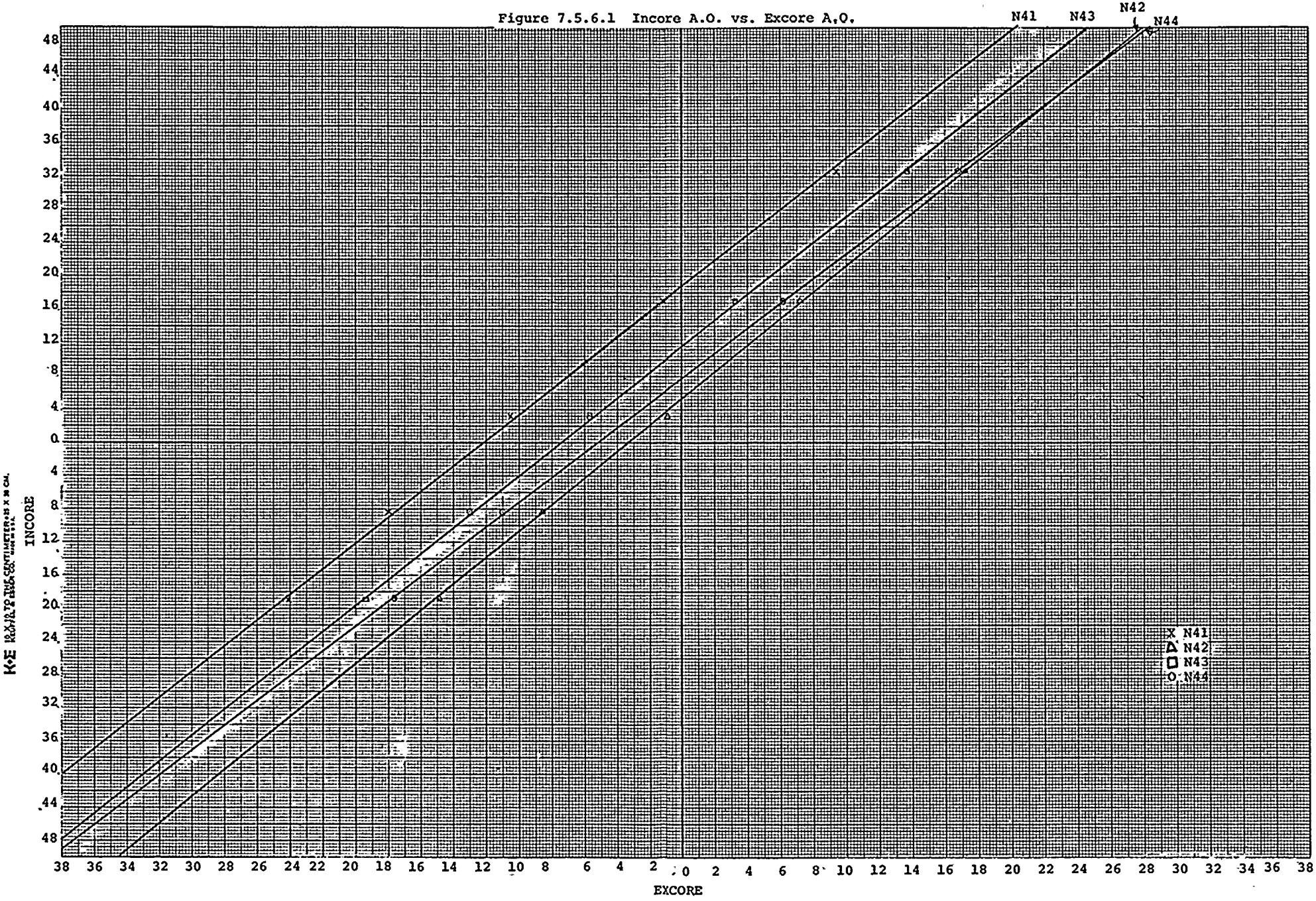

Figure 7.5.6.2

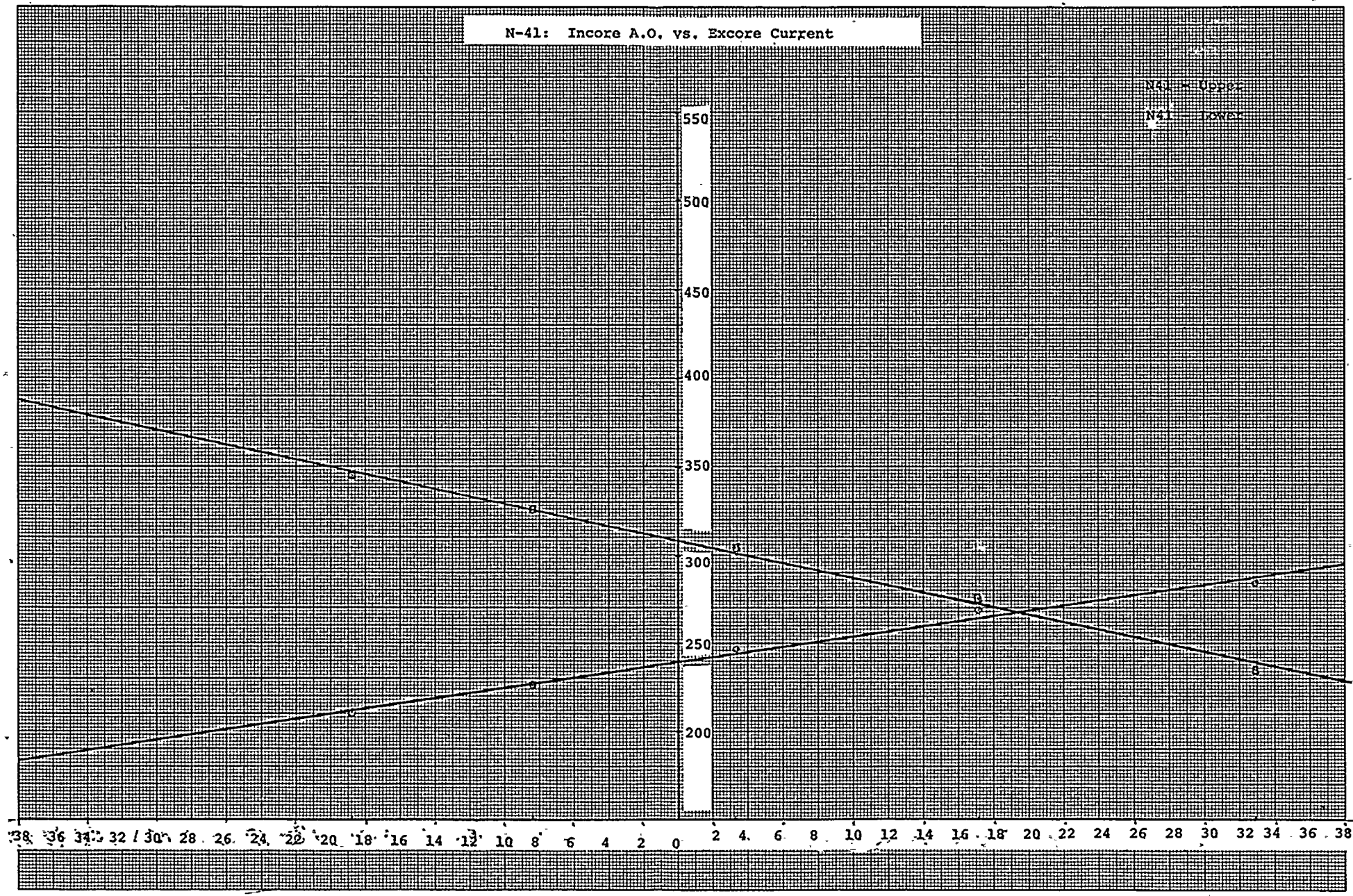
N-41: Incore A.O. vs. Excore Current
N41 - Upper
N41 - Lower
550
500
450
400
350
300
250
200
38 36 34 32 30 28 26 24 22 20 18 16 14 12 10 8 6 4 2 0 2 4 6 8 10 12 14 16 18 20 22 24 26 28 30 32 34 36 38

Figure 7.5.6.3 N-42: Incore A.O. vs. Excore Current

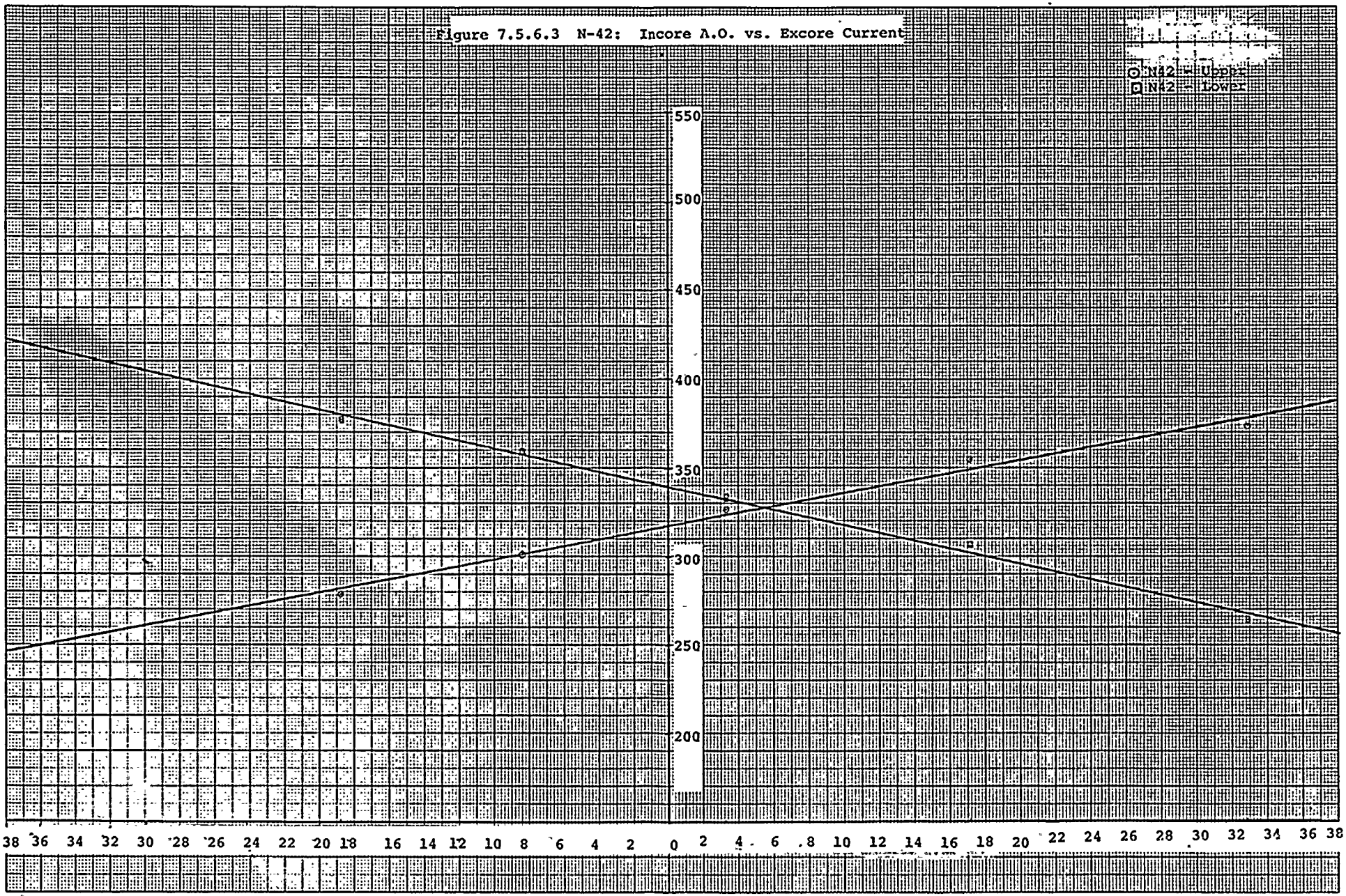

Figure 7.5.6.4 N-43: Incore A.O. vs. Excore Current.

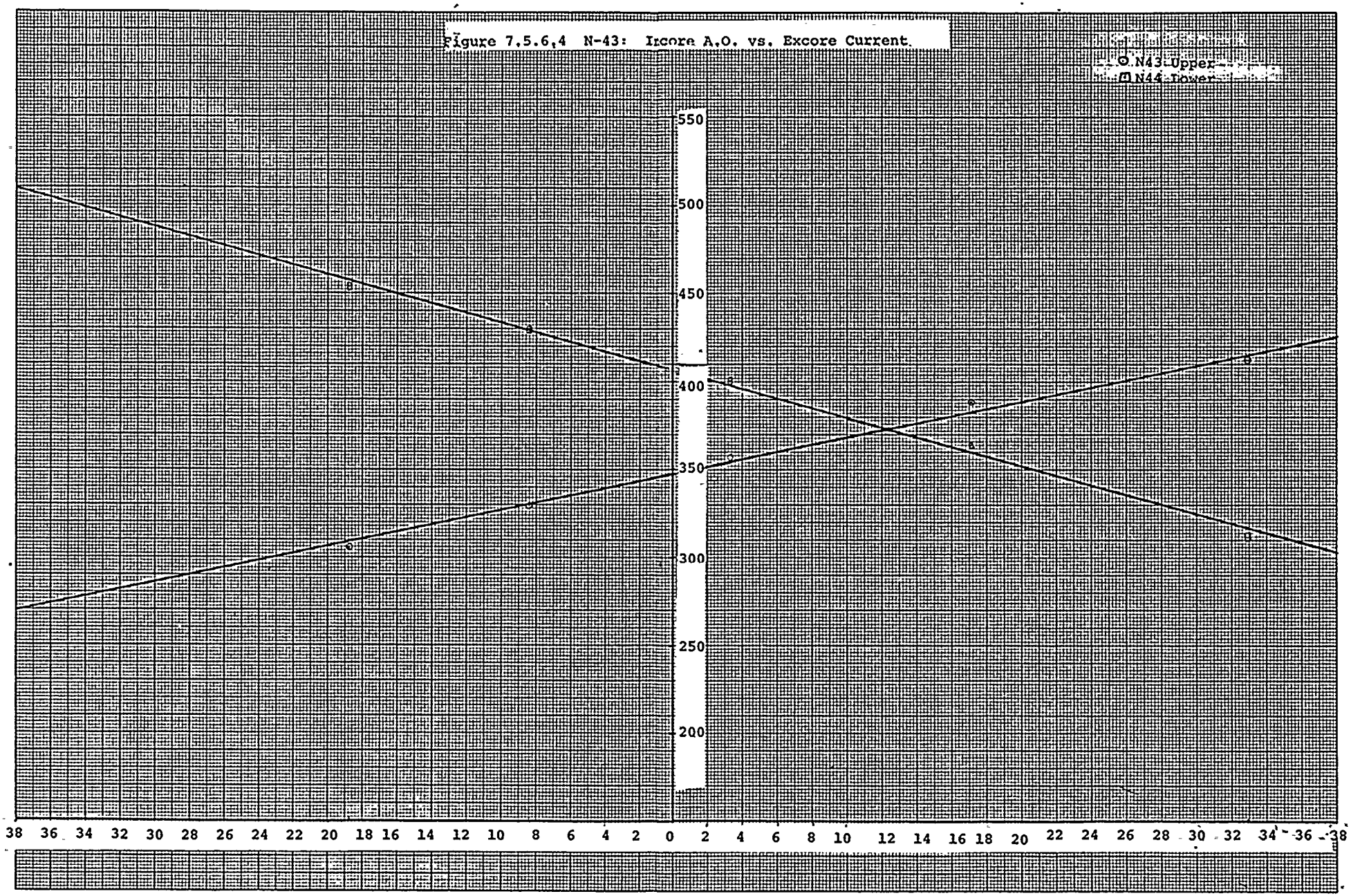

Figure 7.5.6.5 N-44: Incore A.O. vs. Excore Current

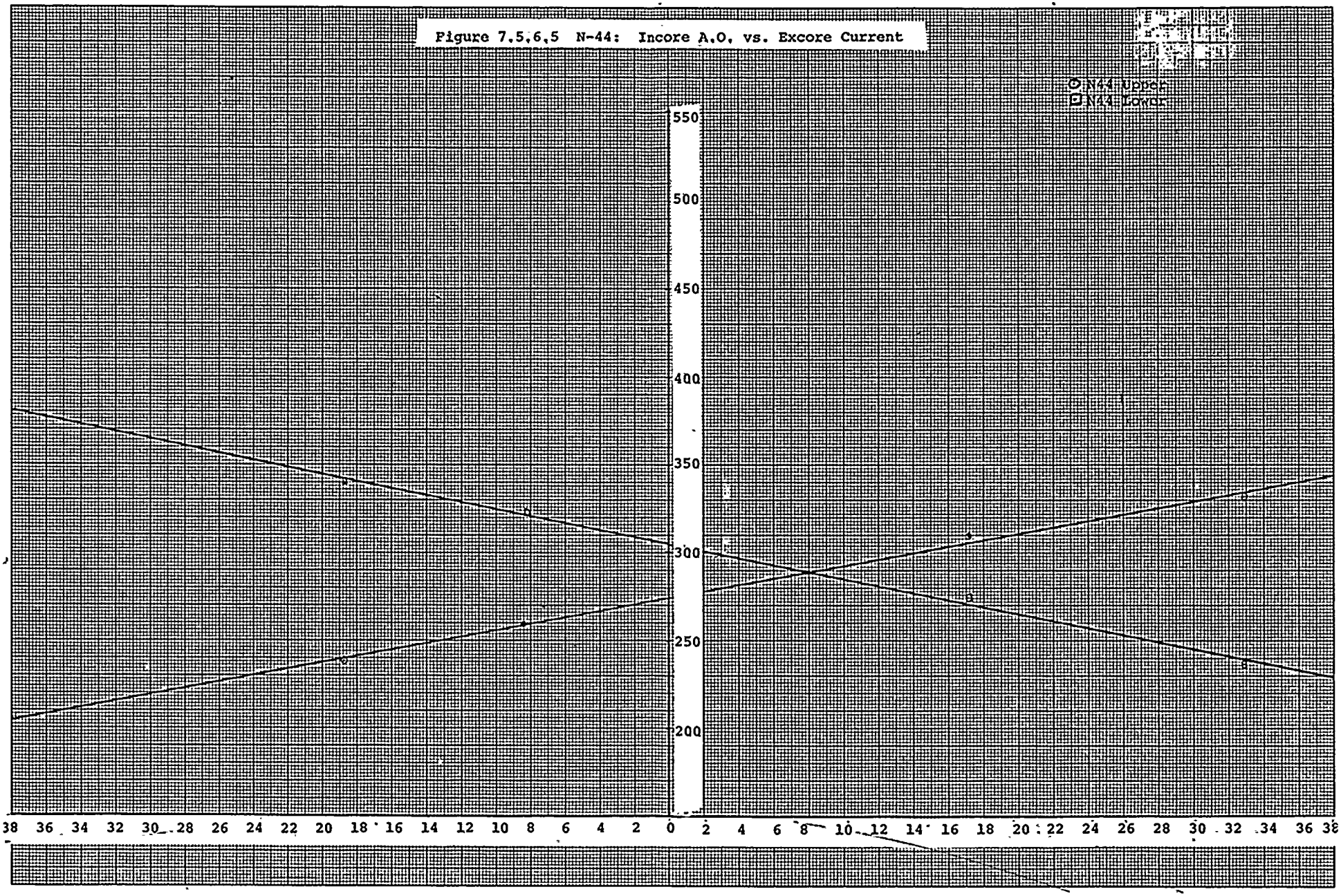

Figure 7.5.6.6 History of Flux Difference, Power Level and Control Bank D Position Versus Time

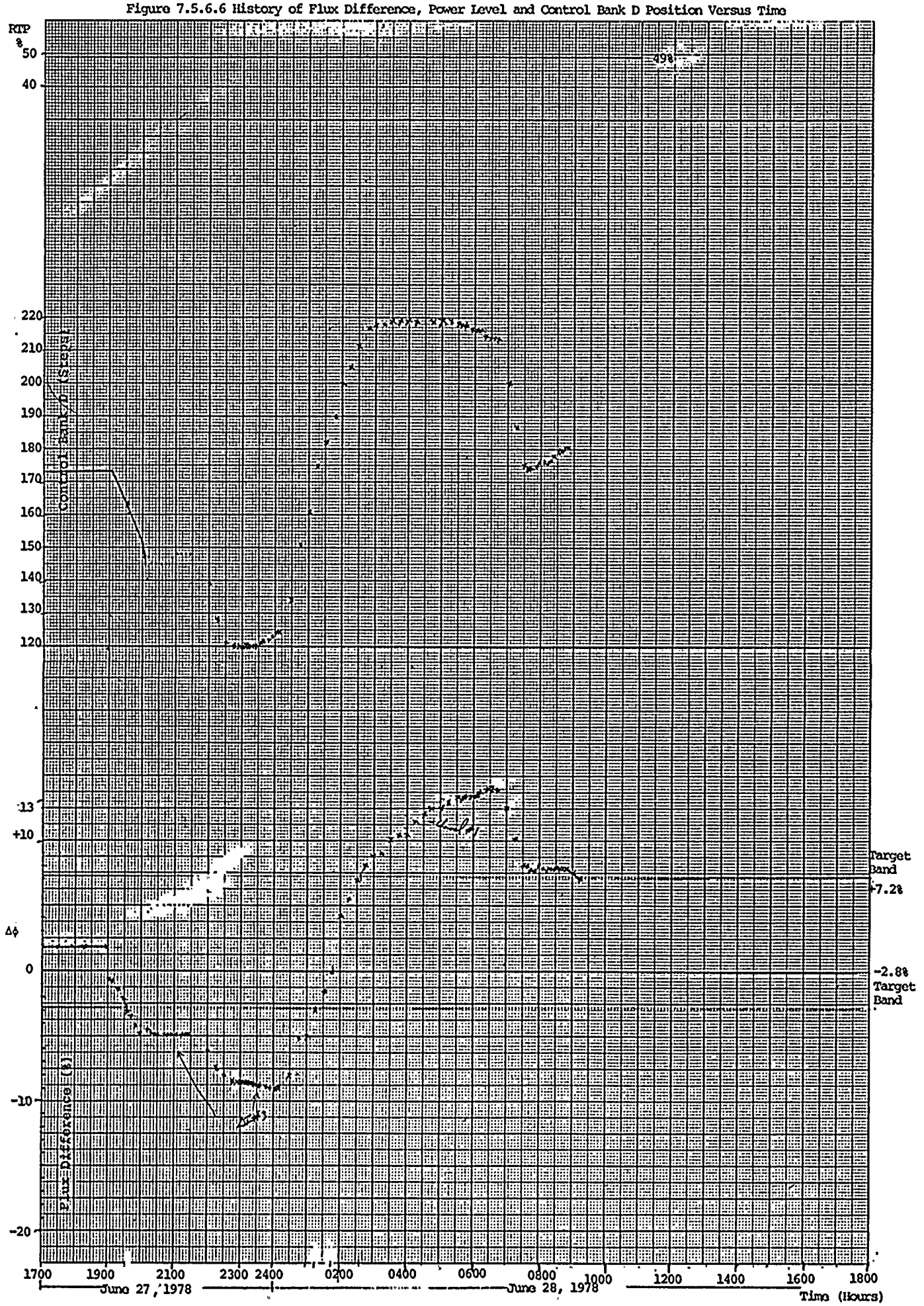

SECTION 8.0

CORE POWER DISTRIBUTION MEASUREMENTS

PURPOSE

The purpose of this section is to describe the core power distribution measurements made to verify design calculations, to show compliance with Technical Specifications, and to provide data for the calibration of the APDMS.

SUMMARY OF RESULTS

Power distribution measurements from incore moveable detector flux maps were obtained at various power levels in the power ascension testing program. All measurements were found to be within Technical Specification limits and the measured horizontal power distribution agreed well with design values. Table 8-1 gives a summary of the peaking factors at the various power levels. Although the power level was initially limited to 97% because of the APDMS, subsequent burnup has allowed the unit to operate at 100%.

DISCUSSION OF TEST

During the power escalation program, flux maps were obtained at each of the major testing plateaus. The power distributions were calculated by the DETECTOR code from raw incore thimble data using analytic factors supplied by the fuel vendor. Figure 8-1 shows the normalized power distribution at 99% power. Figure 8-2 shows the relative errors between measured and design values of assembly $F_{\Delta H}$. As can be seen from the rather small errors (maximum of 11.7% along the periphery) the measured power distribution agrees well with the design predictions.

At 50% power, data for the incore/excore detector calibration was obtained. This data was also used for the initial APDMS calibration (Table 8-2). Due to the penalized values of Fq, as measured by the APDMS ($Fq = Fz \times \bar{R}j$), power level was limited to 97%. Subsequent burnup of 668 MWD/MTU and updating of $\bar{R}j$'s, using the higher power and higher burnup analytical factors, permitted power operation at 100%.

The 100% axial flux difference (ΔI) target was measured using FCFM 103 - 18 at 99.1% power and CBD at 204 steps. The 100% target value is +0.64%. The target band is shown in Figure 8-3.

Table 8-1

Core Power Distribution*

Map No.	Power (%)	$F^N_{\Delta H}$	$F^{L\ 1}_{\Delta H}$	F_Q	F^L_Q	F_{XY}	F^L_{XY}
103-05	36.3	1.4956	1.7023	2.0143	3.8403	1.7287	1.9278
103-11	50.0	1.4714	1.6611	2.4413	3.7011	1.5554	1.7051
103-13	70	1.4751	1.6020	1.8826	2.7543	1.6028	1.6444
103-14	89.5	1.4705	1.5417	1.8353	2.1452	1.5857	1.5825
103-18	99.1	1.4307	1.5128	1.7979	1.9682	1.5399	1.5529

$^1F^L_{\Delta H} = 1.51\ [1.0 + 0.2(1-P)]$

*These are penalized values for peak $F_{\Delta H}$, F_{XY}, F_Q.

NOTE: The peak values do not necessarily have the lowest margin.

Table 8-2 APDMS [Fj(z)]s Limit Check

$$[Fj(z)]s = \frac{(Fq \text{ max limit})\ [k(z)]}{(Rj) \times (P_L) \times (1.03) \times (1+\sigma j) \times (1.07) \times (Fp) \times [\overline{G}(z)max]}$$

Fq max limit = 1.95 Fp = 1.00 G(z)max = 1.00

Power level which APDMS is set up for: $P_L = 0.97$

APDMS Detector	FMS Detector	Thimble Number	Location	New $\overline{R}j$	σj	6.0 ft k(z)=1.000	11.1 ft k(z)=0.935	12.0 ft k(z)=0.505
2	B	12	D10	1.4661	0.02	1.21977	1.14049	.61598
3	C	24	C5	1.4075	0.02	1.27056	1.18797	.64163
4	D	35	L13	1.4047	0.02	1.27308	1.19034	.64291
1	F	54	N6	1.4014	0.02	1.27609	1.19314	.64442
Spare	A	7	D12	1.4380	0.02	1.24301	1.16277	.62802
Spare	E	49	C8	1.4148	0.02	1.26400	1.18184	.63832

103018 MAP 103-18 ANALYZED WITH REV. 500 MWD/MTU FACTORS
AEP - THIMBLE DATA

NUCLEAR PEAKING FACTORS FOR ENTHALPY RISE FOR ASSEMBLAGES IN THE POWER NORMALIZATION-

	R	P	N	M	L	K	J	H	G	F	E	D	C	B	A
1					0.589	0.774	0.880	0.840	0.883	0.814	0.630				
2			0.663	0.968	1.073	0.913	1.188	0.915	1.186	0.937	1.088	0.852	0.584		
3		0.629	1.082	1.032	1.015	1.077	0.926	0.897	0.922	1.058	1.001	0.964	1.008	0.584	
4		0.922	0.972	1.003	1.183	1.200	1.122	1.105	1.128	1.198	1.178	0.992	0.957	0.834	
5	0.634	1.113	1.018	1.192	1.049	1.208	1.205	1.022	1.209	1.198	1.030	1.167	0.978	1.050	0.586
6	0.820	0.934	1.056	1.203	1.202	1.018	1.180	1.110	1.196	1.015	1.185	1.181	1.045	0.901	0.755
7	0.905	1.228	0.920	1.123	1.184	1.162	0.971	0.935	1.009	1.186	1.187	1.116	0.913	1.161	0.842
8	0.878	0.972	0.911	1.087	0.983	1.070	0.919	0.928	0.930	1.099	1.009	1.096	0.888	0.931	0.826
9	0.876	1.198	0.950	1.103	1.182	1.176	0.993	0.926	0.965	1.174	1.200	1.113	0.910	1.160	0.839
10	0.802	0.937	1.085	1.192	1.215	1.023	1.192	1.086	1.149	1.004	1.197	1.181	1.029	0.979	0.821
11	0.636	1.161	1.063	1.179	1.041	1.207	1.188	0.994	1.188	1.196	1.033	1.163	0.969	1.163	0.638
12		0.923	1.033	1.017	1.182	1.198	1.099	1.091	1.125	1.190	1.161	0.969	0.973	0.928	
13		0.636	1.076	1.013	0.995	1.062	0.921	0.878	0.908	1.048	1.017	0.976	1.058	0.634	
14			0.663	0.922	1.100	0.923	1.184	0.916	1.126	0.960	1.126	0.902	0.623		
15					0.630	0.796	0.850	0.836	0.850	0.800	0.619				

FIGURE 8-1

103018 MAP 103-18 ANALYZED WITH REV. 500 MWD/MTU FACTORS

AEP - THIMBLE DATA

RELATIVE ERRORS IN F SUB DELTA H CALCULATED FROM WEIGHTED THEORETICAL FACTORS, (CALC.-MEAS.)/MEAS.

	R	P	N	M	L	K	J	H	G	F	E	D	C	B	A
1					0.006	-0.008	-0.027	-0.000	-0.031	-0.056	-0.060				
2			-0.116	-0.114	0.003	0.015	0.002	0.028	0.005	-0.011	-0.011	0.007	0.004		
3		-0.069	-0.065	-0.062	-0.003	-0.001	0.017	0.025	0.021	0.017	0.011	0.004	0.003	0.004	
4		-0.074	-0.000	0.004	0.015	0.015	0.022	0.022	0.017	0.017	0.019	0.014	0.016	0.024	
5	-0.077	-0.044	-0.016	0.005	0.013	0.014	0.016	0.015	0.013	0.022	0.032	0.026	0.024	0.013	-0.002
6	-0.079	-0.030	0.000	0.000	0.011	0.015	0.028	-0.015	0.014	0.018	0.026	0.019	0.011	0.005	0.001
7	-0.069	-0.046	0.004	0.002	0.017	0.036	0.058	0.043	0.018	0.015	0.014	0.008	0.012	0.009	0.001
8	-0.058	-0.042	-0.011	0.020	0.036	0.044	0.051	0.074	0.040	0.016	0.010	0.011	0.014	-0.000	0.002
9	-0.038	-0.022	-0.028	0.020	0.018	0.024	0.034	0.052	0.064	0.026	0.003	0.011	0.014	0.010	0.004
10	-0.059	-0.034	-0.027	0.009	0.000	0.010	0.018	0.037	0.056	0.029	0.015	0.019	0.027	-0.075	-0.080
11	-0.081	-0.084	-0.057	0.016	0.020	0.014	0.031	0.044	0.031	0.024	0.028	0.029	0.033	-0.085	-0.083
12		-0.075	-0.059	-0.010	0.016	0.016	0.044	0.036	0.020	0.024	0.034	0.039	-0.001	-0.080	
13		-0.079	-0.060	-0.044	0.016	0.013	0.023	0.047	0.037	0.027	-0.005	-0.008	-0.043	-0.075	
14			-0.117	-0.070	-0.021	0.004	0.006	0.028	0.057	-0.035	-0.044	-0.050	-0.060		
15					-0.060	-0.035	0.007	0.005	0.007	-0.039	-0.042				

FIGURE 8-2

THE MEAN VALUE = -0.0026 AND THE STANDARD DEVIATION = 0.0382 FOR THE ABOVE 193 VALUES

THE MEAN OF THE ABSOLUTE VALUES = 0.0290 . THE MAXIMUM MAGNITUDE = 0.1165 AT 14-N

FIGURE 8-3 AXIAL FLUX DIFFERENCE vs. POWER LEVEL

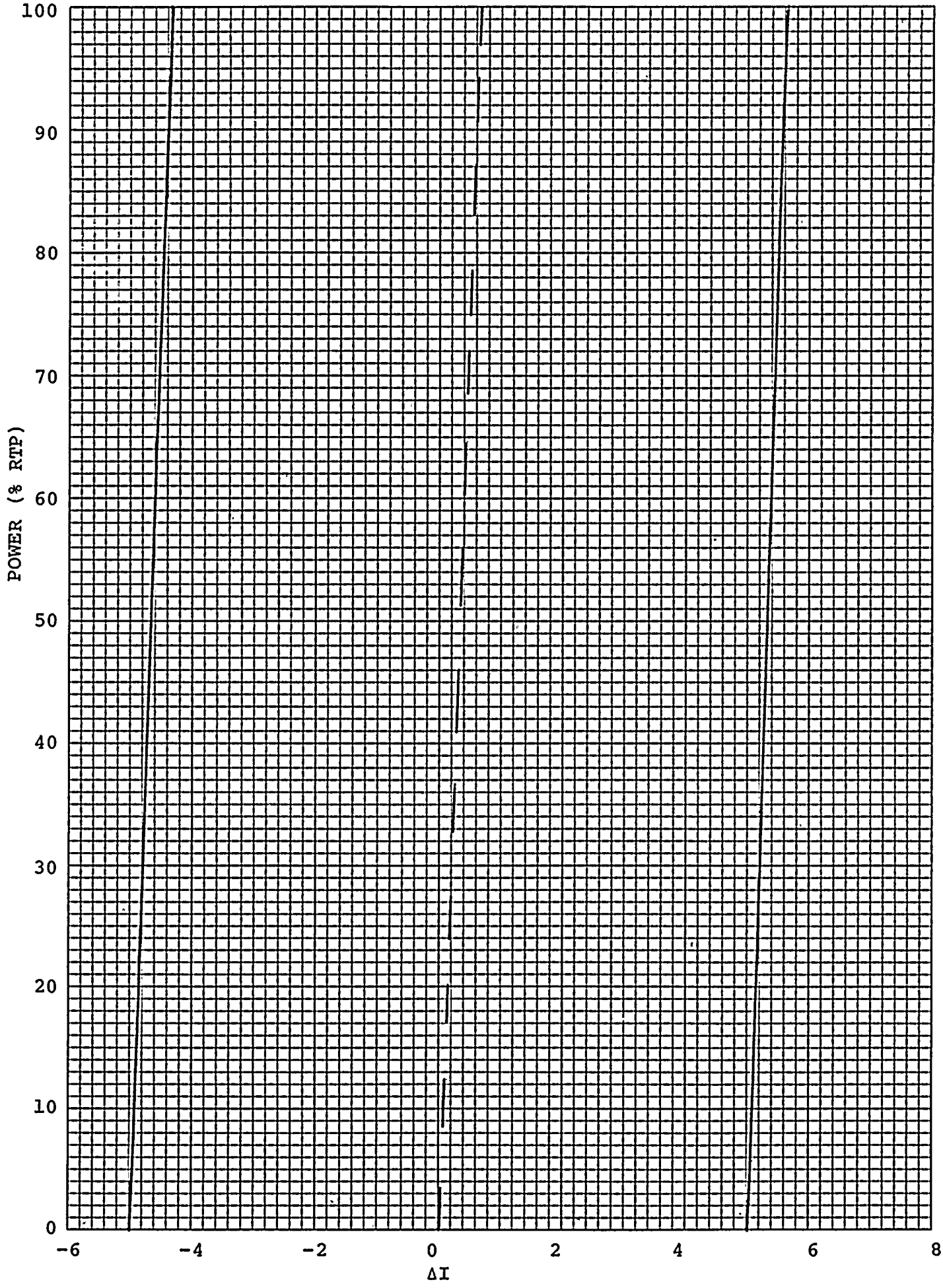

Appendix A

Fuel Examination Core 2

D. C. Cook Nuclear Power Plant Unit 1

CONTENTS

1. Examination Report

   Introduction
   Summary
   Procedure
   Discussion
   Conclusions

2. Table of Fuel Assemblies Examined

3. Figures

   1. Starting Sequence for Inspection
   2. Fuel Assembly Positions Cycle 1
   3. Fuel Assembly Positions Cycle 2
   4. Fuel Assembly Positions Cycle 3
   5. Scratch Line Corrosion Site

Introduction

The Indiana and Michigan Power Company Donald C. Cook Nuclear Power Plant, Unit 1 shut down in April, 1978, for refueling. This concluded the second cycle of operation for the core.

In order to determine the general physical condition of the fuel assemblies, a visual inspection of selected fuel assemblies was performed by the Babcock and Wilcox Company under contract to the American Electric Power Service Corporation.

Summary

Eight (8) fuel assemblies were visually examined using remote underwater television. The fuel assemblies examined were manufactured by Westinghouse Electric Corporation and Exxon Nuclear Corporation and operated in the D. C. Cook Nuclear Power Plant, Unit 1, for either one or two cycles.

The overall condition of the fuel assemblies examined and scheduled for reinsertion in Cycle 3 was good and would not preclude their further utilization. The discharged fuel assemblies were also in good condition.

The following characteristics were observed in the Westinghouse manufactured fuel assemblies:

- o Visible bowing of fuel rods
- o Enhanced corrosion sites along the fuel rod scratch line
- o Fuel rods contacting the lower nozzle
- o CRUD patterns were non-uniform and dull
- o All grids were intact

The following characteristics were observed in the Exxon manufactured fuel assemblies:

- o No visible bowing of fuel rods
- o Fuel rods were bright and no blemishes observed
- o Fuel rods contacting the lower nozzle
- o CRUD was uniform and rods appeared bright
- o Grids were intact and were very bright

Procedure

The fuel assemblies were viewed using a Diamond Power Company ST-5 television camera and closed circuit television monitor. The camera was mounted on a bracket designed to set on the fuel storage rack in the spent fuel. The fuel assemblies were suspended from the fuel handling bridge and lowered past the TV camera; the condition of the fuel assembly was observed and the results recorded on video tape. The starting position for scanning each fuel assembly is shown in Figure 1.

The fuel assembly was lowered past the TV camera starting at the bottom nozzle. Half of the fuel rods (8) were observed in each vertical scan. The fuel assembly was then raised past the TV camera, thereby giving two scans of the left side of

the fuel assembly being viewed. The fuel assembly was then moved to the left so that the right half of the fuel assembly was in view and the same scan repeated to complete the visual observation of the side. The fuel assembly was rotated counterclockwise and the above procedure repeated for each side.

Discussion

The fuel assemblies examined are given in Table 1 with their respective burnups and cycles of operation. The position of each fuel assembly for each cycle of operation are given in Figures 2, 3, and 4. The reactor is presently operating in Cycle 3 (Core 3).

The "B" and "C" fuel assemblies all showed what appears to be enhanced corrosion sites on the scratch line of the fuel rods as illustrated in Figure 5.

The scratch line occurs during fuel assembly manufacture since the fuel rods are inserted through the grid cells without keying open the cells. The hard stops scratch the surface of the cladding as the fuel rods are pushed through the grid cell. This appears to create sites where enhanced corrosion can occur. This condition does not appear to affect the integrity of the fuel rod cladding. The "D" fuel assemblies did not exhibit this phenomena. They were manufactured using keyed open grid cells, thereby eliminating the probability of scratching the surface of the fuel rod cladding during manufacture.

All of the fuel assemblies were manufactured with the fuel rods off the bottom nozzle. The "B" and "C" fuel assemblies showed varying amounts of grid relaxation since not all fuel rods were resting on the lower nozzle. The "D" fuel assemblies showed essentially all the fuel rods resting on the lower nozzle, thereby indicating a somewhat higher degree of grid relaxation.

The "B" and "C" fuel assemblies showed visible rod bow. The "D" fuel assemblies showed no visible evidence of rod bow.

The "B" and "C" fuel assemblies had non-uniform CRUD deposits and were generally dull or non-reflective. The "D" fuel assemblies had a uniform deposit and were bright or reflective.

All grids on all the fuel assemblies were intact and only minor scratches were observed. These scratches were due to general fuel assembly handling.

Conclusions

All the fuel assemblies were in generally good condition. The observation of enhanced corrosion sites and rod bow on the "B" and "C" fuel assemblies do not appear to limit further operation of the fuel assemblies. No unusual features were observed on the "D" fuel assemblies.

All "C" and "D" fuel assemblies were recommended for further operation in Cycle 3 of D. C. Cook, Unit 1.

TABLE 1 FUEL ASSEMBLIES EXAMINED

Fuel Assembly	Burnup, MWD/MTU Cycle 1	Cycle 2	Status
+C11D	17,630	29,410	Cycle 3
+C42D	16,740	27,890	Cycle 3
+B57D	20,610	29,930	Discharge
+B63D	19,570	28,970	Discharge
+B26D	19,850	29,260	Discharge
*D58D	--	13,560	Cycle 3
*D60D	--	13,190	Cycle 3
*D61D	--	13,430	Cycle 3

+Manufactured by Westinghouse - Core 1

*Manufactured by Exxon - First Reload

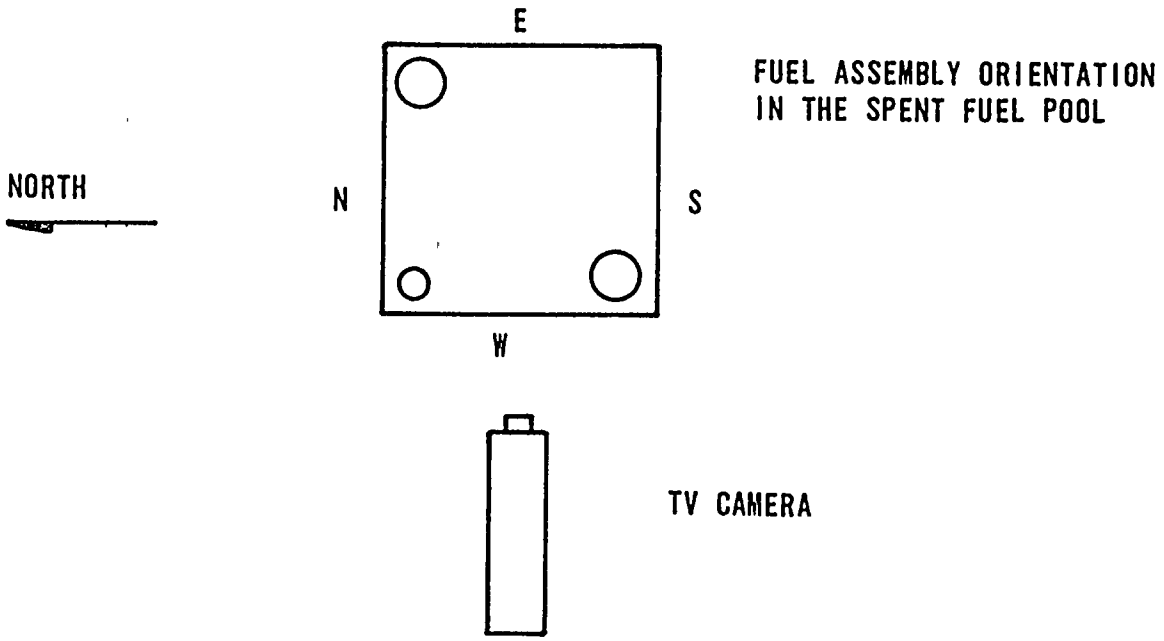

STARTING SEQUENCE FOR INSPECTION

Figure 1

D.C. COOK UNIT 1

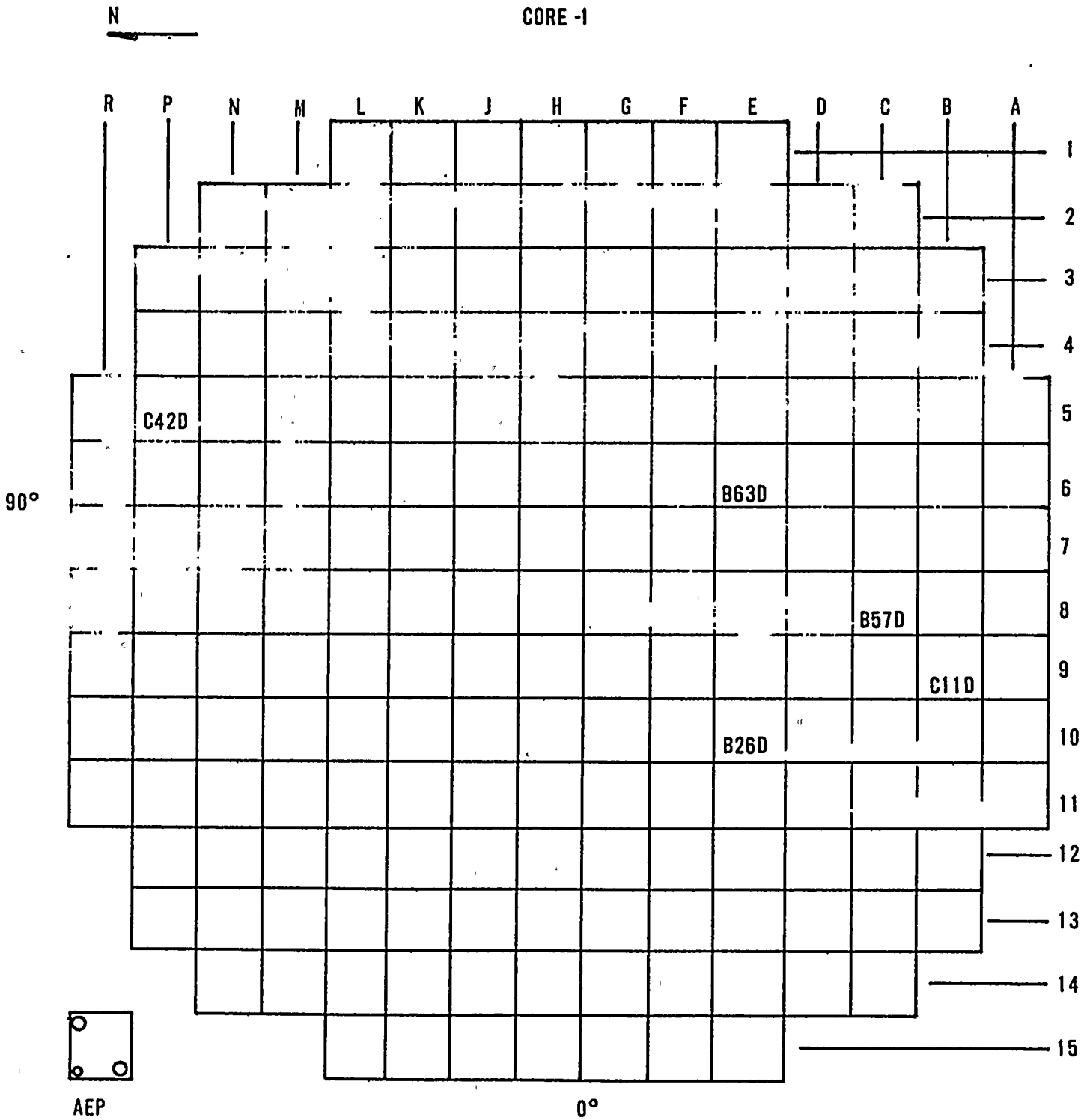

FUEL ASSEMBLY POSITIONS CYCLE 1

Figure 2

D.C. COOK

UNIT 1 CORE 2

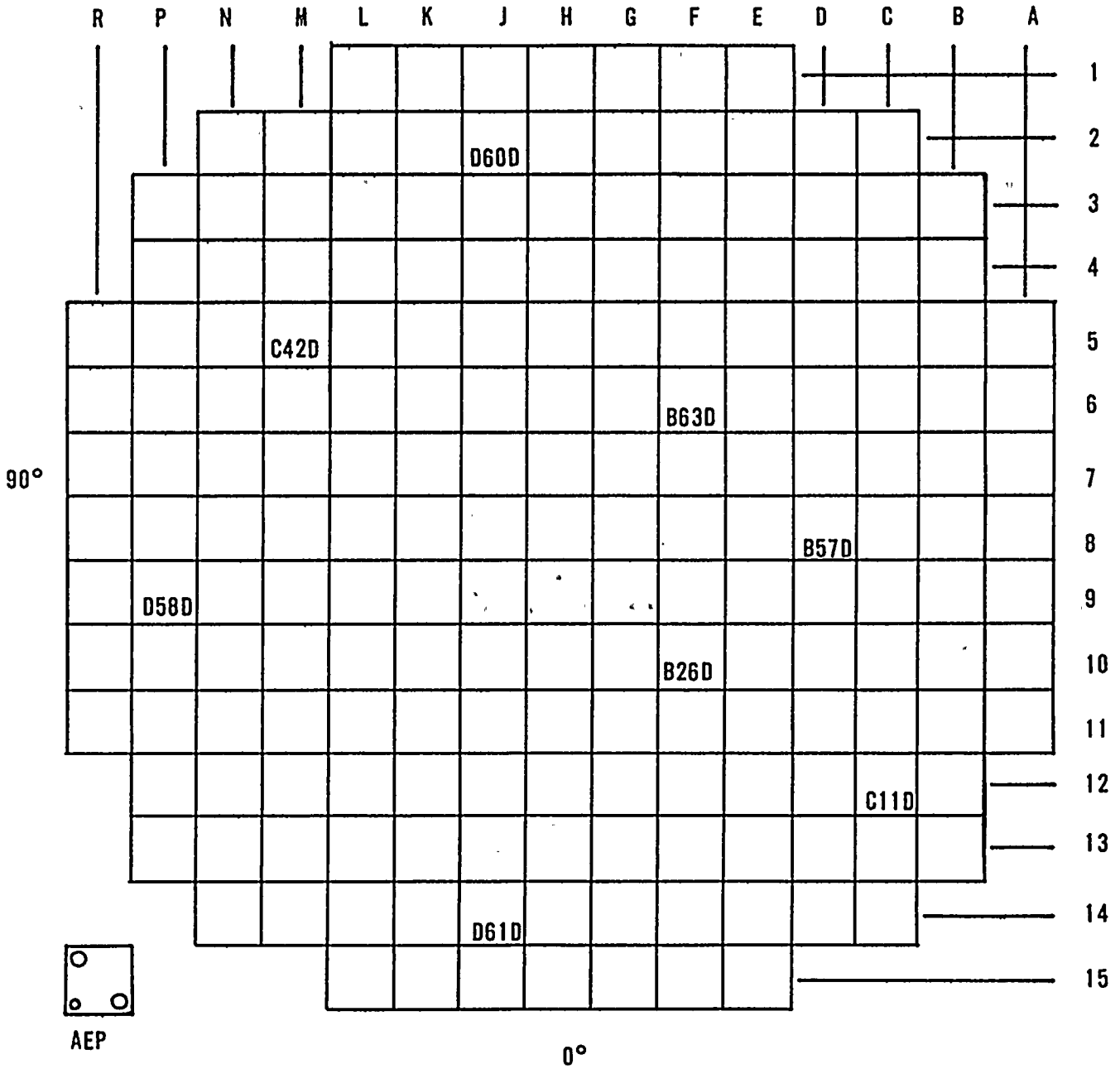

FUEL ASSEMBLY POSITIONS CYCLE 2

Figure 3

D.C. COOK UNIT 1

Core -3

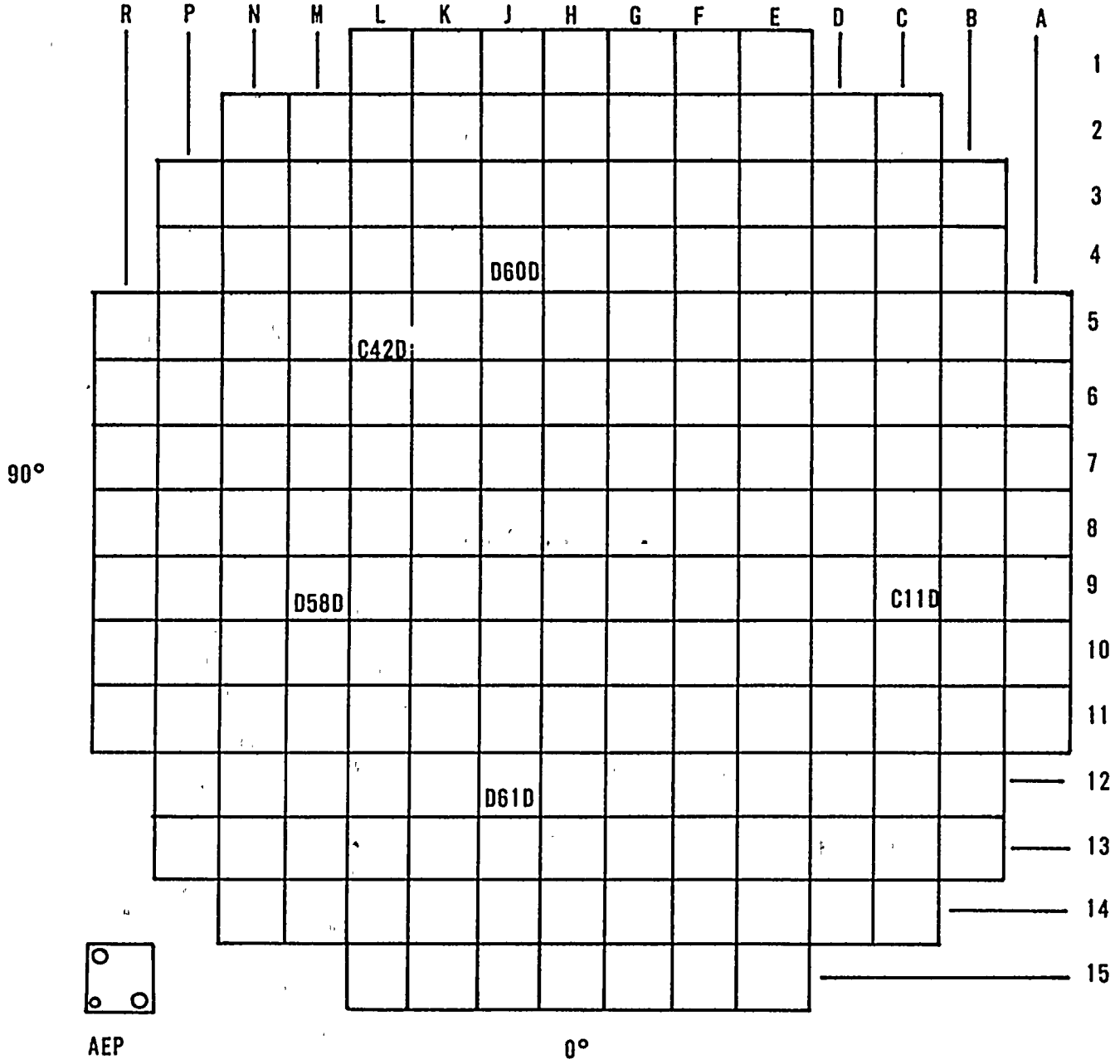

FUEL ASSEMBLY POSITIONS CYCLE 3

Figure 4

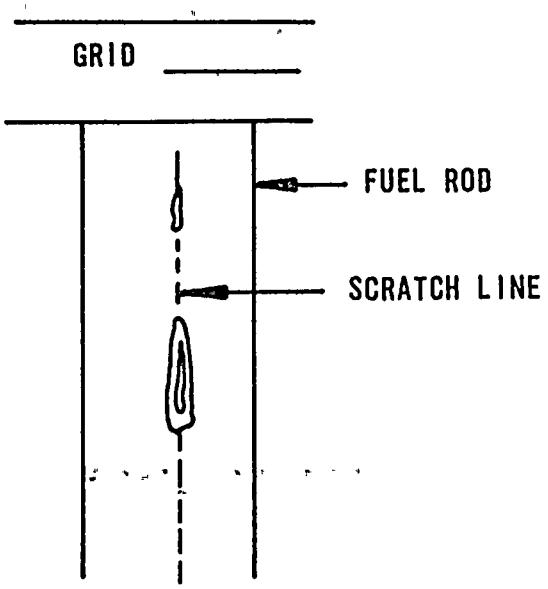

SCRATCH LINE CORROSION SITE
Figure 5

Appendix B

Summary of Exxon Fuel Examination

End of Core 2 D.C. Cook, Unit I

EXXON NUCLEAR COMPANY, Inc.

2101 Horn Rapids Road
P. O. Box 130, Richland, Washington 99352
Phone: (509) 943-8100 Telex: 32-6353

August 31, 1978

Mr. Rod Simms
Donald C. Cook Nuclear Plant
Indiana & Michigan Power Co.
P. O. Box 458
Red Arrow Highway
Bridgman, MI 49106

Dear Rod:

In response to your recent request, this letter summarizes the preliminary results obtained during our 1978 fuel examination at D. C. Cook # 1. All data for the two irradiated assemblies which were examined (D-65 and D-61) have been reduced and are currently being analyzed. The following table is a summary of rod-to-rod spacing measurements performed on D-65 and D-61. Nominal design spacing width is 139 mils.

Bundle	Span	Mean Rod Bow (mils)	95th Percentile Fractional Closure*	No. Of Observations
D-65	1	15.05	0.182	292
	2	16.56	0.208	292
	3	16.65	0.211	301
	4	13.51	0.165	294
	5	11.03	0.140	294
	6	4.40	0.078	295
D-61	1	10.56	0.134	84
	2	18.45	0.222	80
	3	16.54	0.208	162
	4	14.22	0.185	153
	5	10.75	0.135	163
	6	5.70	0.075	161

Measurements to determine the distance between the upper and lower tie plates were performed on D-65. The following figure illustrates the

* 95% of closures are less than value given

orientation of the assembly and the corresponding length measurements. Nominal design length is 153.510 inches.

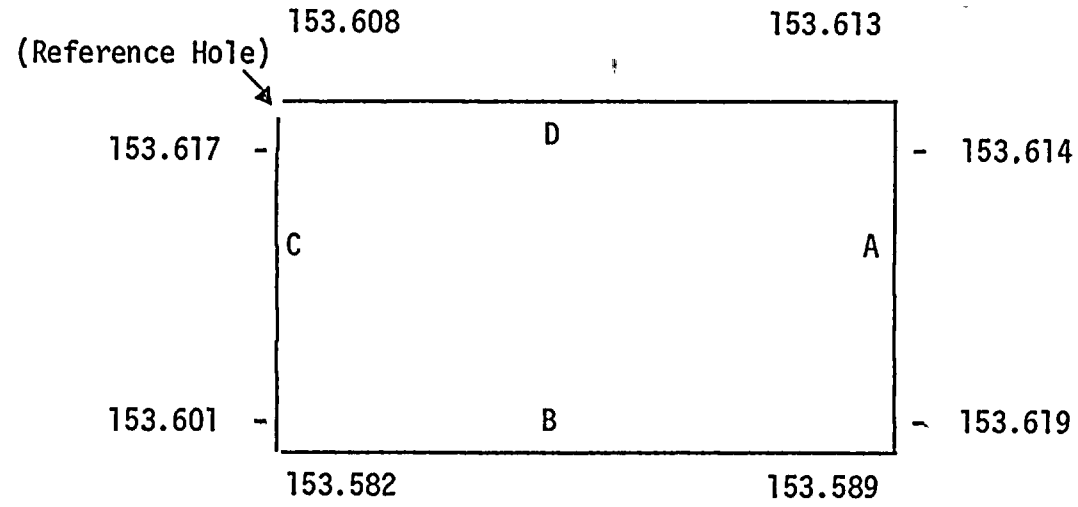

Repeatability of this measurement technique is generally considered to be ± 15 mils.

Television examination, record on video tape, of bundle D-65 showed this assembly to be in very good condition. Four rods had seated themselves onto the lower tie plate during the irradiation cycle; however, this condition is not considered unusual.

I hope you find this information useful in serving your immediate need. The final report should be completed and distributed in the near future.

Sincerely yours,

J. R. Tandy

J. R. Tandy, Engineer
Fuel Performance

JRT:wrg

cc: RJ Ehlers,ENC
GA Sofer, ENC
H. Sobel, American Electric Power
FP Wahlquist, ENC
KN Woods, ENC
File/LB